

## Supplementary Information for:

# Modulating the Performance of an Asymmetric Organocatalyst by Tuning Its Spatial Environment in a Metal-Organic Framework

Lujia Liu, Tian-You Zhou and Shane G. Telfer

*MacDiarmid Institute for Advanced Materials and Nanotechnology, Institute of Fundamental Sciences, Massey University, Palmerston North, New Zealand. Email: s.telfer@massey.ac.nz*

## Contents

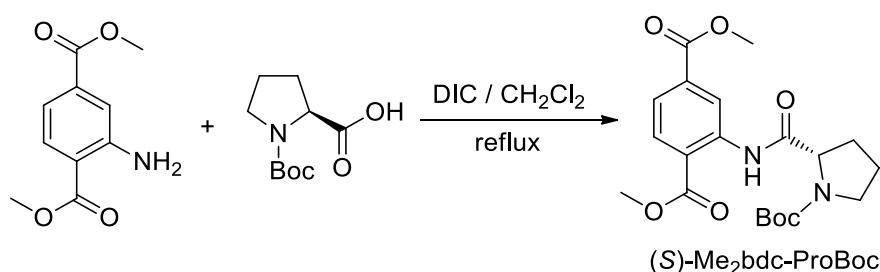
1. General procedures .....	2
2. Ligand synthesis and characterization .....	2
3. HPLC chromatographs of Me2bdc-ProBoc and Me2bdc-Pro .....	5
4. MOF synthesis and characterization .....	7
5. <sup>1</sup> H NMR analysis of digested MOF samples .....	10
6. Single crystal X-ray diffraction .....	28
7. Powder X-ray diffraction .....	31
8. Gas adsorption experiments and calculations .....	32
9. Catalysis of the aldol reaction between acetone and p-nitrobenzaldehyde .....	40
10. Catalysis of the aldol reaction between cyclopentanone and p-nitrobenzaldehyde .....	53
11. Photographs and microscopy images .....	54
12. References .....	56

## 1. General procedures

All starting materials and solvents were used as received from commercial sources without further purification unless otherwise noted. Several compounds were prepared via literature procedures: (*S*)-H<sub>2</sub>bpdC-ProBoc,<sup>1</sup> (*S*)-H<sub>2</sub>bpdC-Pro,<sup>1</sup> H<sub>3</sub>hmtt,<sup>2,3</sup> H<sub>3</sub>hbtt,<sup>2</sup> H<sub>3</sub>hott<sup>2</sup> and H<sub>2</sub>dppdc.<sup>4</sup> Column chromatography was carried out on silica gel (grade 60, mesh size 230-400, Scharlau). NMR spectra were recorded at room temperature (unless otherwise noted) on Bruker-400 and Bruker-500 Avance instruments, with the use of the solvent proton as an internal standard. High performance liquid chromatography (HPLC) was carried out using a Thermo Fisher Dionex Ultimate 3000 system equipped with a UV detector. Elemental analyses were performed by the Campbell Microanalytical Laboratory at the University of Otago, New Zealand.

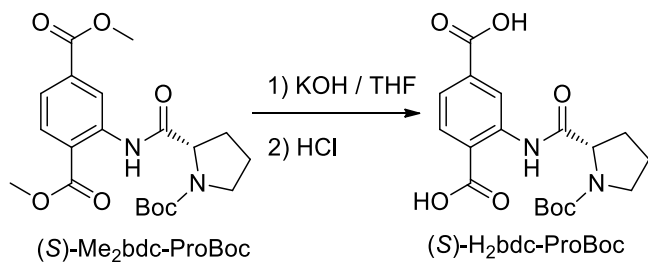
## 2. Ligand synthesis and characterization

### (i) (*S*)-Me<sub>2</sub>bdc-ProBoc



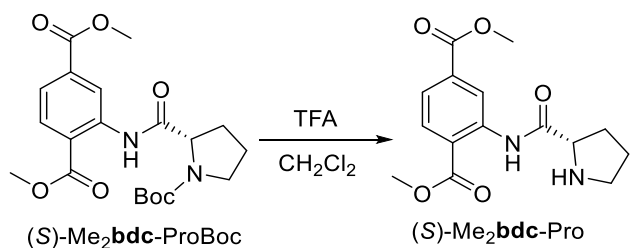
To a solution of *N*-Boc-L-Proline (4.74 g, 22.0 mmol) and DMAP (69 mg, 0.56 mmol) in CH<sub>2</sub>Cl<sub>2</sub> (100 mL), *N,N'*-diisopropylcarbodiimide (1.72 mL, 11.0 mmol) was added dropwise at 0 °C over 1 h. The resulting suspension was gradually added to a solution of dimethyl aminoterephthalate (2.09 g, 10.0 mmol) in CH<sub>2</sub>Cl<sub>2</sub> (100 mL) at 0 °C. The resulting mixture was then refluxed for 3 days. The reaction mixture was concentrated to ~25 mL by evaporating CH<sub>2</sub>Cl<sub>2</sub> *in vacuo* and the insoluble material was removed by filtration. The remaining CH<sub>2</sub>Cl<sub>2</sub> was removed under reduced pressure from the filtrate to afford a pink oil. To this oil, a small amount of 96 % ethanol was added and the product crystallized as large block colorless crystals. Yield: 3.36g (57 %). <sup>1</sup>H NMR (400 MHz, CDCl<sub>3</sub>, complicated by two conformers): δ 1.35-1.50 (s, s, 9H), 1.92-1.96 (m, 2H), 2.19-2.32 (m, 2H), 3.49-3.75 (m, 2H), 3.94 (s, 6H), 4.32-4.47 (s, s, 1 H), 7.75 (s, s, 1H), 8.09 (s, s, 1H), 9.39 (s, 1H), 11.45-11.52 (s, s, 1H). <sup>13</sup>C NMR (125 MHz, CDCl<sub>3</sub>, complicated by two conformers): δ 23.97, 24.52, 28.38, 28.58, 30.55, 31.69, 46.99, 47.32, 52.66, 52.96, 62.22, 62.82, 80.54, 118.71, 121.16, 121.44, 123.59, 130.92, 131.18, 135.52, 141.04, 141.27, 154.39, 155.26, 166.29, 167.77, 172.19, 172.69 ppm. ES-MS (positive mode, CH<sub>3</sub>OH): *m/z* = 430.11 ([C<sub>20</sub>H<sub>26</sub>N<sub>2</sub>O<sub>7</sub>Na]<sup>+</sup>, calcd. 429.16). Anal. calcd. for [C<sub>20</sub>H<sub>26</sub>N<sub>2</sub>O<sub>7</sub>]: C, 59.10; H, 6.45; N, 6.89; Found: C, 59.12; H, 6.43; N, 6.92. HPLC: Daicel Chiralpak AS. Hexane / *i*-PrOH, 95 : 5, 1 mL min<sup>-1</sup>, 254 nm, 25 °C: t<sub>R</sub> = 15.2 min. e.e. = 100 %. (*R*)-Me<sub>2</sub>bdc-ProBoc was prepared with the same procedure with its <sup>1</sup>H NMR data identical to the *S* enantiomer. t<sub>R</sub> = 11.3 min. e.e. = 100 %. Alternative HPLC condition: Daicel Chiralpak AS. Hexane / *i*-PrOH, 90 : 10, 1 mL min<sup>-1</sup>, 254 nm, 25 °C: t<sub>R</sub> (*S* enantiomer) = 10.1 min, t<sub>R</sub> (*R* enantiomer) = 7.7 min. The absolute structures of the two enantiomers were confirmed by single-crystal X-ray diffraction experiments as detailed later.

## (ii) (S)-H<sub>2</sub>bdc-ProBoc



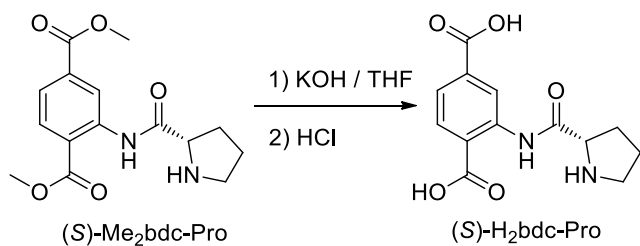
(S)-Me<sub>2</sub>bdc-ProBoc (1.076 g, 2.647 mmol) was suspended in a 1: 1 (v/v) mixture of THF and 1 M aq. KOH (50 mL). The suspension was heated to 50 °C and the reaction was monitored by TLC. Reaction was completed in 3 hours and THF was removed *in vacuo*. The remaining solution was acidified with 1 M aq. HCl to pH = 2. The white precipitate was isolated by filtration and washed with H<sub>2</sub>O then dried under a dynamic vacuum. Yield: 0.923 g (92%). <sup>1</sup>H NMR (500 MHz, DMSO-*d*<sub>6</sub>, complicated by two conformers): δ 1.24-1.41 (s, s, 9H), 1.83-1.87 (m, 2H), 1.95-1.99 (m, 1H), 2.20-2.32 (m, 1H) 3.39-3.44 (m, 1H), 3.49-3.55 (m, 1H), 4.16-4.20 (m, 1H), 7.67 (d, *J* = 8.2 Hz, 1H), 8.08 (d, *J* = 8.2 Hz, 1H), 9.16-9.20 (s, s, 1H), 11.7 (s, 1H), 11.3-14.1 (s, s, br, 2H). <sup>13</sup>C NMR (125 MHz, DMSO-*d*<sub>6</sub>): δ 23.28, 23.94, 27.83, 28.02, 30.05, 30.95, 46.50, 46.77, 61.81, 62.07, 79.03, 79.31, 120.08, 123.13, 131.42, 135.47, 140.52, 153.06, 154.02, 166.48, 168.96, 169.08, 171.77, 172.00 ppm. <sup>13</sup>C NMR (100 MHz, KOH / D<sub>2</sub>O / dioxane): δ 24.23, 24.61, 28.17, 28.33, 30.94, 31.55, 47.39, 47.91, 63.38, 82.59, 121.09, 121.14, 124.69, 127.62, 131.31, 137.86, 140.08, 156.41, 157.11, 174.39, 174.66, 175.13 ppm. ESI (negative mode, CH<sub>3</sub>OH): *m/z* = 377.1347 ([C<sub>18</sub>H<sub>21</sub>N<sub>2</sub>O<sub>7</sub>]<sup>-</sup>, calcd. 377.1343). Anal. calcd. for [C<sub>18</sub>H<sub>22</sub>N<sub>2</sub>O<sub>7</sub>·2H<sub>2</sub>O]: C, 52.17; H, 6.32; N, 6.76; Found: C, 52.62; 6.24; 6.80.

## (iii) (S)-Me<sub>2</sub>bdc-Pro



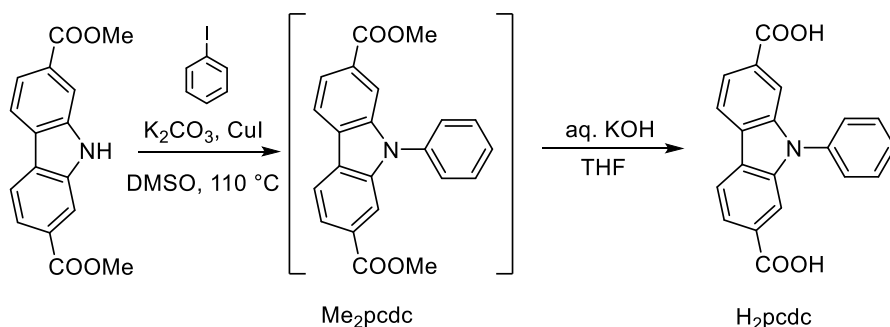
To a solution of (S)-Me<sub>2</sub>bdc-ProBoc (1.204 g, 2.962 mmol) in CH<sub>2</sub>Cl<sub>2</sub> (25 mL), trifluoroacetic acid (25 mL) was added dropwise at 0 °C. After 10 min, the reaction mixture was allowed to warm to room temperature and reacted for a further 30 min. Solvents were removed under reduced pressure and the remaining material was partitioned between CH<sub>2</sub>Cl<sub>2</sub> and sat. aq. NaHCO<sub>3</sub>. The organic layer was dried over Na<sub>2</sub>SO<sub>4</sub> to afford the product as a white solid. Yield: 0.857 g (95 %). <sup>1</sup>H NMR (500 MHz, CDCl<sub>3</sub>): δ 1.71-1.84 (m, 2H), 2.03-2.10 (m, 1H), 2.19-2.27 (m, 1H), 3.05-3.10 (m, 1H), 3.13-3.18 (m, 1H), 3.92-3.96 (m, 7H), 7.55 (dd, *J* = 8.2 Hz, 1.5 Hz, 1H), 8.08 (d, *J* = 8.3 Hz, 1H), 9.39 (d, *J* = 1.4 Hz, 1H), 12.2 (m, 1H). <sup>13</sup>C NMR (125 MHz, CDCl<sub>3</sub>): δ 26.33, 31.28, 47.55, 52.61, 52.72, 61.95, 119.52, 121.61, 123.43, 131.16, 135.18, 140.81, 166.38, 167.38, 175.18 ppm. ESI (positive mode, methanol): *m/z* = 307.1277 ([C<sub>15</sub>H<sub>19</sub>N<sub>2</sub>O<sub>5</sub>]<sup>+</sup>, calcd. 307.1288). Anal. calcd. for [C<sub>15</sub>H<sub>18</sub>N<sub>2</sub>O<sub>5</sub>]: C, 58.82; H, 5.92; N, 9.15; found: C, 58.75; H, 5.97; N, 9.17. HPLC: Chiralpak AD-H. Hexane/*i*-PrOH, 45:55 to 20:80 gradient, 0.75 mL min<sup>-1</sup>, 25 °C: t<sub>R</sub> = 16.8 min. e.e. = 100 %. (*R*)-Me<sub>2</sub>bdc-Pro was prepared with the same procedure with its <sup>1</sup>H NMR data identical to the *S* enantiomer. t<sub>R</sub> = 8.7 min. e.e. = 100 %.

#### (iv) (S)-H<sub>2</sub>bdc-Pro



(S)-Me<sub>2</sub>bdc-Pro (225 mg, 0.735 mmol) was suspended in a 1: 1 (v/v) mixture of THF and 1 M aq. KOH (10 mL). The suspension was refluxed for 14 hours. After the reaction, THF was removed *in vacuo*. The remaining solution was acidified with aq. HCl to pH = 2. The yellow precipitate was isolated by filtration and washed with H<sub>2</sub>O and dried under dynamic vacuum to afford the product. Yield: 134.3 mg (58%). <sup>1</sup>H NMR (500 MHz, DMSO-*d*<sub>6</sub>): δ 1.94-2.00 (m, 2H), 2.03-2.10 (m, 1H), 2.34-2.41 (m, 1H), 3.21-3.31 (m, 2H) 4.53 (t, *J* = 7.6 Hz, 1H), 7.64 (dd, *J* = 8.2 Hz, 1.3 Hz, 1H), 8.06 (d, *J* = 7.9 Hz, 1H), 8.9 (s, 1H). <sup>13</sup>C NMR (175 MHz, DMSO-*d*<sub>6</sub>): δ 23.84, 29.02, 45.46, 60.90, 119.68, 123.04, 131.13, 132.30, 139.81, 167.11, 168.37 ppm. ES-MS (negative mode, CH<sub>3</sub>OH): *m/z* = 277.86 ([C<sub>13</sub>H<sub>13</sub>N<sub>2</sub>O<sub>5</sub>]<sup>-</sup>, calcd. 277.08). ES-MS (positive mode, CH<sub>3</sub>OH): *m/z* = 279.38 ([C<sub>13</sub>H<sub>15</sub>N<sub>2</sub>O<sub>5</sub>]<sup>+</sup>, calcd. 279.10). Anal. calcd. for [C<sub>13</sub>H<sub>14</sub>N<sub>2</sub>O<sub>5</sub>·0.33H<sub>2</sub>O]: C, 54.93; H, 5.20; N, 9.85; found: C, 54.87; 5.00; 9.84.

#### (v) H<sub>2</sub>pcdc



A green suspension of dimethyl 9H-carbazole-2,7-dicarboxylate (100 mg, 0.35 mmol), iodobenzene (0.18 mL, 1.06 mmol), K<sub>2</sub>CO<sub>3</sub> (98 mg, 0.71 mmol), CuI (6.7 mg, 0.035 mmol) and D-proline (4.1 mg, 0.035 mmol) in DMSO was heated at 110 °C in microwave for 18 hours to give a brown suspension. This suspension was extracted by DCM and the organic layer was washed with water three times to remove DMSO. A white solid was obtained after purification by column with DCM/hexane (1/1). This Me<sub>2</sub>pcdc product was dissolved in a 1:1 (v/v) mixture of THF and 1 M aq. KOH (10 mL). The suspension was refluxed for 14 hours. After the reaction, THF was removed under vacuum. The remaining solution was acidified with 3 M aq. HCl to pH = 2. A yellow precipitate was isolated by filtration and washed with H<sub>2</sub>O and dried under dynamic vacuum to afford the product (70 mg, yield 60%). <sup>1</sup>H NMR (500 MHz, DMSO-*d*<sub>6</sub>) δ 13.13 – 13.07 (s, 2H), 8.43 (d, *J* = 7.7 Hz, 2H), 7.93 (m, 4H), 7.76 (d, *J* = 7.5 Hz, 2H), 7.70 (d, *J* = 7.5 Hz, 2H), 7.65 (t, *J* = 7.4 Hz, 1H). <sup>13</sup>C NMR (125 MHz, DMSO-*d*<sub>6</sub>): δ 111.58, 121.68, 121.90, 125.77, 127.67, 129.08, 129.93, 130.99, 136.40, 141.55, 167.90 ppm. ESI (negative mode, CH<sub>3</sub>OH): *m/z* = 330.0771 ([C<sub>20</sub>H<sub>12</sub>NO<sub>4</sub>]<sup>-</sup>, calcd. 330.0761).

### 3. HPLC chromatographs of Me<sub>2</sub>bdc-ProBoc and Me<sub>2</sub>bdc-Pro

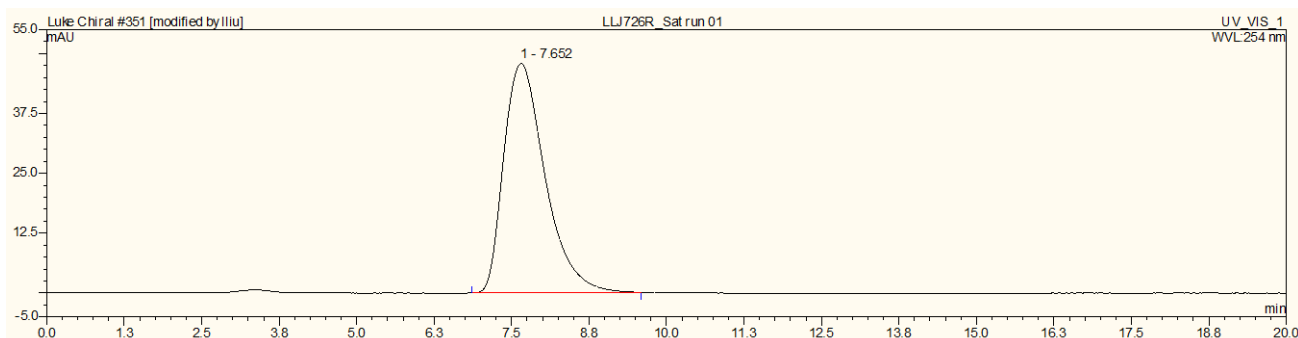


**Figure S1** Chromatogram of (*R*)-Me<sub>2</sub>bdc-ProBoc.

Conditions: Daicel Chiralpak AS. Hexane / *i*-PrOH, 90 : 10, 1 mL min<sup>-1</sup>, 254 nm, 25 °C

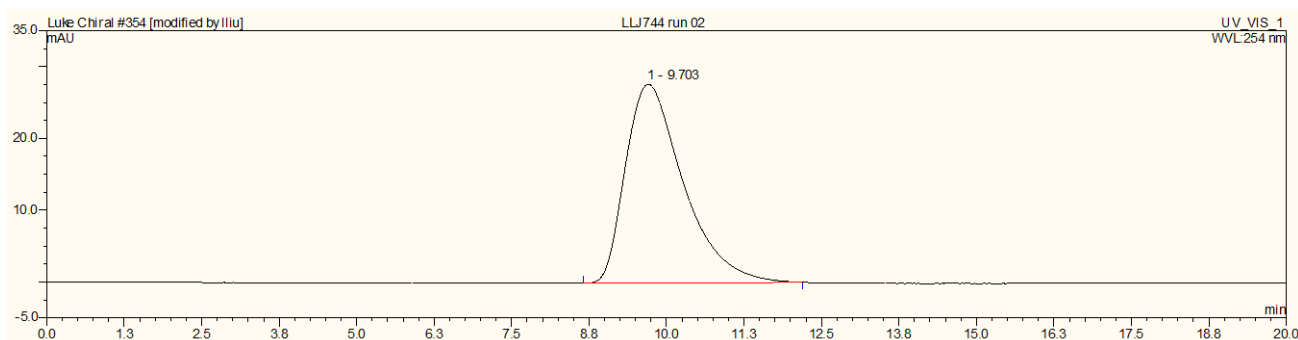


**Figure S2** Chromatogram of (*S*)-Me<sub>2</sub>bdc-ProBoc.

Conditions: Daicel Chiralpak AS. Hexane / *i*-PrOH, 90 : 10, 1 mL min<sup>-1</sup>, 254 nm, 25 °C

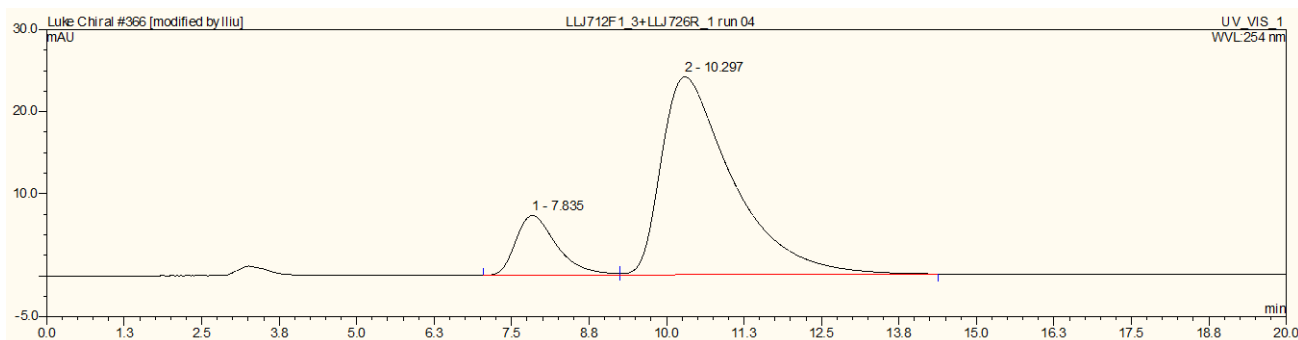


**Figure S3** Chromatogram of a (*R*)-Me<sub>2</sub>bdc-ProBoc / (*S*)-Me<sub>2</sub>bdc-ProBoc mixture (~ 1:3)

Conditions: Daicel Chiralpak AS. Hexane / *i*-PrOH, 90 : 10, 1 mL min<sup>-1</sup>, 254 nm, 25 °C

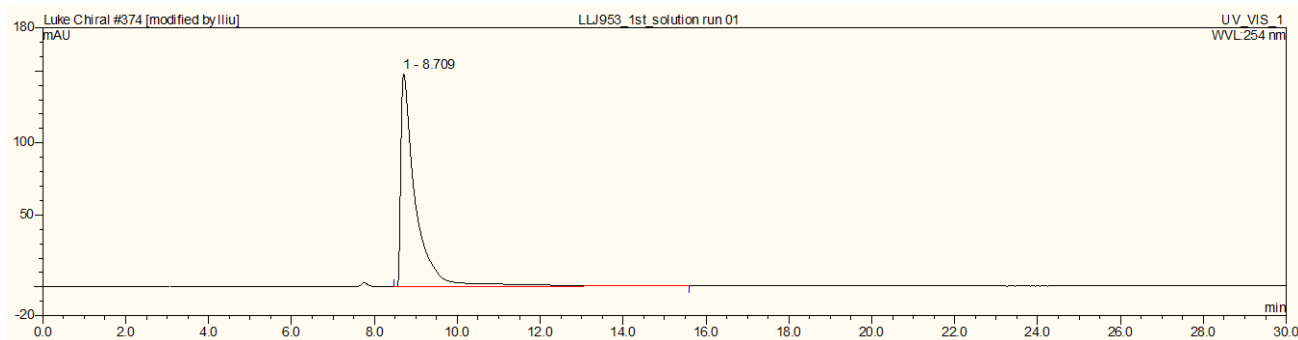


**Figure S4** Chromatogram of (*R*)-Me<sub>2</sub>bdc-Pro.

Conditions: Daicel Chiralpak AD-H. Hexane / *i*-PrOH, 55 : 45 to 20 : 80 gradient, 0.75 mL min<sup>-1</sup>, 254 nm, 25 °C

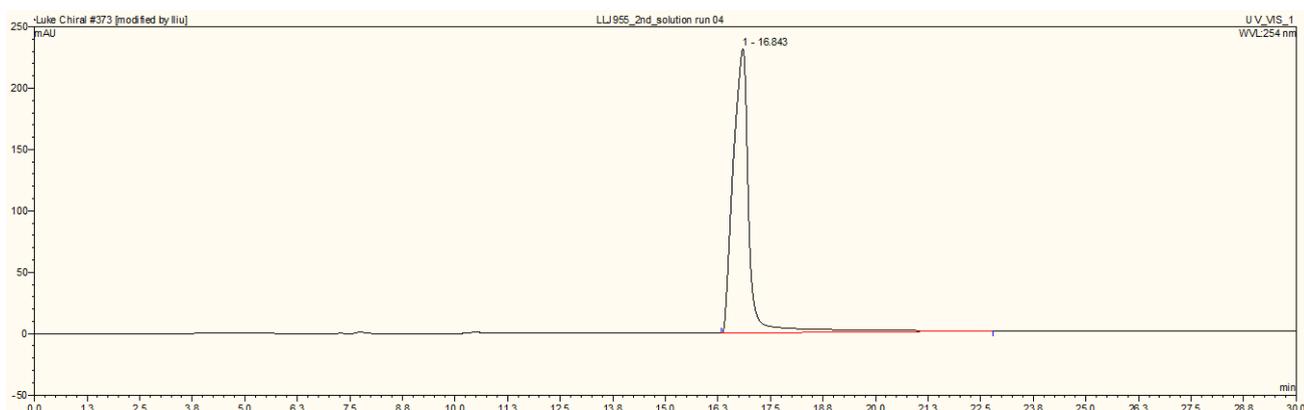


**Figure S5** Chromatogram of (*S*)-Me<sub>2</sub>bdc-Pro.

Conditions: Daicel Chiralpak AD-H. Hexane / *i*-PrOH, 55 : 45 to 20 : 80 gradient, 0.75 mL min<sup>-1</sup>, 254 nm, 25 °C

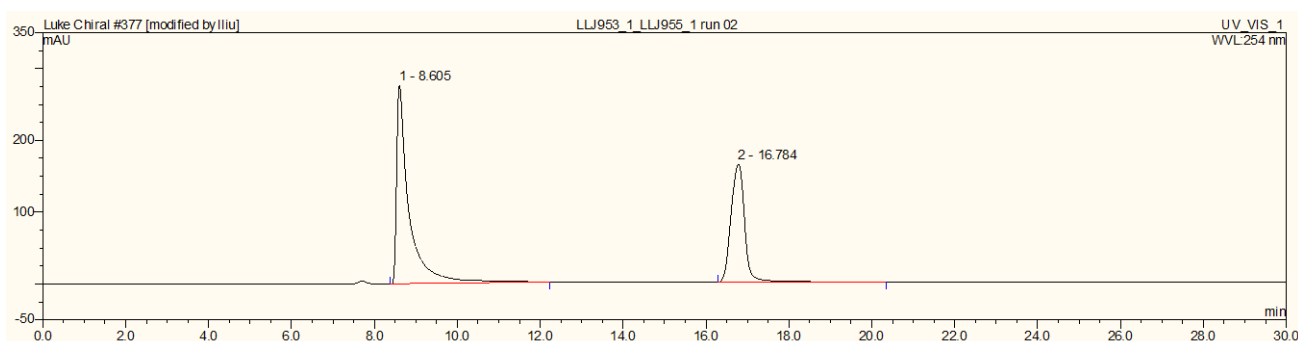


**Figure S6** Chromatogram of a (*R*)-Me<sub>2</sub>bdc-Pro/(*S*)-Me<sub>2</sub>bdc-Pro mixture (~ 3:2).

Conditions: Daicel Chiralpak AD-H. Hexane / *i*-PrOH, 55 : 45 to 20 : 80 gradient, 0.75 mL min<sup>-1</sup>, 254 nm, 25 °C

## 4. MOF synthesis and characterization

### (a) $[\text{Zn}_4\text{O}(\text{bdc})_{1/2}(\text{bpdc-ProBoc})_{1/2}(\text{hmtt})_{4/3}]$ and $[\text{Zn}_4\text{O}(\text{bdc})_{1/2}(\text{bpdc-Pro})_{1/2}(\text{hmtt})_{4/3}]$

$\text{H}_3\text{hmtt}$  (23.0 mg, 41.2  $\mu\text{mol}$ ), (*S*)- $\text{H}_2\text{bpdc-ProBoc}$  (18.7 mg, 41.2  $\mu\text{mol}$ ), terephthalic acid (6.9 mg, 41.2  $\mu\text{mol}$ ) and  $\text{Zn}(\text{NO}_3)_2 \cdot 4\text{H}_2\text{O}$  (75.4 mg, 288.2  $\mu\text{mol}$ ) were dissolved in a mixed solvent of DEF (5 mL) and water (0.18 mL) in a 20 mL scintillation vials. The reaction was carried out in an 85 °C isothermal oven for 17 hours to obtain colourless crystals of  $[\text{Zn}_4\text{O}(\text{bdc})_{1/2}(\text{bpdc-ProBoc})_{1/2}(\text{hmtt})_{4/3}]$ . The mother liquor was replaced with anhydrous DMF and this process was repeated five times. The DMF was then replaced with fresh anhydrous acetone and the solvent replenished five times within an hour. Occluded solvent was removed under a dynamic vacuum. Anal. calcd. for  $[\text{C}_{128}\text{H}_{100}\text{N}_2\text{O}_{29}\text{Zn}_8] \cdot 2.5\text{H}_2\text{O}$ : C, 56.98; H, 3.92; N, 1.04; Found: C, 56.93; H, 3.85; N, 1.00.

$[\text{Zn}_4\text{O}(\text{bdc})_{1/2}(\text{bpdc-ProBoc})_{1/2}(\text{hmtt})_{4/3}]$  crystals were gradually heated at a rate of 20 °C / min to 200 °C and held for 20 hours under dynamic vacuum to afford  $[\text{Zn}_4\text{O}(\text{bdc})_{1/2}(\text{bpdc-Pro})_{1/2}(\text{hmtt})_{4/3}]$  as colourless crystals. Yield: 22.5 mg. Anal. calcd. for  $[\text{C}_{123}\text{H}_92\text{N}_2\text{O}_{27}\text{Zn}_8] \cdot 8\text{H}_2\text{O}$ : C, 54.77; H, 4.04; N, 1.04; found: C, 54.69; H, 3.84; N, 1.00.

### (b) Direct synthesis of $[\text{Zn}_4\text{O}(\text{bdc})_{1/2}(\text{bpdc-Pro}')_{1/2}(\text{hmtt})_{4/3}]$ starting from $\text{H}_2\text{bpdc-Pro}$

$\text{H}_3\text{hmtt}$  (22.1 mg, 39.6  $\mu\text{mol}$ ), (*S*)- $\text{H}_2\text{bpdc-Pro}$  (8.8 mg, 23  $\mu\text{mol}$ ), terephthalic acid (10.3 mg, 62.0  $\mu\text{mol}$ ) and  $\text{Zn}(\text{NO}_3)_2 \cdot 4\text{H}_2\text{O}$  (84.1 mg, 322  $\mu\text{mol}$ ) were dissolved in a mixed solvent of DEF (5 mL) and water (0.15 mL) in a 20 mL scintillation vials which had been treated with Sigmacote. The reaction was carried out in an 85 °C isothermal oven for 17 hours to obtain orange crystals. The mother liquor was replaced with anhydrous DMF and this process was repeated five times. The DMF was then replaced with fresh anhydrous  $\text{CH}_2\text{Cl}_2$  and the solvent replenished five times within an hour. Occluded solvent was removed by gradually heating the crystals at a rate of 1 °C / min and holding the temperature at 80 °C five hours under a dynamic vacuum. Yield: 24.7 mg.

### (c) $[\text{Zn}_4\text{O}(\text{bdc})_{1/2}(\text{bpdc-Pro})_{1/2}(\text{hett})_{4/3}]$

$\text{H}_3\text{hett}$  (26.1 mg, 40.5  $\mu\text{mol}$ ), (*S*)- $\text{H}_2\text{bpdc-ProBoc}$  (18.4 mg, 40.5  $\mu\text{mol}$ ), terephthalic acid (6.8 mg, 40.5  $\mu\text{mol}$ ) and  $\text{Zn}(\text{NO}_3)_2 \cdot 4\text{H}_2\text{O}$  (74.0 mg, 283.2  $\mu\text{mol}$ ) were dissolved in a mixed solvent of DEF (5 mL) and water (0.18 mL). The reaction was carried out in an 85 °C isothermal oven for 17 hours to obtain yellow crystals. The mother liquor was replaced with anhydrous DMF and this process was repeated five times. The DMF was then replaced with fresh anhydrous acetone and the solvent replenished five times within an hour. The acetone-occluded crystals were thermolyzed to generate the title compound by heating the crystals at a rate of 20 °C / min and holding the temperature at 200 °C for 20 hours under a dynamic vacuum. Yield: 25.1 mg. Anal. calcd. for  $[\text{C}_{139}\text{H}_{124}\text{N}_2\text{O}_{27}\text{Zn}_8] \cdot 7.5\text{H}_2\text{O}$ : C, 57.32; H, 4.81; N, 0.96; found: C, 57.02; H, 4.40; N, 0.85.

**(d) [Zn<sub>4</sub>O(bdc)<sub>1/2</sub>(bpdc-Pro)<sub>1/2</sub>(hbtt)<sub>4/3</sub>]**

H<sub>3</sub>hbtt (33.5 mg, 41.2 μmol), (S)-H<sub>2</sub>bpdc-ProBoc (18.7 mg, 41.2 μmol), terephthalic acid (6.9 mg, 41.2 μmol) and Zn(NO<sub>3</sub>)<sub>2</sub>·4H<sub>2</sub>O (75.4 mg, 288.2 μmol) were dissolved in a mixed solvent of DEF (5 mL) and water (0.18 mL) in a 20 mL scintillation vials. The reaction was carried out in an 85 °C isothermal oven for 17 hours to obtain yellow crystals. The mother liquor was replaced with anhydrous DMF and this process was repeated five times. The DMF was then replaced with fresh anhydrous acetone and the solvent replenished five times within an hour. The acetone-occluded crystals were thermolyzed to generate the title compound by heating the crystals at a rate of 20 °C / min and holding the temperature at 200 °C for 20 hours under a dynamic vacuum. Yield: 29.5 mg. Anal. calcd. for [C<sub>171</sub>H<sub>188</sub>N<sub>2</sub>O<sub>27</sub>Zn<sub>8</sub>].4.5H<sub>2</sub>O: C, 62.10; H, 6.00; N, 0.85; found: C, 61.99; H, 5.82; N, 0.80.

**(e) [Zn<sub>4</sub>O(bdc)<sub>1/2</sub>(bpdc-Pro)<sub>1/2</sub>(hott)<sub>4/3</sub>]**

H<sub>3</sub>hmtt (47.5 mg, 41.2 μmol), (S)-H<sub>2</sub>bpdc-ProBoc (18.7 mg, 41.2 μmol), terephthalic acid (6.9 mg, 41.2 μmol) and Zn(NO<sub>3</sub>)<sub>2</sub>·4H<sub>2</sub>O (75.4 mg, 288.2 μmol) were dissolved in a mixed solvent of DEF (5 mL) and water (0.18 mL) in a 20 mL scintillation vials. The reaction was carried out in an 85 °C isothermal oven for 24 hours to obtain yellow crystals of [Zn<sub>4</sub>O(bdc)<sub>1/2</sub>(bpdc-ProBoc)<sub>1/2</sub>(hott)<sub>4/3</sub>]. The mother liquor was replaced with anhydrous DMF and this process was repeated five times. The DMF was then replaced with fresh anhydrous CH<sub>2</sub>Cl<sub>2</sub> and the solvent replenished five times within an hour. The acetone-occluded crystals were thermolyzed to generate the title MOF by heating the crystals at a rate of 20 °C / min and holding the temperature at 200 °C for 20 hours under a dynamic vacuum. Yield: 41.0 mg. Anal. calcd. for [C<sub>235</sub>H<sub>316</sub>N<sub>2</sub>O<sub>27</sub>Zn<sub>8</sub>].12H<sub>2</sub>O: C, 65.03; H, 7.90; N, 0.65; Found: C, 64.94; H, 7.70; N, 0.54.

**(f) [Zn<sub>4</sub>O(bdc-ProBoc)<sub>1/2</sub>(bpdc)<sub>1/2</sub>(hmtt)<sub>4/3</sub>] and [Zn<sub>4</sub>O(bdc-Pro)<sub>1/2</sub>(bpdc)<sub>1/2</sub>(hmtt)<sub>4/3</sub>]**

H<sub>3</sub>hmtt (23.0 mg, 41.2 μmol), H<sub>2</sub>bpdc (9.9 mg, 41.2 μmol), (S)-H<sub>2</sub>bdc-ProBoc (15.6 mg, 41.2 μmol) and Zn(NO<sub>3</sub>)<sub>2</sub>·4H<sub>2</sub>O (75.4 mg, 288.2 μmol) were dissolved in a mixed solvent of DEF (5 mL) and water (0.18 mL) in a 20 mL scintillation vials. The reaction was carried out in an 85 °C isothermal oven for 18 hours to obtain colourless crystals of [Zn<sub>4</sub>O(bdc-ProBoc)<sub>1/2</sub>(bpdc)<sub>1/2</sub>(hmtt)<sub>4/3</sub>]. The mother liquor was replaced with anhydrous DMF and this process was repeated five times. The DMF was then replaced with fresh anhydrous acetone and the solvent replenished five times within an hour. acetone-occluded crystals were thermolyzed to generate [Zn<sub>4</sub>O(bdc-Pro)<sub>1/2</sub>(bpdc)<sub>1/2</sub>(hmtt)<sub>4/3</sub>] by heating the crystals at a rate of 20 °C / min and holding the temperature at 200 °C for 20 hours under a dynamic vacuum. Yield: 25.4 mg. Anal. calcd. for [C<sub>123</sub>H<sub>92</sub>N<sub>2</sub>O<sub>27</sub>Zn<sub>8</sub>].5.5H<sub>2</sub>O: C, 55.70; H, 3.91; N, 1.06; Found: C, 55.42; H, 3.57; N, 0.95.

**(g) Direct synthesis of [Zn<sub>4</sub>O(bdc-Pro)<sub>1/2</sub>(bpdc)<sub>1/2</sub>(hmtt)<sub>4/3</sub>] starting from H<sub>2</sub>bdc-Pro**

H<sub>3</sub>hmtt (41.8 mg, 74.8 μmol), H<sub>2</sub>bpdc (23.4 mg, 96.6 μmol) (S)-H<sub>2</sub>bdc-Pro (23.6 mg, 75.0 μmol), and Zn(NO<sub>3</sub>)<sub>2</sub>·4H<sub>2</sub>O (140.8 mg, 538.6 μmol) were dissolved in a mixed solvent of DEF (10 mL) and water (0.3 mL) in a 50 mL Schott which had been treated with Sigmacote. The reaction was carried out in an 85 °C isothermal

oven for 9.5 hours to obtain orange crystals. The mother liquor was replaced with anhydrous DMF and this process was repeated five times. The DMF was then replaced with fresh anhydrous CH<sub>2</sub>Cl<sub>2</sub> and the solvent replenished five times within an hour. Occluded solvent was removed by gradually heating the crystals at a rate of 1 °C / min and holding the temperature at 80 °C five hours under a dynamic vacuum. Yield: 42.4 mg.

**(h) [Zn<sub>4</sub>O(bdc-Pro)<sub>1/2</sub>(bpdc)<sub>1/2</sub>(hett)<sub>4/3</sub>]**

H<sub>3</sub>hett (26.1 mg, 40.5 μmol), H<sub>2</sub>bpdc (18.4 mg, 40.5 μmol), (S)-H<sub>2</sub>bdc-ProBoc (6.8 mg, 40.5 μmol) and Zn(NO<sub>3</sub>)<sub>2</sub>·4H<sub>2</sub>O (74.0 mg, 283.2 μmol) were dissolved in a mixed solvent of DEF (5 mL) and water (0.18 mL). The reaction was carried out in an 85 °C isothermal oven for 17 hours to obtain yellow crystals. The mother liquor was replaced with anhydrous DMF and this process was repeated five times. The DMF was then replaced with fresh anhydrous acetone and the solvent replenished five times within an hour. The acetone-occluded crystals were thermolyzed to generate the title compound by heating the crystals at a rate of 20 °C / min and holding the temperature at 200 °C for 20 hours under a dynamic vacuum. Yield: 25.4 mg.

**(i) [Zn<sub>4</sub>O(bdc-Pro)<sub>1/2</sub>(bpdc)<sub>1/2</sub>(hbtt)<sub>4/3</sub>]**

H<sub>3</sub>hbtt (33.5 mg, 41.2 μmol), H<sub>2</sub>bpdc (9.9 mg, 41.2 μmol), (S)-H<sub>2</sub>bdc-ProBoc (15.6 mg, 41.2 μmol) and Zn(NO<sub>3</sub>)<sub>2</sub>·4H<sub>2</sub>O (75.4 mg, 288.2 μmol) were dissolved in a mixed solvent of DEF (5 mL) and water (0.18 mL) in a 20 mL scintillation vials. The reaction was carried out in an 85 °C isothermal oven for 18 hours to obtain colourless crystals. The reaction was carried out in an 85 °C isothermal oven for 17 hours to obtain yellow crystals. The mother liquor was replaced with anhydrous DMF and this process was repeated five times. The DMF was then replaced with fresh anhydrous acetone and the solvent replenished five times within an hour. The acetone-occluded crystals were thermolyzed to generate the title compound by heating the crystals at a rate of 20 °C / min and holding the temperature at 200 °C for 20 hours under a dynamic vacuum. Yield: 29.5 mg.

**(j) [Zn<sub>4</sub>O(bdc-Pro)<sub>1/2</sub>(bpdc)<sub>1/2</sub>(hott)<sub>4/3</sub>]**

H<sub>3</sub>hott (47.5 mg, 41.2 μmol), H<sub>2</sub>bpdc (9.9 mg, 41.2 μmol), (S)-H<sub>2</sub>bdc-ProBoc (15.6 mg, 41.2 μmol) and Zn(NO<sub>3</sub>)<sub>2</sub>·4H<sub>2</sub>O (75.4 mg, 288.2 μmol) were dissolved in a mixed solvent of DEF (5 mL) and water (0.18 mL) in a 20 mL scintillation vials. The reaction was carried out in an 85 °C isothermal oven for 18 hours to obtain colourless crystals. The reaction was carried out in an 85 °C isothermal oven for 24 hours to obtain yellow crystals. The mother liquor was replaced with anhydrous DMF and this process was repeated five times. The DMF was then replaced with fresh anhydrous acetone and the solvent replenished five times within an hour. The acetone-occluded crystals were thermolyzed to generate the title compound by heating the crystals at a rate of 20 °C / min and holding the temperature at 200 °C for 20 hours under a dynamic vacuum. Yield: 41.0 mg.

**(k) [Zn<sub>4</sub>O(ndc)<sub>1/2</sub>(bpdc-Pro)<sub>1/2</sub>(hmtt)<sub>4/3</sub>]**

The synthesis of [Zn<sub>4</sub>O(ndc)<sub>1/2</sub>(bpdc-Pro)<sub>1/2</sub>(hmtt)<sub>4/3</sub>] was similar to the procedure of [Zn<sub>4</sub>O(bdc)<sub>1/2</sub>(bpdc-Pro)<sub>1/2</sub>(hmtt)<sub>4/3</sub>] except for replacing bdc by ndc.

**(l) [Zn<sub>4</sub>O(ndc)<sub>1/2</sub>(bpdc-Pro)<sub>1/2</sub>(hbtt)<sub>4/3</sub>]**

The synthesis of [Zn<sub>4</sub>O(ndc)<sub>1/2</sub>(bpdc-Pro)<sub>1/2</sub>(hbtt)<sub>4/3</sub>] was similar to the procedure of [Zn<sub>4</sub>O(bdc)<sub>1/2</sub>(bpdc-Pro)<sub>1/2</sub>(hbtt)<sub>4/3</sub>] except for replacing bdc by ndc.

**(m) [Zn<sub>4</sub>O(ndc)<sub>1/2</sub>(bpdc-Pro)<sub>1/2</sub>(hott)<sub>4/3</sub>]**

The synthesis of [Zn<sub>4</sub>O(ndc)<sub>1/2</sub>(bpdc-Pro)<sub>1/2</sub>(hott)<sub>4/3</sub>] was similar to the procedure of [Zn<sub>4</sub>O(bdc)<sub>1/2</sub>(bpdc-Pro)<sub>1/2</sub>(hott)<sub>4/3</sub>] except for replacing bdc by ndc.

**(n) [Zn<sub>4</sub>O(bdc-Pro)<sub>1/2</sub>(dppdc)<sub>1/2</sub>(hmtt)<sub>4/3</sub>]**

H<sub>3</sub>hmtt (23.0 mg, 41.2 μmol), H<sub>2</sub>dppdc (9.9 mg, 41.2 μmol) (S)-H<sub>2</sub>bdc-ProBoc (17.9 mg, 47.5 μmol), benzoic acid (55 mg, 0.45 mmol) and Zn(NO<sub>3</sub>)<sub>2</sub>·4H<sub>2</sub>O (75.4 mg, 0.29 mmol) were dissolved in a mixed solvent of DEF (5 mL) and water (0.175 mL) in a 20 mL vial. The reaction was carried out in an 85 °C isothermal oven for 48 hours to obtain yellow crystals. The mother liquor was replaced with anhydrous DMF and this process was repeated five times. The DMF was then replaced with anhydrous acetone and the solvent replenished five times within an hour. Acetone-occluded crystals were thermolyzed to produce [Zn<sub>4</sub>O(bdc-Pro)<sub>1/2</sub>(dppdc)<sub>1/2</sub>(hmtt)<sub>4/3</sub>] by heating at a rate of 20 °C / min and holding the temperature at 200 °C for 20 hours under a dynamic vacuum. Yield: 24.0 mg.

**(o) [Zn<sub>4</sub>O(bdc-Pro)<sub>1/2</sub>(pcdc)<sub>1/2</sub>(hmtt)<sub>4/3</sub>]**

H<sub>3</sub>hmtt (23.0 mg, 41.2 μmol), H<sub>2</sub>pcdc (9.9 mg, 41.2 μmol) (S)-H<sub>2</sub>bdc-ProBoc (17.9 mg, 47.5 μmol), benzoic acid (55 mg, 0.45 mmol) and Zn(NO<sub>3</sub>)<sub>2</sub>·4H<sub>2</sub>O (75.4 mg, 0.29 mmol) were dissolved in a mixed solvent of DEF (5 mL) and water (0.175 mL) in a 20 mL vial. The reaction was carried out in an 85 °C isothermal oven for 48 hours to obtain yellow crystals. The mother liquor was replaced with anhydrous DMF and this process was repeated five times. The DMF was then replaced with anhydrous acetone and the solvent replenished five times within an hour. Acetone-occluded crystals were thermolyzed to produce [Zn<sub>4</sub>O(bdc-Pro)<sub>1/2</sub>(pcdc)<sub>1/2</sub>(hmtt)<sub>4/3</sub>] by heating the crystals at a rate of 20 °C / min and holding the temperature at 200 °C for 20 hours under a dynamic vacuum. Yield: 25.0 mg.

## 5. <sup>1</sup>H NMR analysis of digested MOF samples

For <sup>1</sup>H NMR spectroscopy, The desolvated crystals were digested using the following protocol: 23 μL of a 35% DCI solution in D<sub>2</sub>O was mixed with 1 mL of DMSO-*d*<sub>6</sub> to give a DCI/DMSO-*d*<sub>6</sub> stock solution. Around 5 mg of MOF was digested in 150 μL of this stock solution together with 450 μL of DMSO-*d*<sub>6</sub>. Spectra were acquired immediately following dissolution. Spectra for all MOFs are presented below.

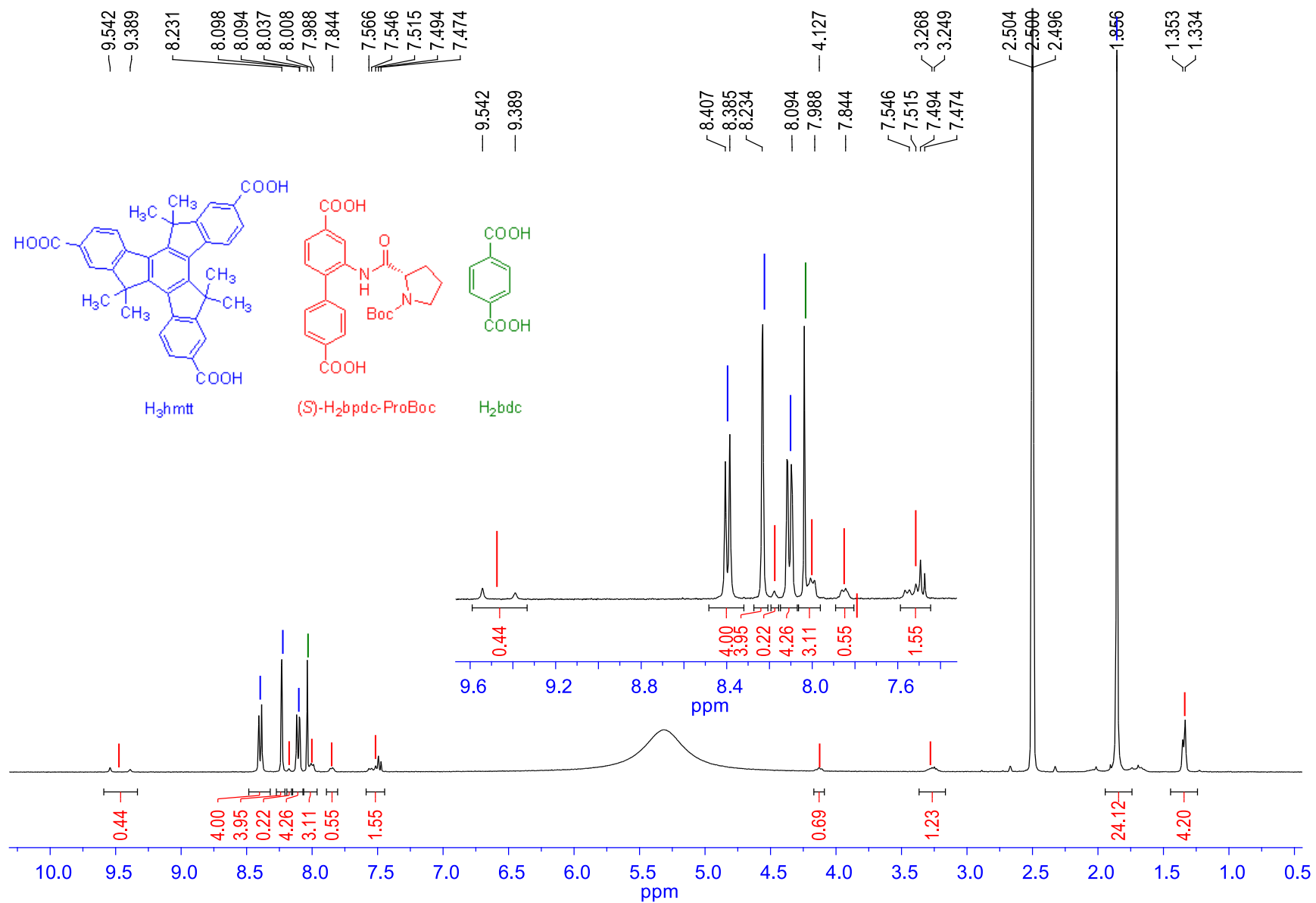


**Figure S7** <sup>1</sup>H NMR spectrum of digested [Zn<sub>4</sub>O(bdc)<sub>1/2</sub>(bpdc-ProBoc)<sub>1/2</sub>(hmtt)<sub>4/3</sub>] showing integrals that match with the formula. Note that two sets of proton peaks of H<sub>2</sub>bpdc-ProBoc are attributed to its two conformers in solution.

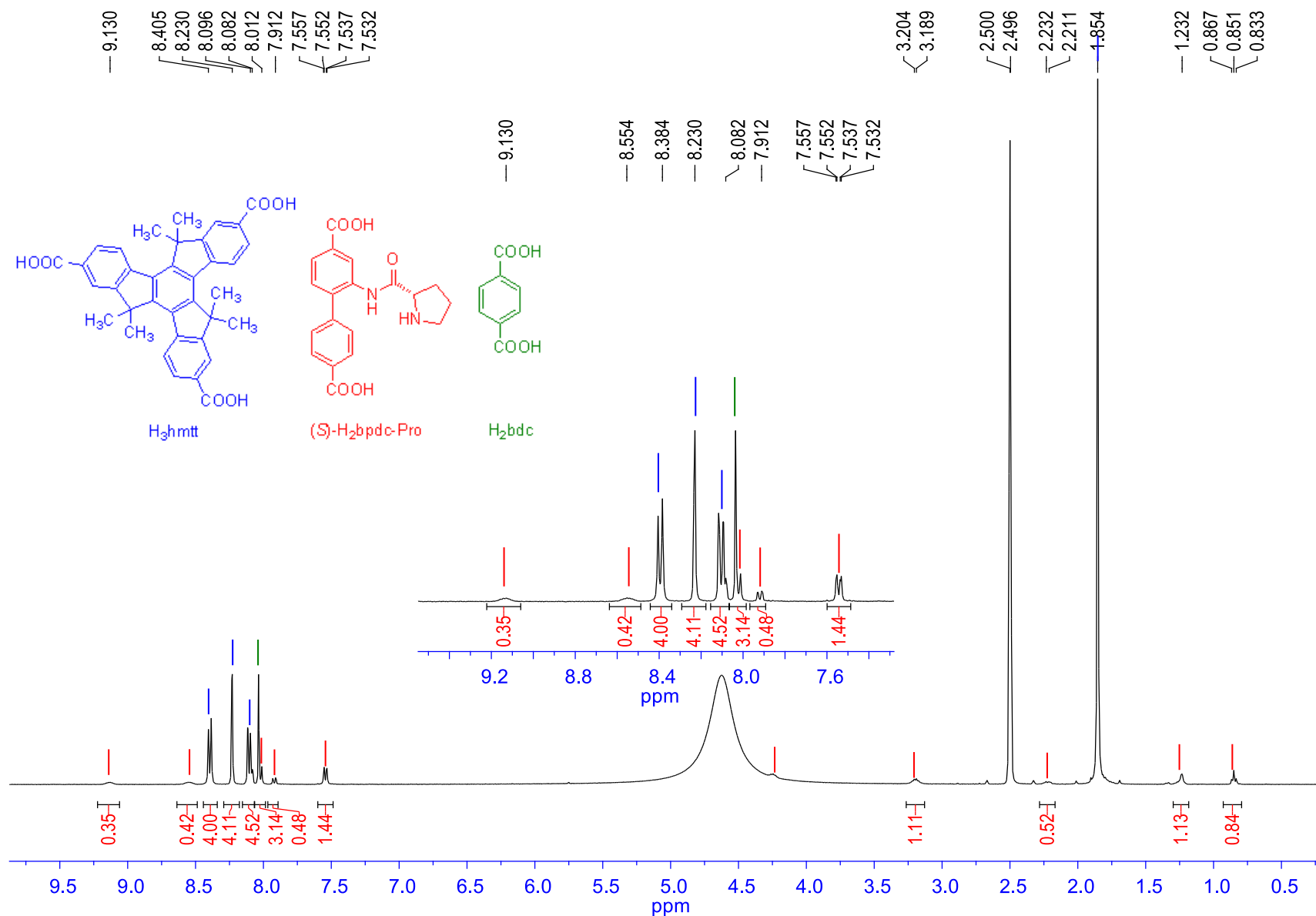


**Figure S8** <sup>1</sup>H NMR spectra of digested [Zn<sub>4</sub>O(bdc)<sub>1/2</sub>(bpdc-Pro)<sub>1/2</sub>(hmtt)<sub>4/3</sub>] showing integrals that match with the formula. The Boc group was completely removed after thermolysis as indicated by the complete disappearance of the Boc protons which would otherwise appear at 1.33 and 1.35 ppm.

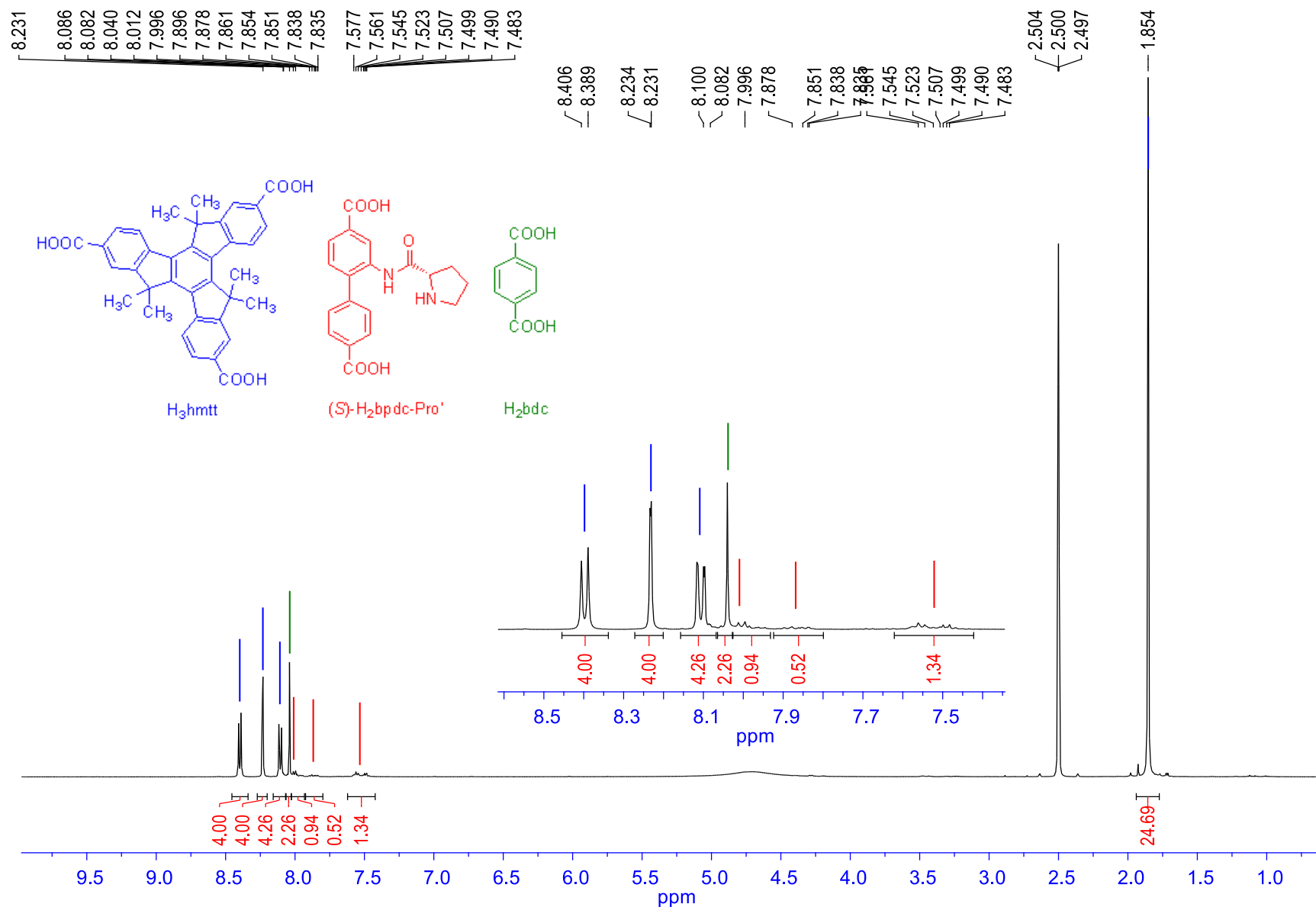


**Figure S9** <sup>1</sup>H NMR spectrum of digested [Zn<sub>4</sub>O(bdc)<sub>1/2</sub>(bpdc-Pro')<sub>1/2</sub>(hmtt)<sub>4/3</sub>] that had been directly synthesized from H<sub>2</sub>bpdc-Pro. Additional signals in the aromatic region indicate that side reactions occur to the bpdc-Pro ligand during the course of MOF synthesis.

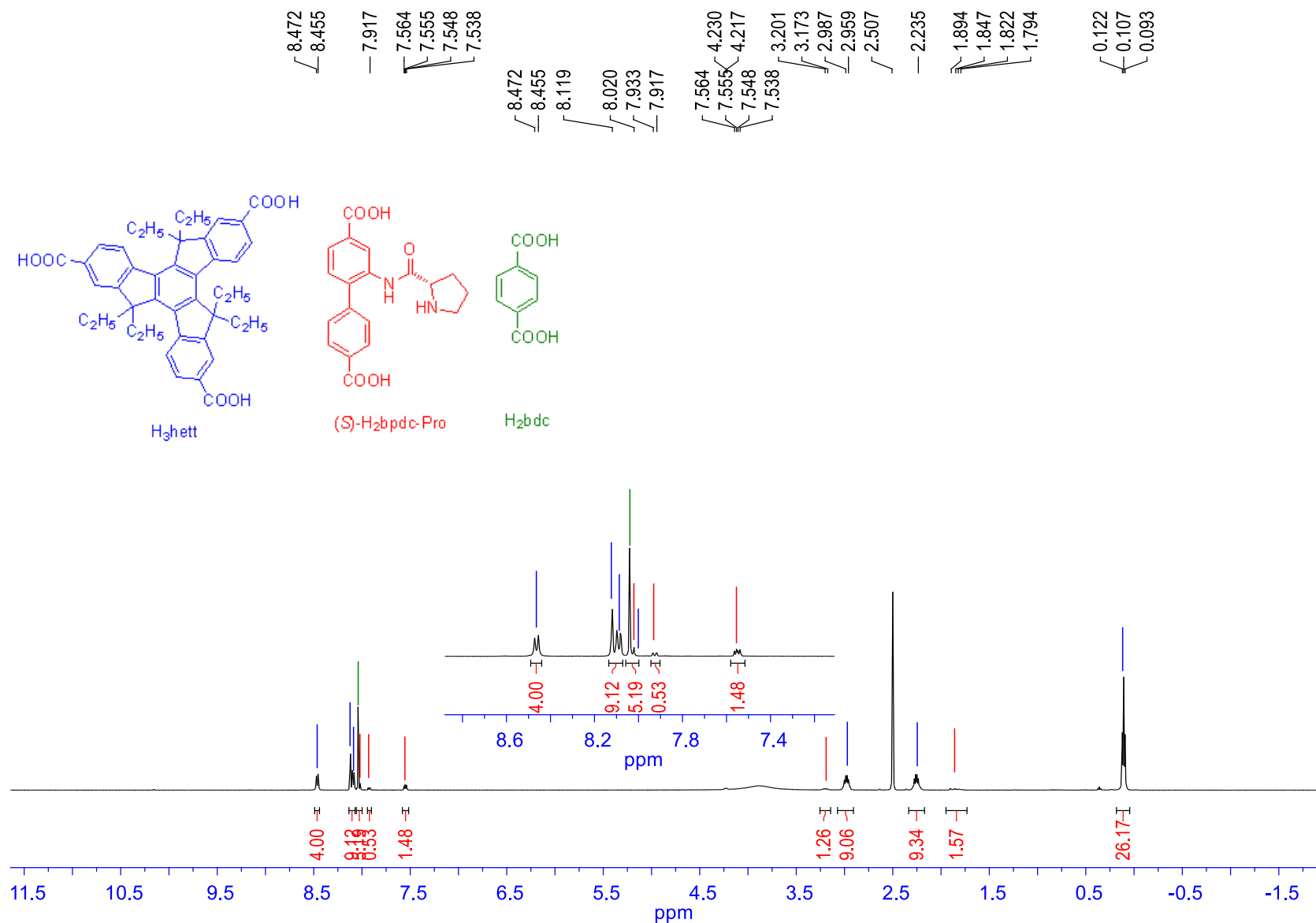


**Figure S10** <sup>1</sup>H NMR spectra of digested [Zn<sub>4</sub>O(bdc)<sub>1/2</sub>(bpdc-Pro)<sub>1/2</sub>(hett)<sub>4/3</sub>] showing integrals that match with the formula. The Boc group was completely removed after thermolysis as indicated by the complete disappearance of the Boc protons which would otherwise appear at 1.33 and 1.35 ppm.

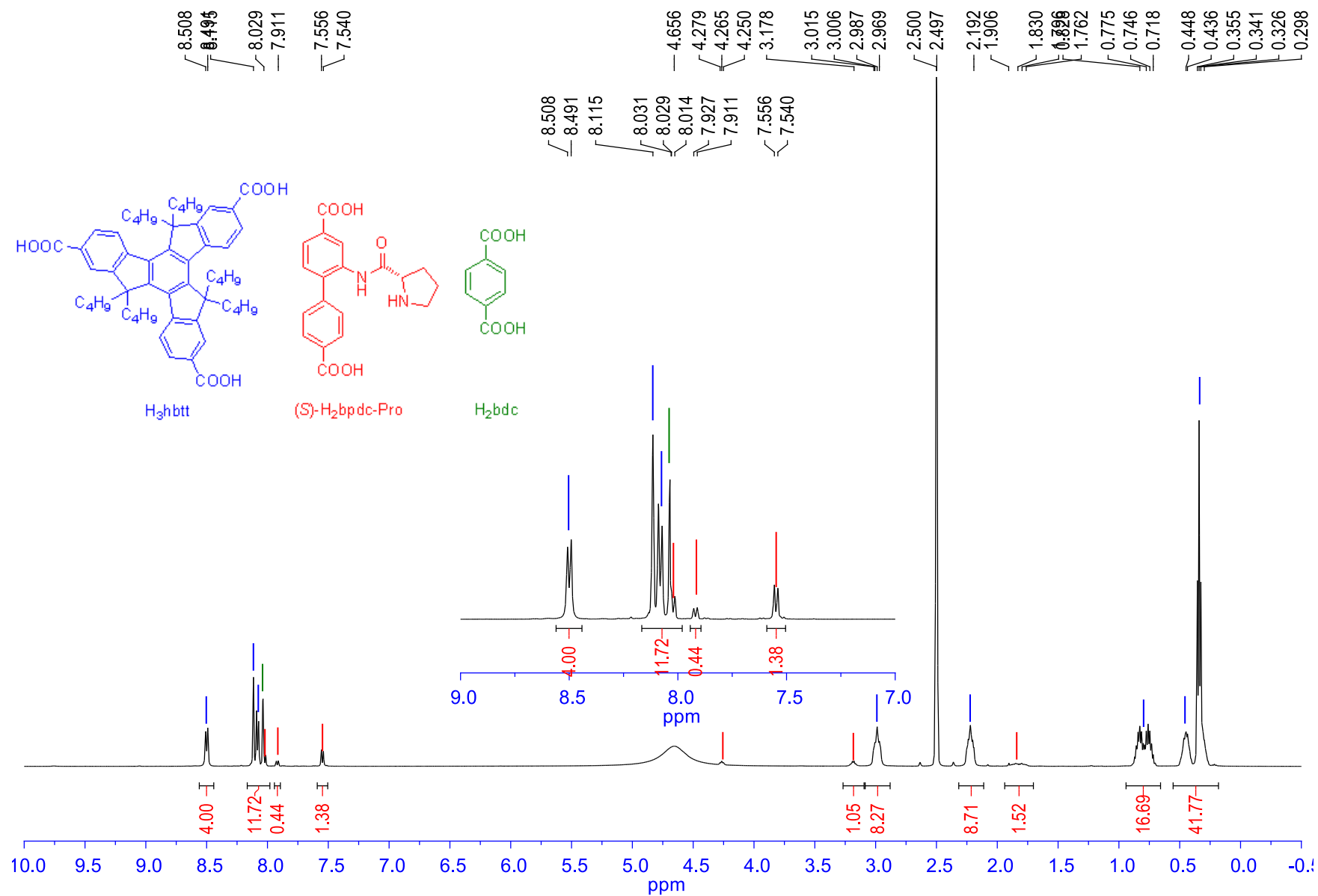


**Figure S11** <sup>1</sup>H NMR spectra of digested [Zn<sub>4</sub>O(bdc)<sub>1/2</sub>(bpdc-Pro)<sub>1/2</sub>(hbt)<sub>4/3</sub>] showing integrals that match with the formula. The Boc group was completely removed after thermolysis as indicated by the complete disappearance of the Boc protons which would otherwise appear at 1.33 and 1.35 ppm.

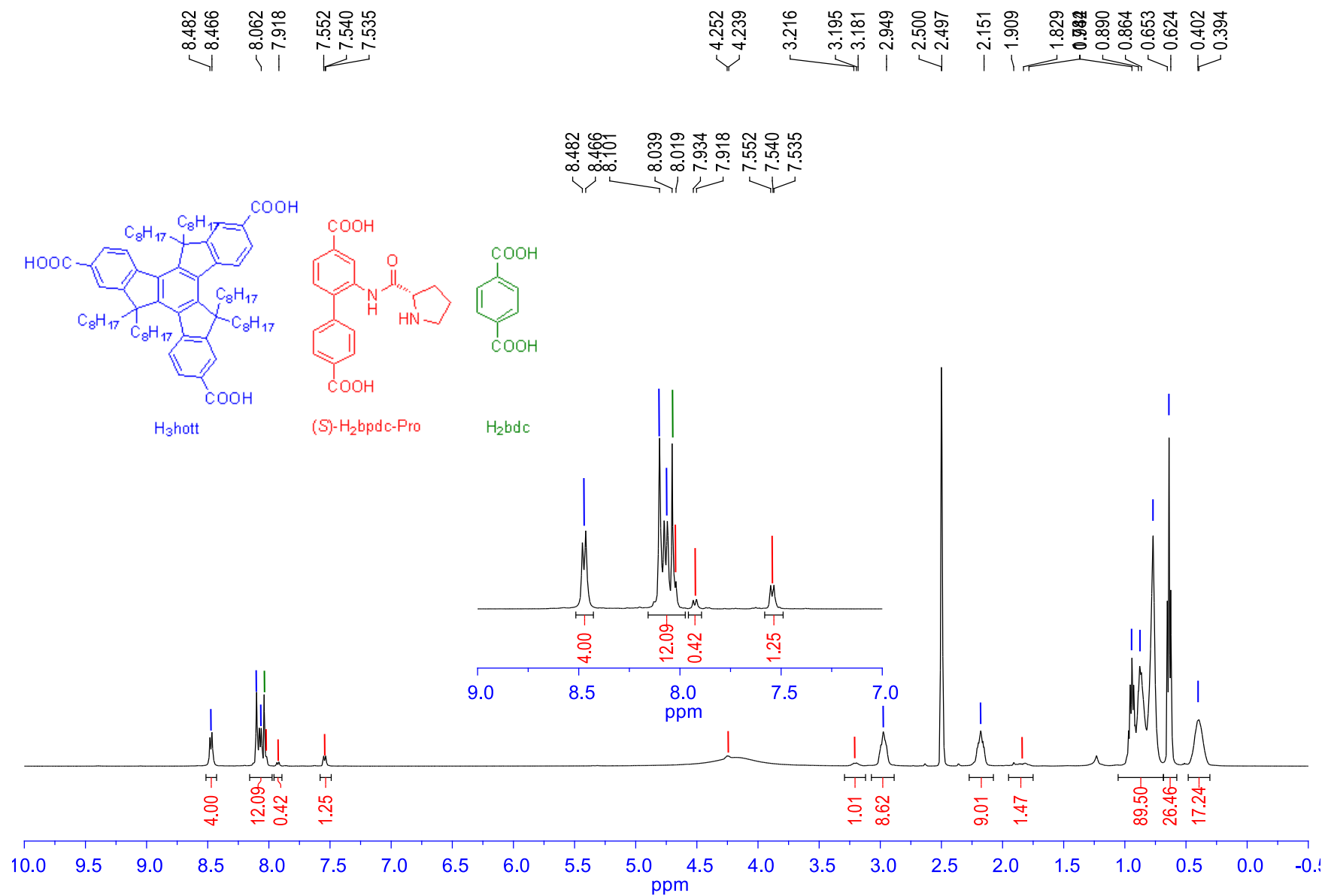


**Figure S12** <sup>1</sup>H NMR spectra of digested [Zn<sub>4</sub>O(bdc)<sub>1/2</sub>(bpdc-Pro)<sub>1/2</sub>(hott)<sub>4/3</sub>] showing integrals that match with the formula. The Boc group was completely removed after thermolysis as indicated by the complete disappearance of the Boc protons which would otherwise appear at 1.33 and 1.35 ppm.

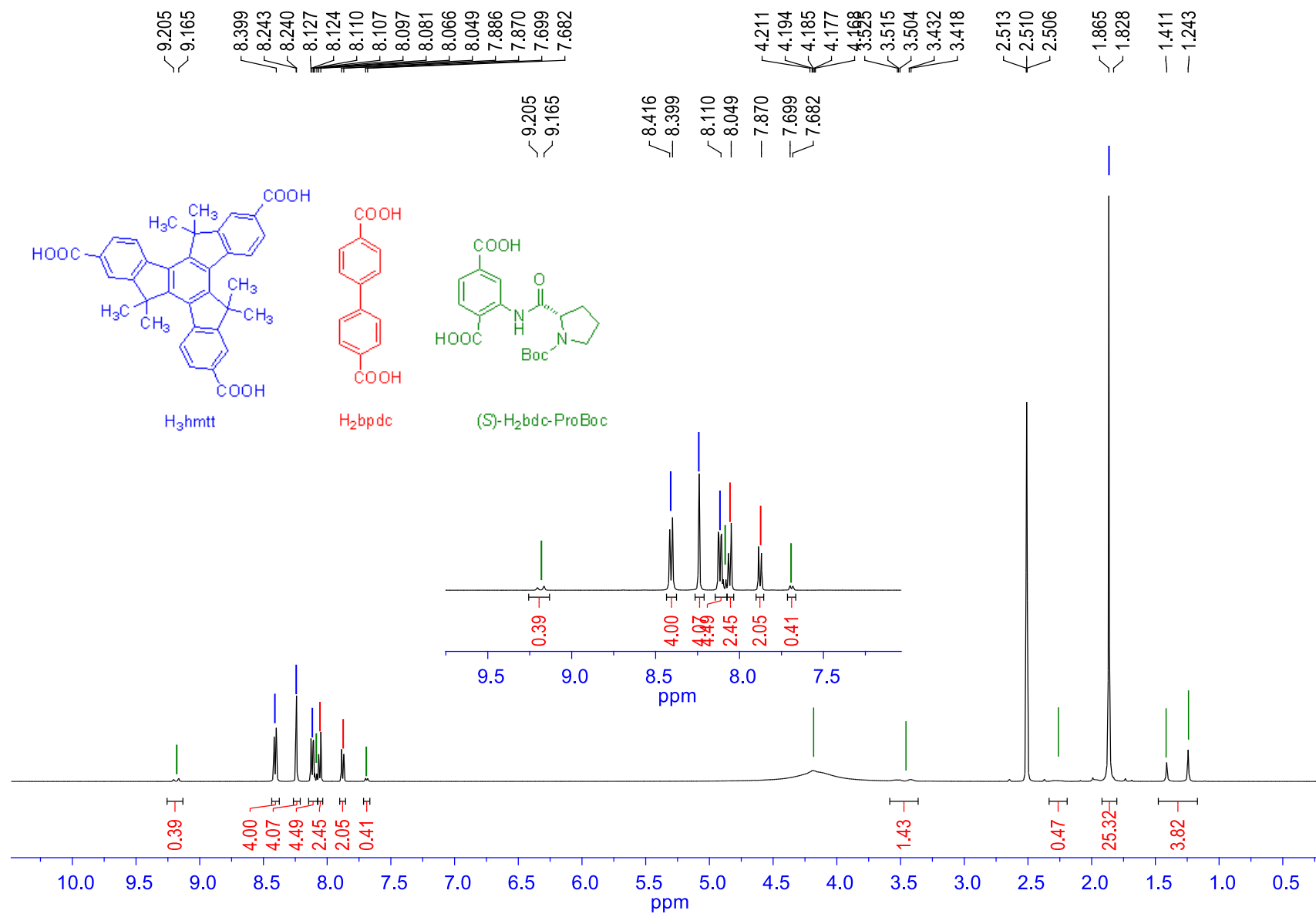


**Figure S13** <sup>1</sup>H NMR spectra of digested [Zn<sub>4</sub>O(bdc-ProBoc)<sub>1/2</sub>(bpdc)<sub>1/2</sub>(hmtt)<sub>4/3</sub>] showing integrals that match with the formula. Note that two sets of proton peaks of H<sub>2</sub>bdc-ProBoc are attributed to its two conformers in solution.

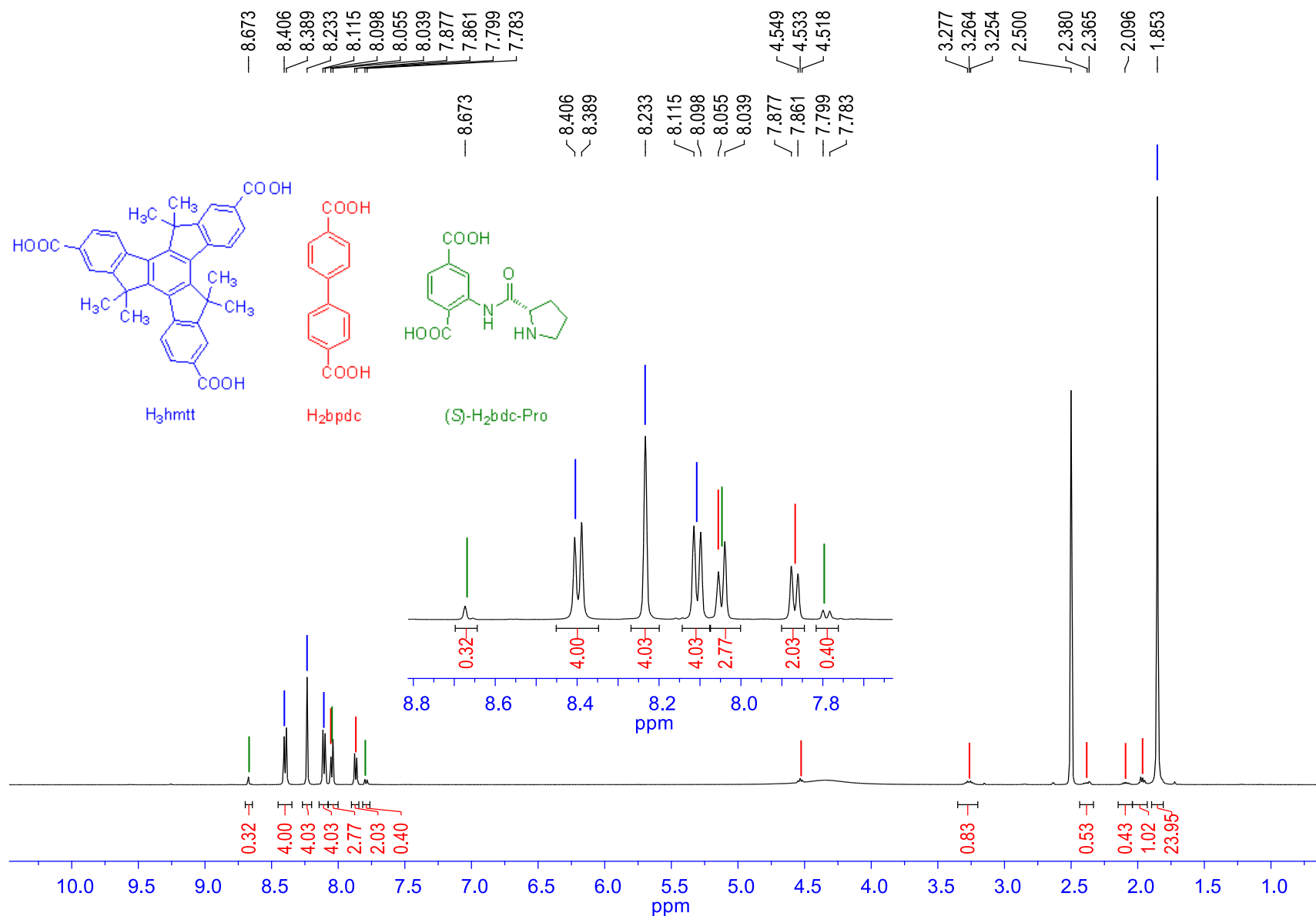


**Figure S14** <sup>1</sup>H NMR spectra of digested [Zn<sub>4</sub>O(bdc-Pro)<sub>1/2</sub>(bpdc)<sub>1/2</sub>(hmtt)<sub>4/3</sub>] showing integrals that match with the formula. The Boc group was completely removed after thermolysis as indicated by the complete disappearance of the Boc protons which would otherwise appear at 1.24 and 1.41 ppm.

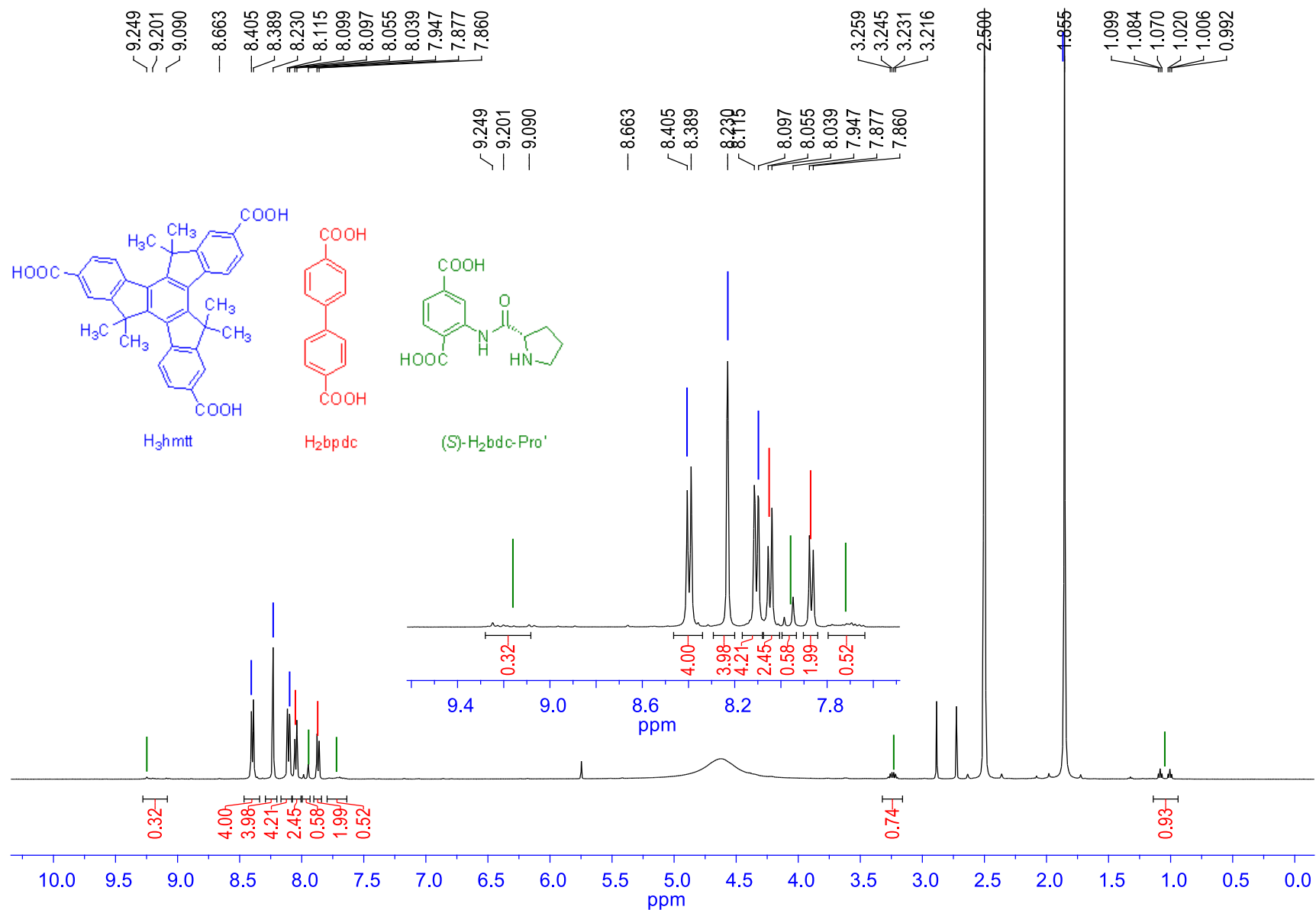


**Figure S15** <sup>1</sup>H NMR spectrum of digested [Zn<sub>4</sub>O(bdc-Pro')<sub>1/2</sub>(bpdc)<sub>1/2</sub>(hmtt)<sub>4/3</sub>] that had been directly synthesized from H<sub>2</sub>bdc-Pro. Additional signals in the aromatic region indicate that side reactions occur to the bdc-Pro ligand during the course of MOF synthesis.

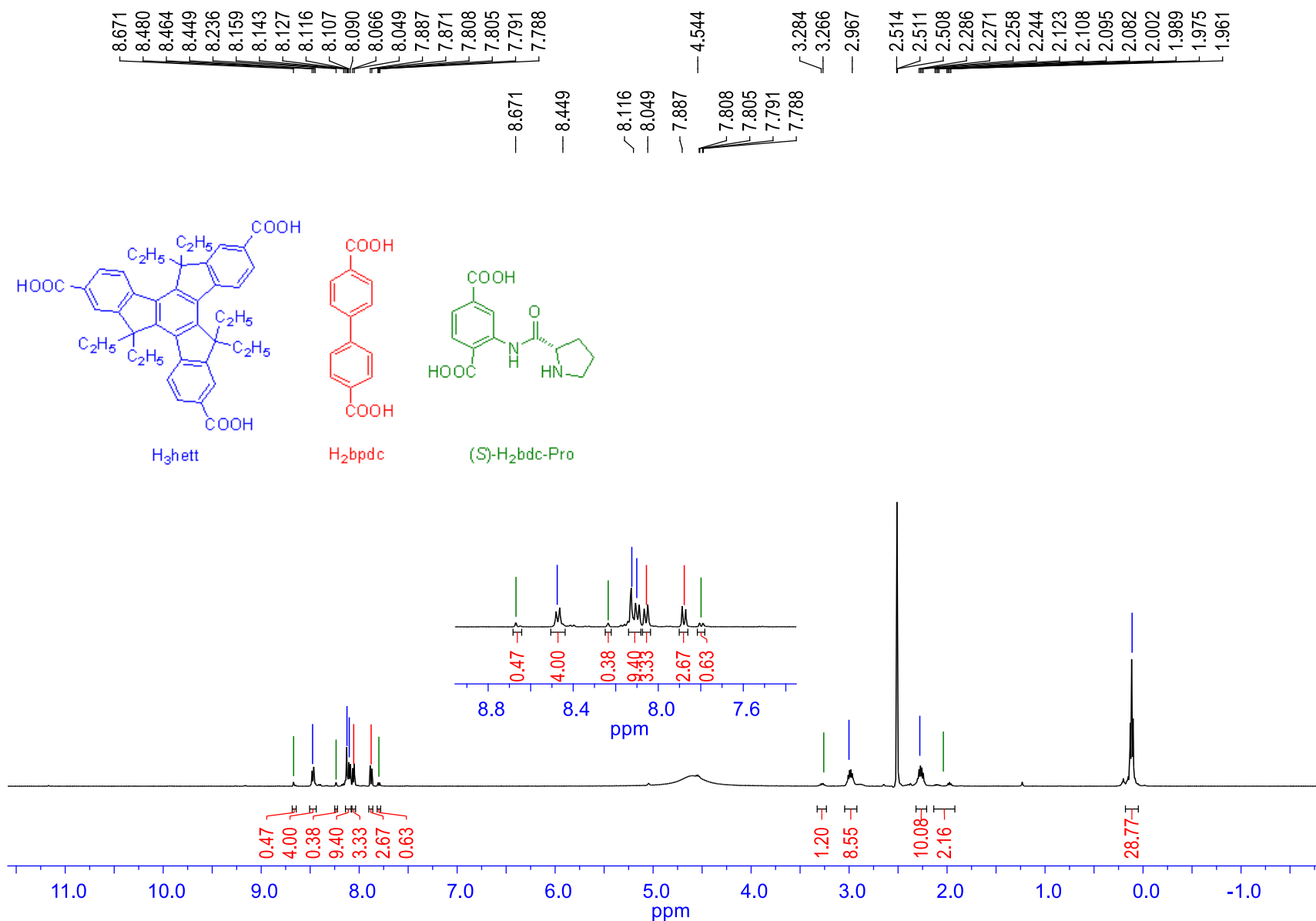


**Figure S16** <sup>1</sup>H NMR spectra of digested [Zn<sub>4</sub>O(bdc-Pro)<sub>1/2</sub>(bpdc)<sub>1/2</sub>(hett)<sub>4/3</sub>] showing integrals that match with the formula. The Boc group was completely removed after thermolysis as indicated by the complete disappearance of the Boc protons which would otherwise appear at 1.24 and 1.41 ppm.

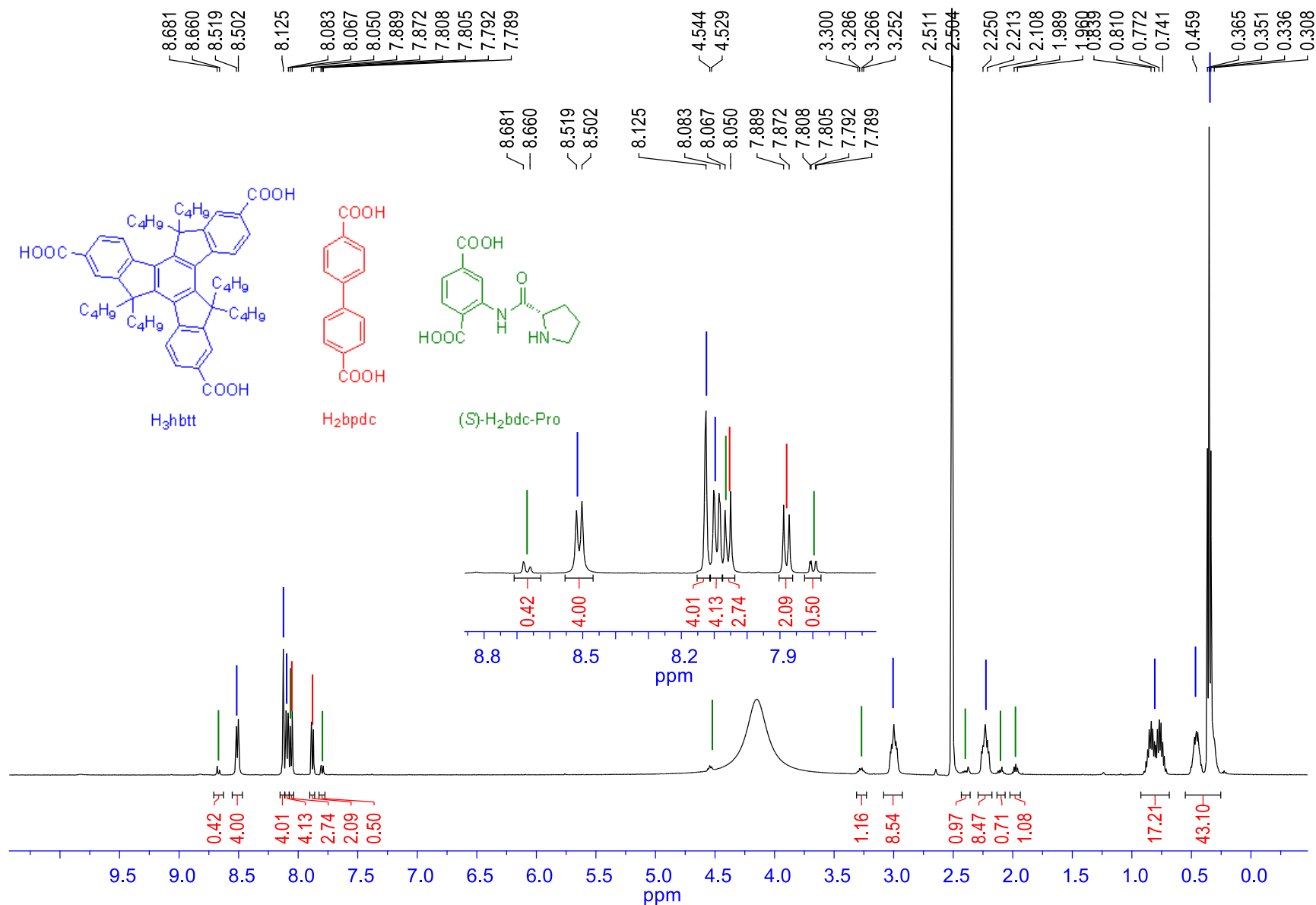


**Figure S17** <sup>1</sup>H NMR spectra of digested [Zn<sub>4</sub>O(bdc-Pro)<sub>1/2</sub>(bpdc)<sub>1/2</sub>(hbt)<sub>4/3</sub>] showing integrals that match with the formula. The Boc group was completely removed after thermolysis as indicated by the complete disappearance of the Boc protons which would otherwise appear at 1.24 and 1.41 ppm.

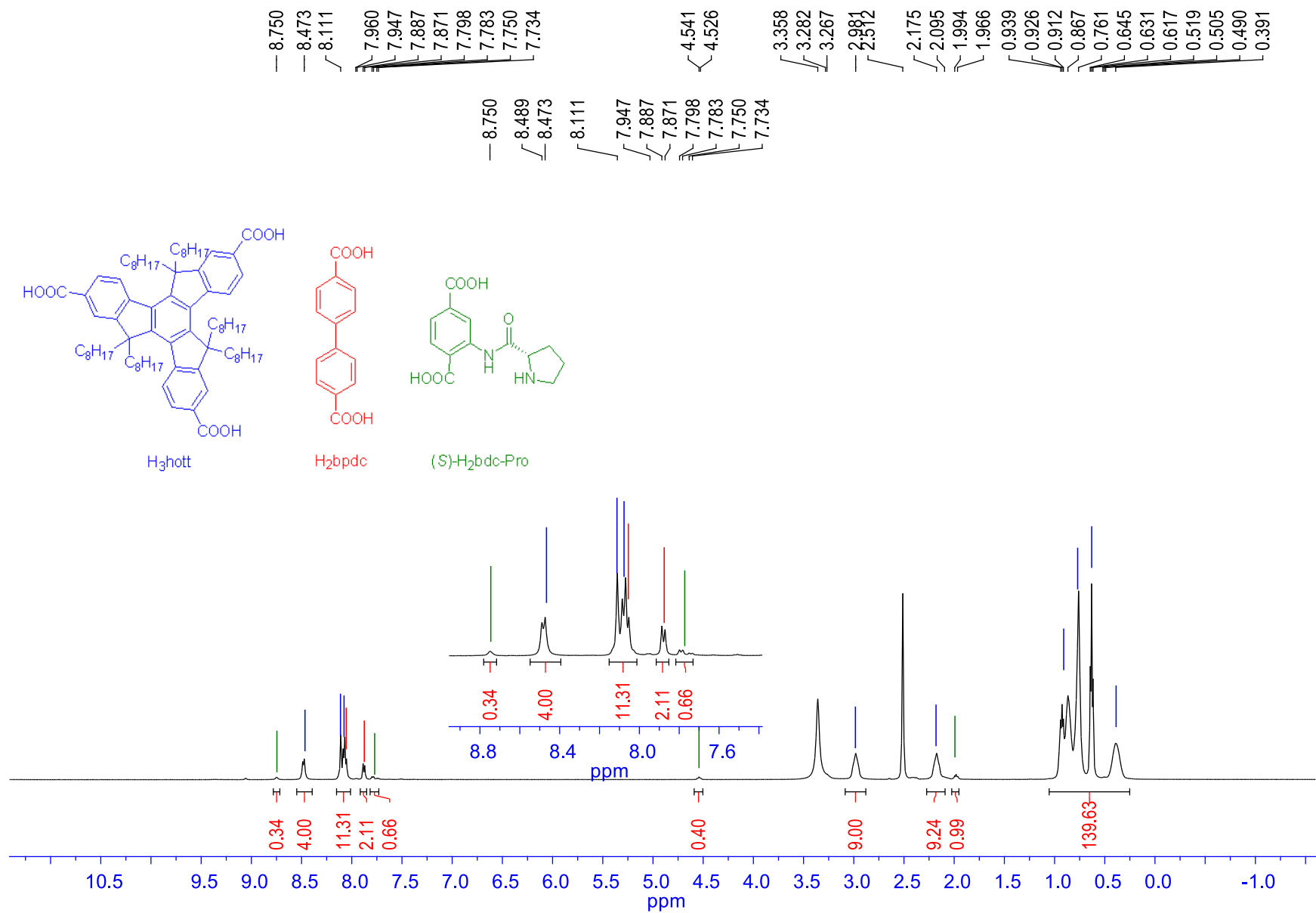


**Figure S18** <sup>1</sup>H NMR spectra of digested [Zn<sub>4</sub>O(bdc-Pro)<sub>1/2</sub>(bpdc)<sub>1/2</sub>(hott)<sub>4/3</sub>] showing integrals that match with the formula. The Boc group was completely removed after thermolysis as indicated by the complete disappearance of the Boc protons which would otherwise appear at 1.24 and 1.41 ppm.

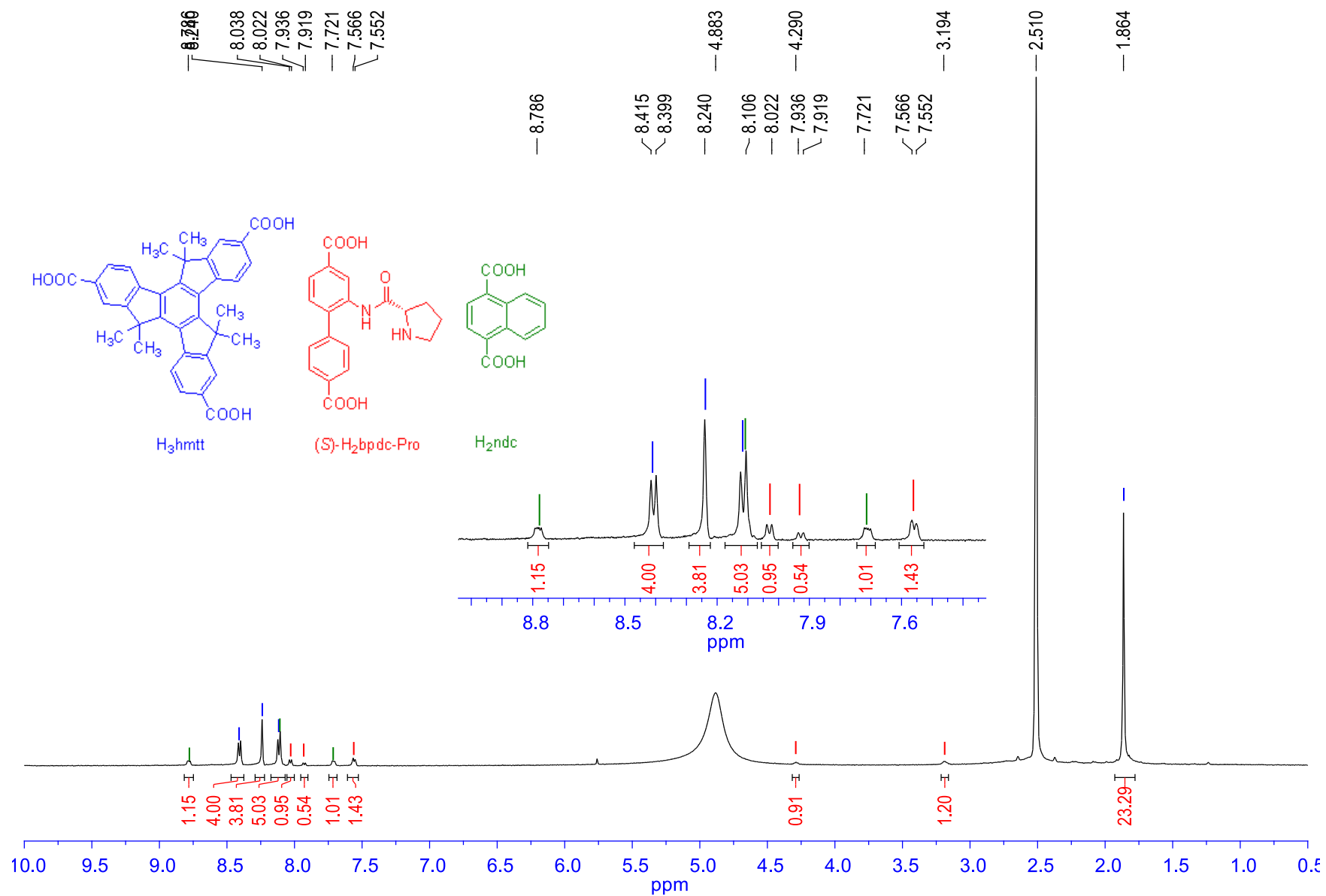


**Figure S19** <sup>1</sup>H NMR spectra of digested [Zn<sub>4</sub>O(ndc)<sub>1/2</sub>(bpdc-Pro)<sub>1/2</sub>(hmtt)<sub>4/3</sub>] showing integrals that match with the formula. The Boc group was completely removed after thermolysis as indicated by the complete disappearance of the Boc protons which would otherwise appear at 1.33 and 1.35 ppm.

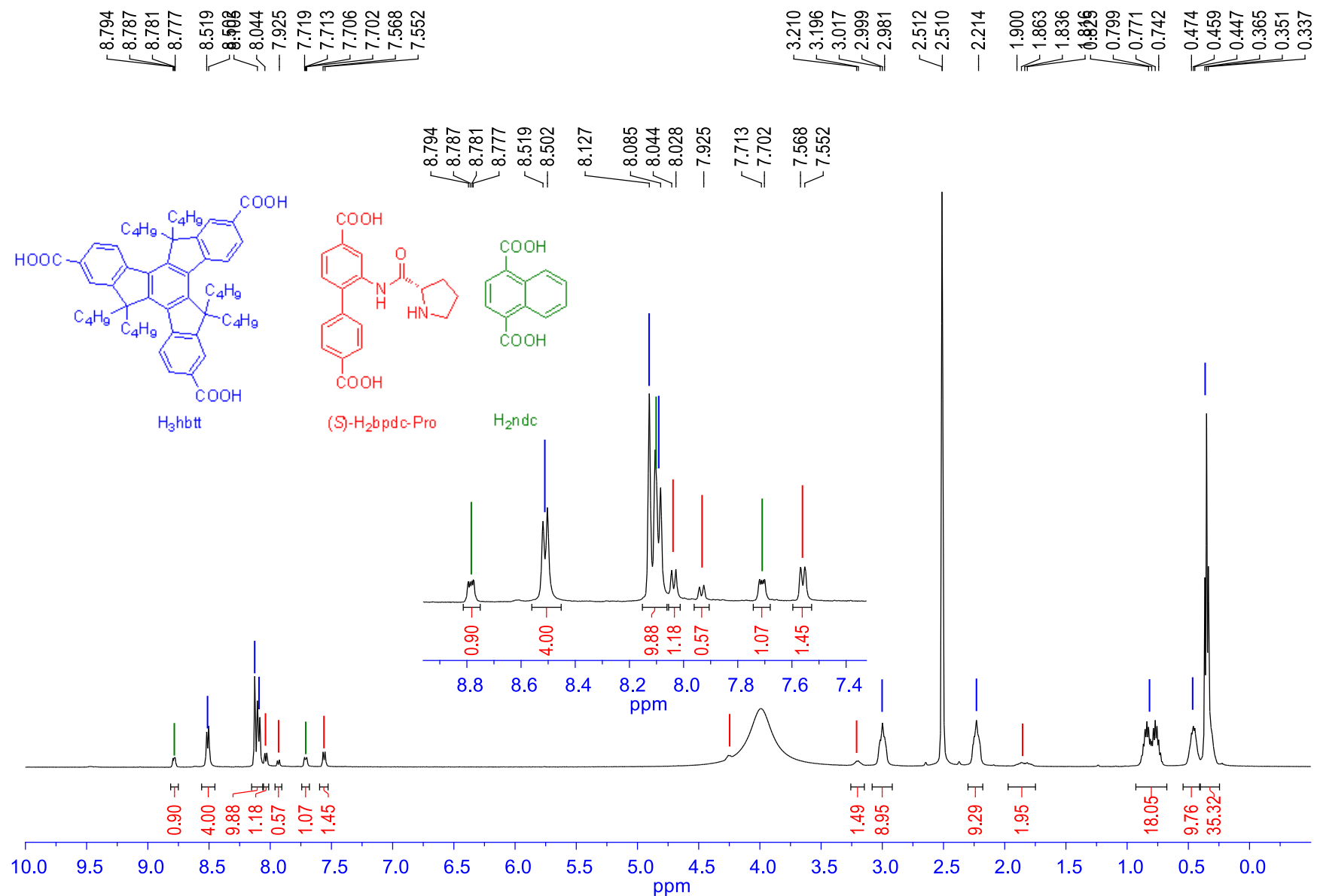


**Figure S20** <sup>1</sup>H NMR spectra of digested [Zn<sub>4</sub>O(ndc)<sub>1/2</sub>(bpdc-Pro)<sub>1/2</sub>(hbtt)<sub>4/3</sub>] showing integrals that match with the formula. The Boc group was completely removed after thermolysis as indicated by the complete disappearance of the Boc protons which would otherwise appear at 1.33 and 1.35 ppm.

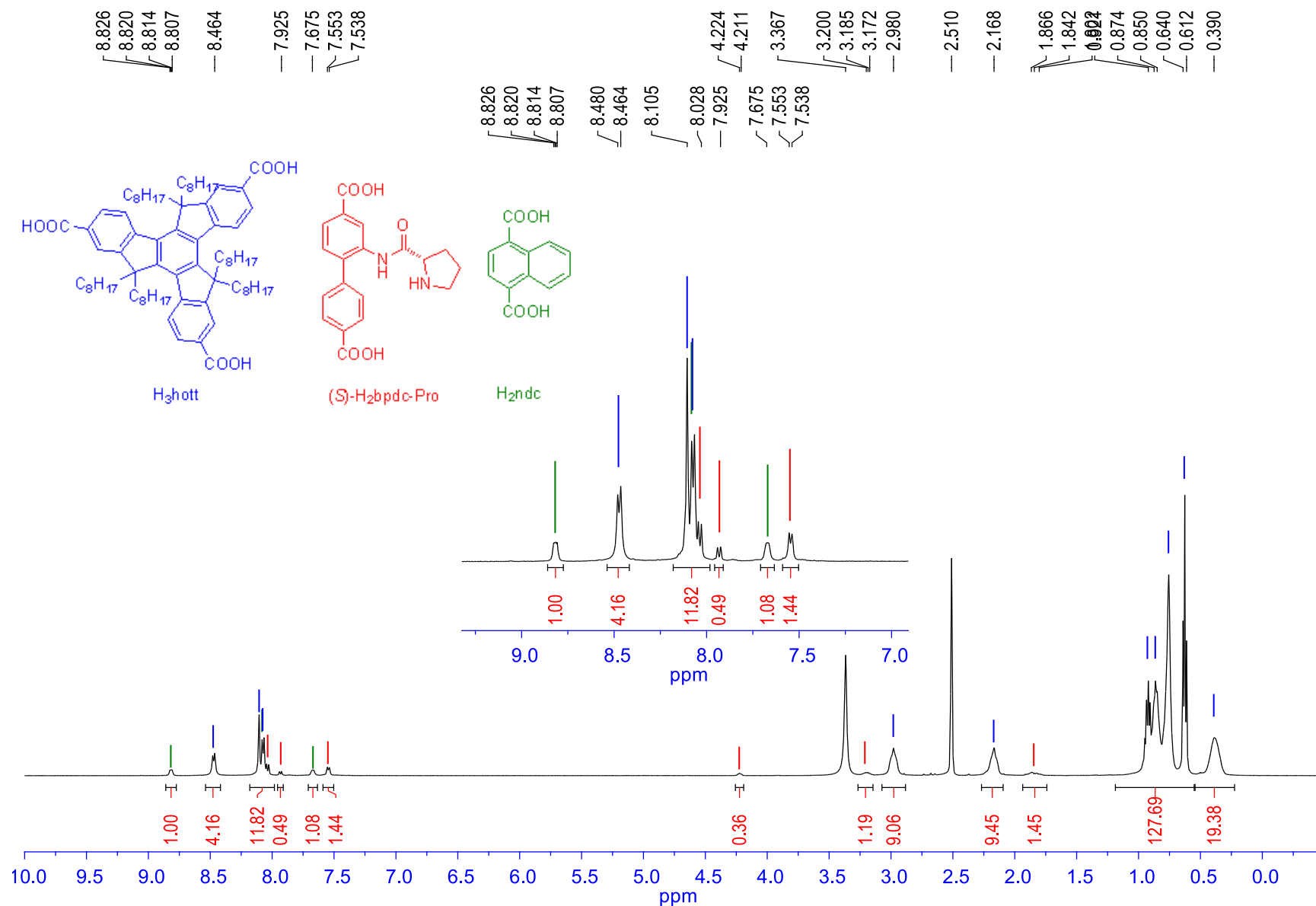


**Figure S21** <sup>1</sup>H NMR spectra of digested [Zn<sub>4</sub>O(ndc)<sub>1/2</sub>(bpdc-Pro)<sub>1/2</sub>(hott)<sub>4/3</sub>] showing integrals that match with the formula. The Boc group was completely removed after thermolysis as indicated by the complete disappearance of the Boc protons which would otherwise appear at 1.33 and 1.35 ppm.

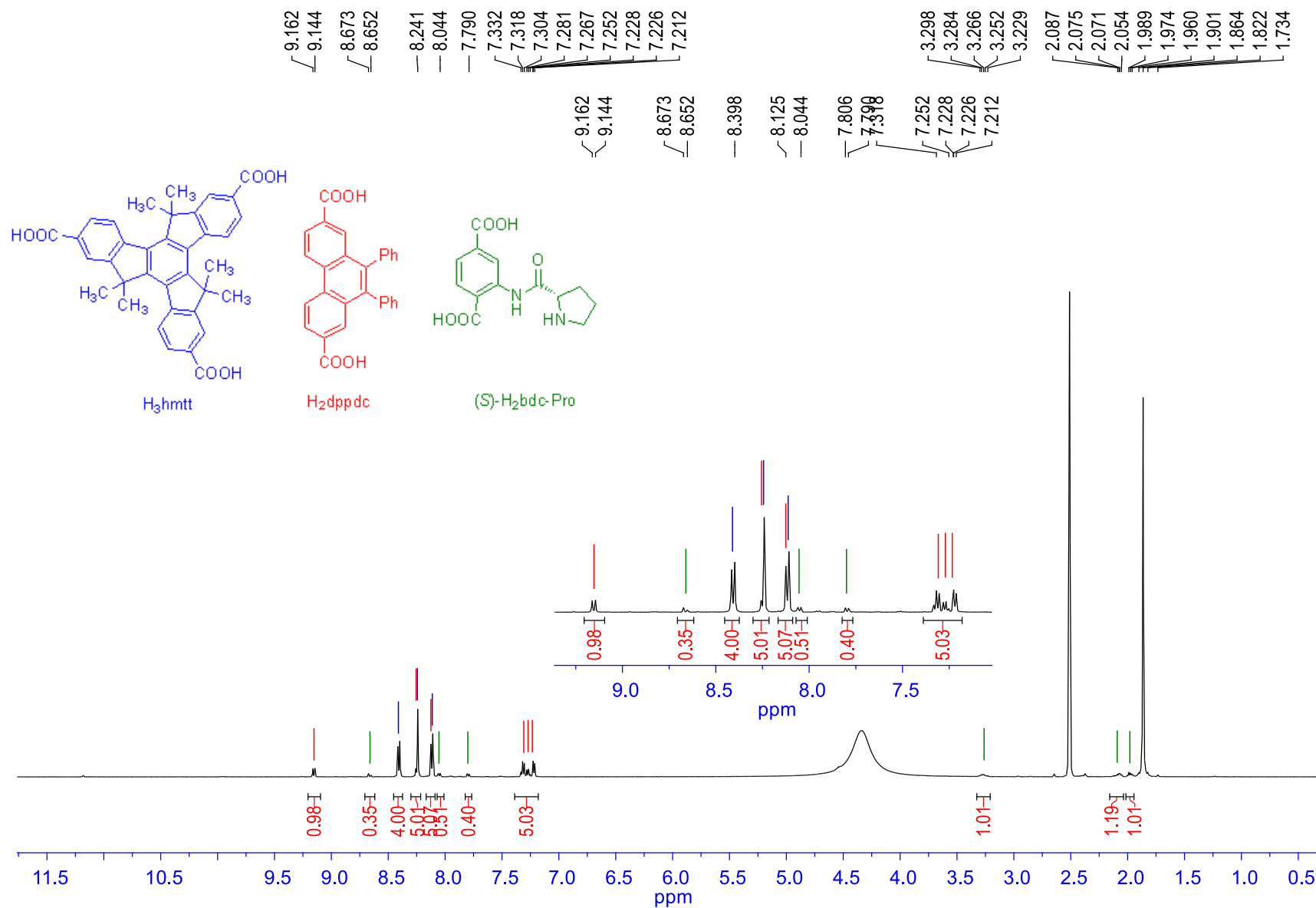


**Figure S22** <sup>1</sup>H NMR spectra of digested [Zn<sub>4</sub>O(bdc-Pro)<sub>1/2</sub>(dppdc)<sub>1/2</sub>(hmtt)<sub>4/3</sub>] showing integrals that match with the formula. The Boc group was completely removed after thermolysis as indicated by the complete disappearance of the Boc protons which would otherwise appear at 1.24 and 1.41 ppm.

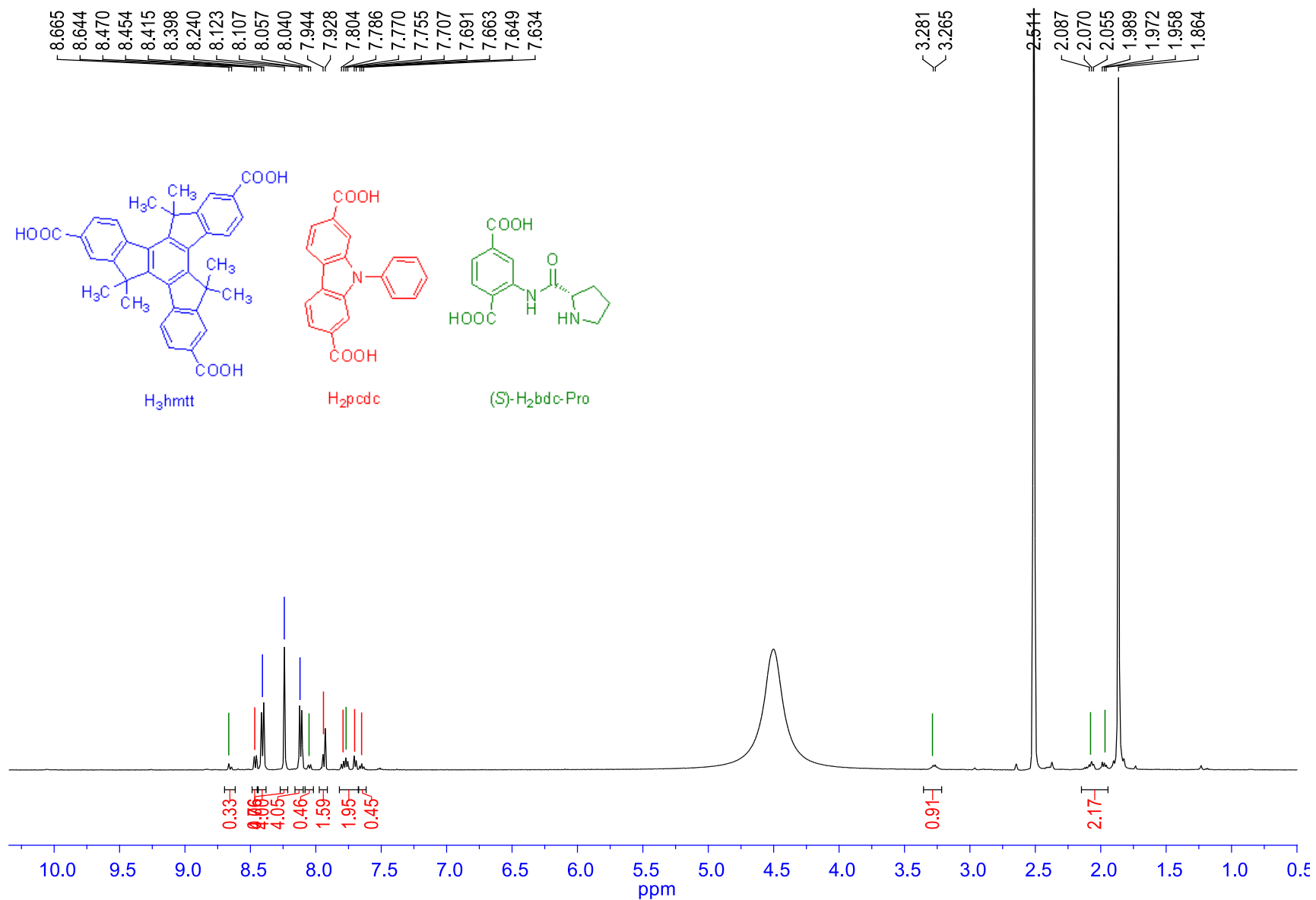


**Figure S23** <sup>1</sup>H NMR spectra of digested [Zn<sub>4</sub>O(bdc-Pro)<sub>1/2</sub>(pcdc)<sub>1/2</sub>(hmtt)<sub>4/3</sub>] showing integrals that match with the formula. The Boc group was completely removed after thermolysis as indicated by the complete disappearance of the Boc protons which would otherwise appear at 1.24 and 1.41 ppm.

## 6. Single crystal X-ray diffraction

### General

Data collections were performed on a Rigaku Spider diffractometer equipped with a MicroMax MM007 rotating anode generator ( $\text{Cu}_\alpha$  radiation), high-flux Osmic multilayer mirror optics, and a curved image-plate detector. Data were integrated and scaled and averaged with FS Process.<sup>5</sup> XPREP<sup>6</sup> was used to determine the space group and the structures were solved using direct methods under SHELXS<sup>6</sup> or SHELXT and refined with SHELXL<sup>6</sup> using OLEX 2.<sup>7</sup>

### Crystallography of MOFs

As-synthesized MOF crystals were soaked in fresh dry DMF and DMF was replenished several times within a day. The crystals were soaked overnight then the solvent was exchanged with dry dichloromethane and the dichloromethane was again replenished several times. The crystals were soaked in fresh dry dichloromethane overnight before being activated under dynamic vacuum at 80 or 200 °C for various periods of time. The vacuum oven was back filled with nitrogen to produce crystals suitable for single crystal X-ray diffraction analyses.

All zinc, oxygen and carbon atoms from the ligand backbone and SBU were found in the electron density difference maps and refined anisotropically. Ideal positions for all hydrogen atoms were calculated and refined using a riding model. The first four non-hydrogen atoms coming off the bpdc or bdc ring of (S)-bpdc-ProBoc, (S)-bpdc-Pro, and (S)-bdc-Pro were found on electron density difference maps despite their low occupancy due to the disorder of these groups over four positions due to crystallographic symmetry and additional positional disorder. To complete the models of the pyrrolidiny rings, their relative atomic coordinates were taken from single crystal x-ray structure of (S)-Me<sub>2</sub>bdc-Pro using the FRAG command in Olex 2. Fixed isotropic atomic displacement parameters (0.1) were often used to allow a sensible and stable refinement.

### Space group determination of MOFs

Single X-ray crystallography of  $[\text{Zn}_4\text{O}(\text{bpdc-ProBoc})_{1/2}(\text{bdc})_{1/2}(\text{hmtt})_{4/3}]$  shows that the framework diffracts to high Bragg angles. The best fit of the systematic absences and the  $|E^2 - 1|$  value (0.977) are given by the centrosymmetric *Pm-3* space group. This is the same space group as MUF-77-methyl. However, this space group cannot be strictly correct since it contains symmetry elements that are incompatible with the enantiopure prolinyl moiety. The chiral space group *P23* is also a viable choice. However, the refinement was still carried out in *Pm-3* for the following reasons. 1) The atoms of the pyrrolidiny ring and Boc group of the proline unit, which encompass the chiral part of the MOF, were not visible on electron density difference map. 2) The prolinyl group is disordered by crystallographic symmetry over the 2, 2', 6, and 6' positions in the same way in both space groups. 3) Refinement in *P23* resulted in unrealistic bond length values. 4) Refinement in *P23* ended up with a Flack parameter very close to 0.5, again indicating that a racemic twinned model better fits experimental data, which is unrealistic.

The *Pm-3* space group was used for all MOFs on the basis of the foregoing discussion.

### Crystallography of (*S*)-Me<sub>2</sub>bdc-ProBoc and (*R*)-Me<sub>2</sub>bdc-ProBoc

Data collections were carried out at -120 °C. All carbon, oxygen and nitrogen atoms were found in the electron density difference maps and refined anisotropically. Due to the excellent data resolution and quality, all hydrogen atoms were found in the electron density difference maps and refined isotropically. Totally refined hydrogen atoms aroused some alerts from the checkcif reports. To eliminate these alerts, only six hydrogen atoms on the two *tert*-butyl groups of (*R*)-Me<sub>2</sub>bdc-ProBoc were placed in calculated positions. Extinction corrections were used for both structures.

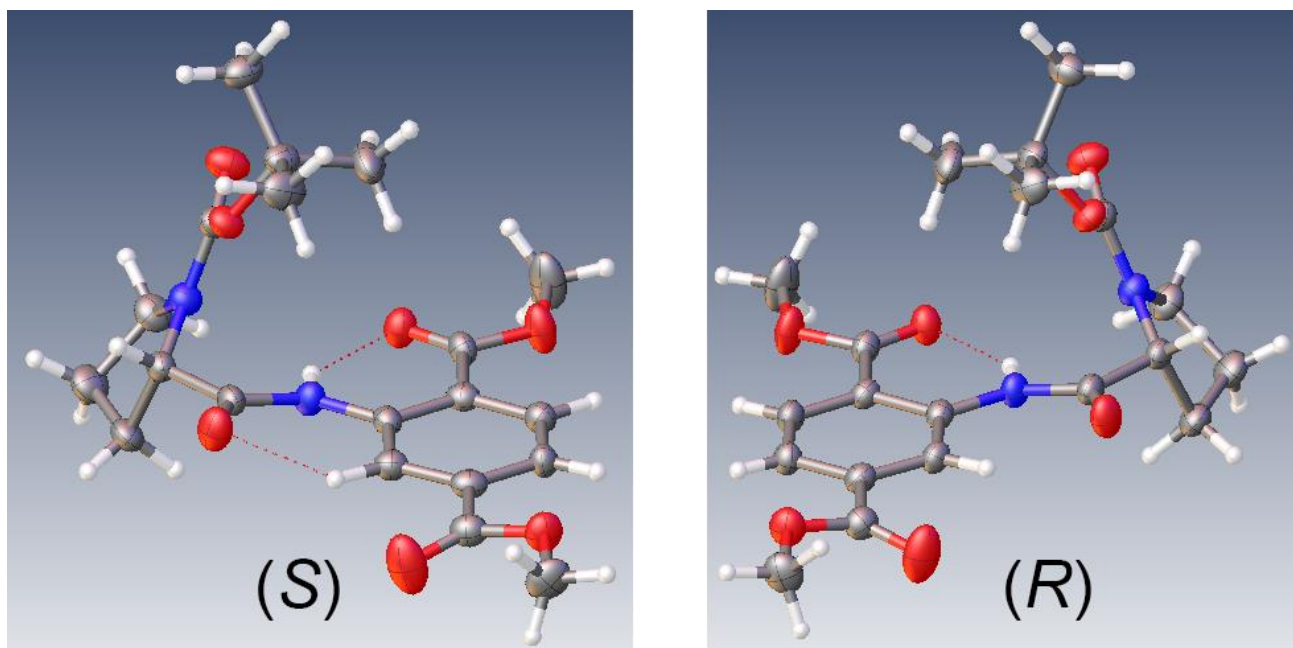


**Figure S24** ORTEP diagrams of the structures of (*S*)-Me<sub>2</sub>bdc-ProBoc and (*R*)-Me<sub>2</sub>bdc-ProBoc, as determined by single crystal X-ray diffraction, showing 50% probability of the atomic displacement ellipsoids.

Graphics were generated using Olex 2.<sup>7</sup>

**Table S1** Crystallographic data summary.

Compound	[Zn <sub>4</sub> O(bpdc-ProBoc) <sub>1/2</sub> (bdc) <sub>1/2</sub> (hmtt) <sub>4/3</sub> ]	[Zn <sub>4</sub> O(bpdc-Pro) <sub>1/2</sub> (bdc) <sub>1/2</sub> (hmtt) <sub>4/3</sub> ]	[Zn <sub>4</sub> O(bpdc) <sub>1/2</sub> (bdc-Pro) <sub>1/2</sub> (hmtt) <sub>4/3</sub> ]	( <i>R</i> )-Me <sub>2</sub> bdc-ProBoc	( <i>S</i> )-Me <sub>2</sub> bdc-ProBoc
CCDC deposition number	1529606	1523841	1523842	1529507	1529508
Formula	C <sub>64</sub> H <sub>50</sub> NO <sub>14.5</sub> Zn <sub>4</sub>	C <sub>61.5</sub> H <sub>46</sub> NO <sub>13.5</sub> Zn <sub>4</sub>	C <sub>61.5</sub> H <sub>46</sub> NO <sub>13.5</sub> Zn <sub>4</sub>	C <sub>20</sub> H <sub>26</sub> N <sub>2</sub> O <sub>7</sub>	C <sub>20</sub> H <sub>26</sub> N <sub>2</sub> O <sub>7</sub>
Formula weight	1326.53	1276.47	1276.47	406.43	406.43
Crystal size (mm)	0.80 × 0.80 × 0.74	0.73 × 0.65 × 0.62	0.60 × 0.55 × 0.50	0.59 × 0.43 × 0.36	1.31 × 1.16 × 0.43
Temperature (K)	290(2)	291(2)	293(2)	153(2)	153(2)
Wavelength (Å)	1.54178	1.54178	1.54178	1.54178	1.54178
Crystal system	cubic	cubic	cubic	orthorhombic	orthorhombic
Space group	<i>Pm</i> -3	<i>Pm</i> -3	<i>Pm</i> -3	<i>C</i> 222 <sub>1</sub>	<i>C</i> 222 <sub>1</sub>
Unit cell length (Å)	29.9444(6)	29.9461(3)	29.9603(3)	a = 12.0860(2) b = 15.1870(3) c = 22.6210(16)	a = 12.1049(3) b = 15.1987(3) c = 22.6397(16)
Unit cell volume (Å <sup>3</sup> )	26850.2(16)	26854.7(8)	26892.9(8)	4152.1(3)	4165.2(3)
Z	6	6	6	8	8
D <sub>calc</sub> (g cm <sup>-3</sup> )	0.492	0.474	0.473	1.300	1.296
μ (mm <sup>-1</sup> )	0.794	0.782	0.781	0.826	0.824
F(000)	4062	3900	3900	1728	1728
Reflns coll./unique, R <sub>int</sub>	103365 / 9316, 0.052	103850 / 9315, 0.031	60444 / 9235, 0.018	20026 / 4011, 0.0347	16530 / 3980, 0.0428
Data range	6.6° < θ < 72° or 6.7 Å > d > 0.81 Å	6.6° < θ < 72° or 6.7 Å > d > 0.81 Å	6.6° < θ < 72° or 6.7 Å > d > 0.81 Å	7.0° < θ < 72° or 6.3 Å > d > 0.81 Å	7.0° < θ < 72° or 6.3 Å > d > 0.81 Å
Completeness	99.7%	99.7%	99.6%	99.7%	99.6%
T <sub>min</sub> , T <sub>max</sub>	0.39, 1.00	0.76, 1.00	0.73, 1.00	0.81, 1.00	0.75, 1.00
R indices for data with I > 2σ(I)	R <sub>1</sub> = 0.0681 wR <sub>2</sub> = 0.1865	R <sub>1</sub> = 0.0372 wR <sub>2</sub> = 0.1034	R <sub>1</sub> = 0.0364 wR <sub>2</sub> = 0.1615	R <sub>1</sub> = 0.0296; wR <sub>2</sub> = 0.0699	R <sub>1</sub> = 0.0307; wR <sub>2</sub> = 0.0714
R indices for all data	R <sub>1</sub> = 0.0795 wR <sub>2</sub> = 0.1945	R <sub>1</sub> = 0.0414 wR <sub>2</sub> = 0.1170	R <sub>1</sub> = 0.0395 wR <sub>2</sub> = 0.1649	R <sub>1</sub> = 0.0342; wR <sub>2</sub> = 0.0741	R <sub>1</sub> = 0.0360; wR <sub>2</sub> = 0.0849
Largest difference peak and hole (e Å <sup>-3</sup> )	0.48 / -0.71	0.24 / -0.47	0.29 / -0.47	0.18 / -0.14	0.17 / -0.19

## 7. Powder X-ray diffraction

All powder X-ray diffraction experiments were carried out on a Rigaku Spider X-ray diffractometer with Cu K $\alpha$  radiation (Rigaku MM007 microfocus rotating-anode generator), monochromated and focused with high-flux Osmic multilayer mirror optics, and a curved image plate detector. The data were obtained from desolvated MOF samples that were ground then fixed to a mount with a minimum amount of Fomblin oil. A very broad scattering peak due to this oil is sometimes observed between  $2\theta = 7^\circ$  and  $2\theta 20^\circ$ . The two-dimensional images of the Debye rings were integrated with 2DP<sup>8</sup> to give  $2\theta$  vs I diffractograms. The predicted powder patterns of the MOFs were generated from their single-crystal structures using Mercury.

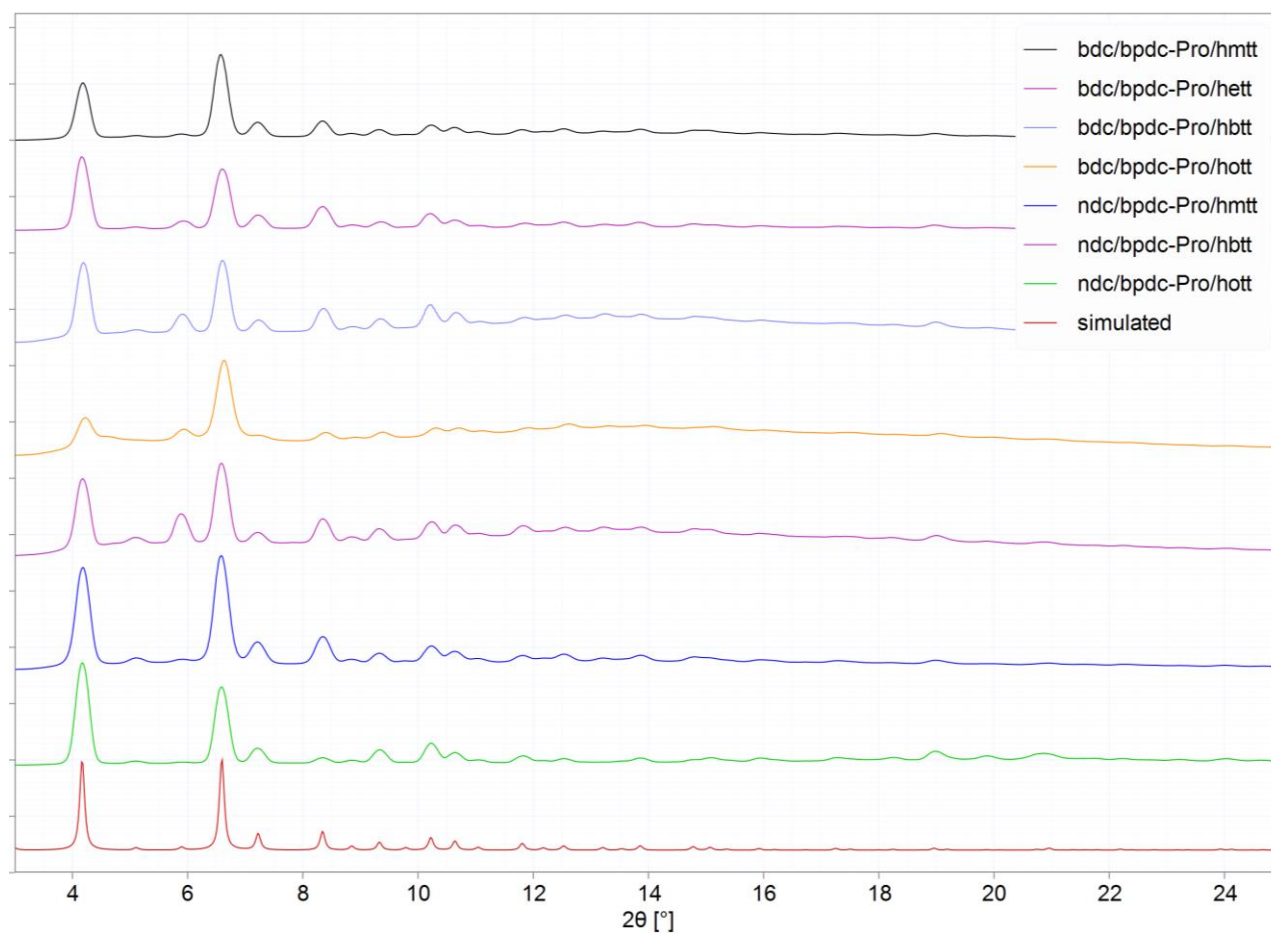


**Figure S25** Powder XRD patterns of all the MOF catalysts that contain bpdC-Pro (From top to bottom:  $[\text{Zn}_4\text{O}(\text{bdc})_{1/2}(\text{bpdC-Pro})_{1/2}(\text{hmtt})_{4/3}]$ ,  $[\text{Zn}_4\text{O}(\text{bdc})_{1/2}(\text{bpdC-Pro})_{1/2}(\text{hett})_{4/3}]$ ,  $[\text{Zn}_4\text{O}(\text{bdc})_{1/2}(\text{bpdC-Pro})_{1/2}(\text{hbtt})_{4/3}]$ ,  $[\text{Zn}_4\text{O}(\text{bdc})_{1/2}(\text{bpdC-Pro})_{1/2}(\text{hott})_{4/3}]$ ,  $[\text{Zn}_4\text{O}(\text{ndc})_{1/2}(\text{bpdC-Pro})_{1/2}(\text{hmtt})_{4/3}]$ ,  $[\text{Zn}_4\text{O}(\text{ndc})_{1/2}(\text{bpdC-Pro})_{1/2}(\text{hbtt})_{4/3}]$ ,  $[\text{Zn}_4\text{O}(\text{ndc})_{1/2}(\text{bpdC-Pro})_{1/2}(\text{hott})_{4/3}]$  and simulated generic powder XRD pattern for MUF-77).

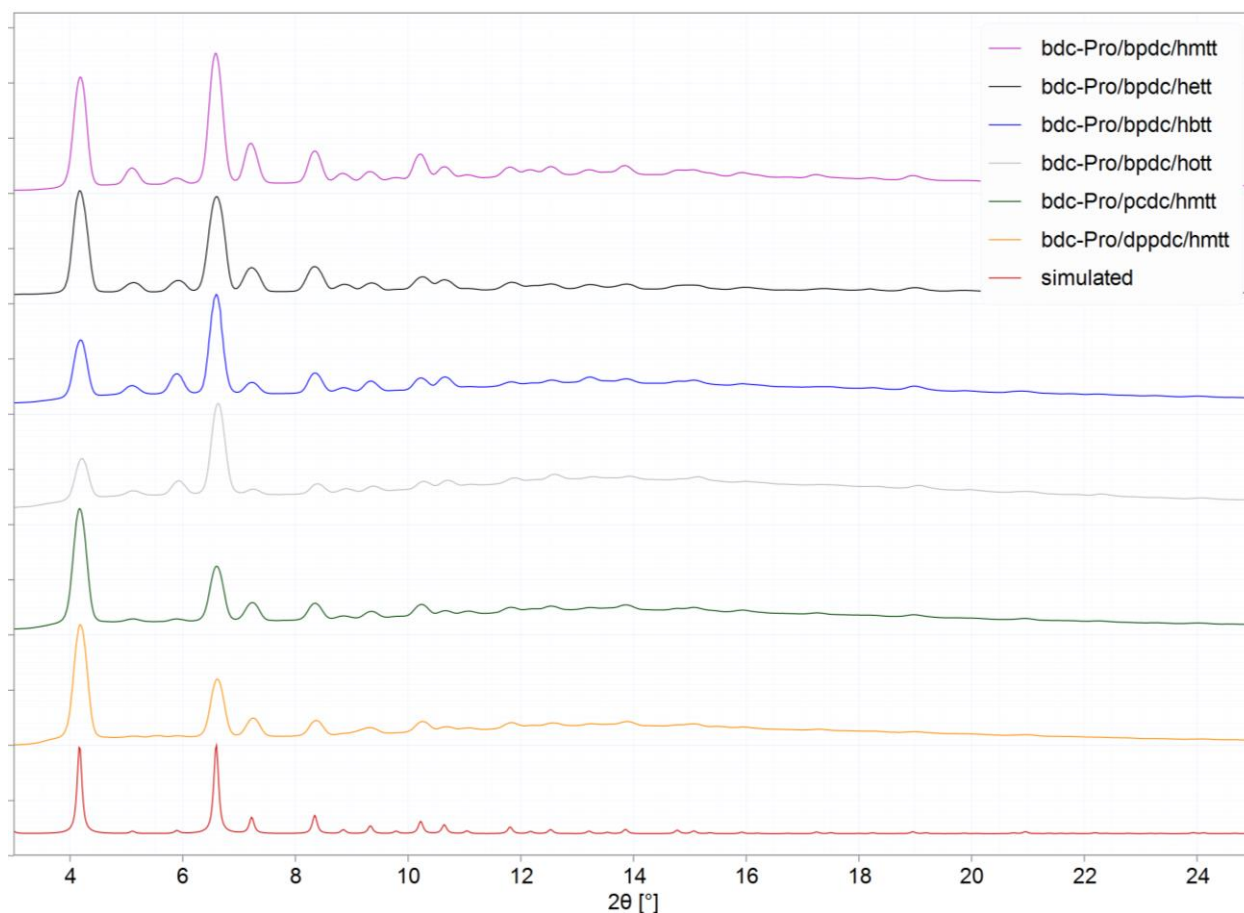


**Figure S26** Powder XRD patterns of all the MOF catalysts that contain bdc-Pro (From top to bottom:  $[\text{Zn}_4\text{O}(\text{bdc-Pro})_{1/2}(\text{bpdc})_{1/2}(\text{hmtt})_{4/3}]$ ,  $[\text{Zn}_4\text{O}(\text{bdc-Pro})_{1/2}(\text{bpdc})_{1/2}(\text{hett})_{4/3}]$ ,  $[\text{Zn}_4\text{O}(\text{bdc-Pro})_{1/2}(\text{bpdc})_{1/2}(\text{hbtt})_{4/3}]$ ,  $[\text{Zn}_4\text{O}(\text{bdc-Pro})_{1/2}(\text{bpdc})_{1/2}(\text{hott})_{4/3}]$ ,  $[\text{Zn}_4\text{O}(\text{bdc-Pro})_{1/2}(\text{pcdc})_{1/2}(\text{hmtt})_{4/3}]$ ,  $[\text{Zn}_4\text{O}(\text{bdc-Pro})_{1/2}(\text{dppdc})_{1/2}(\text{hmtt})_{4/3}]$  and simulated generic powder XRD pattern for MUF-77.)

## 8. Gas adsorption experiments and calculations

$\text{N}_2$  adsorption isotherms were measured by a volumetric method using a Quantachrome Autosorb iQ2 instrument with ultra-high purity gases. Freshly prepared, Boc-protected MOF samples were washed with DMF then activated by soaking in dry  $\text{CH}_2\text{Cl}_2$  for several days then transferred to a pre-dried and weighed analysis tube. Excess  $\text{CH}_2\text{Cl}_2$  was removed under vacuum and the tube back filled with argon before being heated at  $1^\circ\text{C}$  per minute to  $80^\circ\text{C}$  under vacuum. The sample was then held under a dynamic vacuum at  $10^{-6}$  Torr for 10 hours. Accurate sample masses were calculated using degassed samples after sample tubes were backfilled with nitrogen. After measuring their  $\text{N}_2$  adsorption isotherms, these Boc-protected MOF samples were subsequently heated in their original analysis tubes to  $200^\circ\text{C}$  with a heating rate of  $20^\circ\text{C}/\text{min}$  and holding the temperature at  $200^\circ\text{C}$  for 20 hours under a dynamic vacuum. This procedure completely thermolyzed the Boc protecting groups to generate MOF catalysts.  $\text{N}_2$  adsorption isotherms for these MOF catalysts were subsequently measured and accurate sample masses were determined using the same method.

BET surface areas were calculated from N<sub>2</sub> adsorption isotherms at 77 K according to the following procedures:<sup>9</sup>

1) The isotherm region where  $v(1 - P/P_0)$  increases versus  $P/P_0$ , where  $v$  is the amount of N<sub>2</sub> adsorbed, was identified.

2) Within this isotherm region, sequential data points that led to a positive intercept in the plot of  $\frac{P/P_0}{v(1-P/P_0)}$  against  $P/P_0$ , were found. This plot yields a slope  $a$ , and a positive intercept  $b$ . The amount of gas molecules adsorbed in the initial monolayer is  $v_m = \frac{1}{a+b}$ .

3) The BET surface area was calculated according to the following equation:

$$A_{BET} = v_m(\text{cm}^3 \text{g}^{-1}) * \frac{1(\text{mol})}{22400(\text{cm}^3)} * \sigma_0(\text{\AA}^2) * N_A(\text{mol}^{-1}) * 10^{-20} \left(\frac{\text{m}^2}{\text{\AA}^2}\right)$$

Where  $N_A$  is Avogadro's constant, and  $\sigma_0$  is the cross-sectional area of a N<sub>2</sub> molecule, which is 16.2 Å<sup>2</sup>.

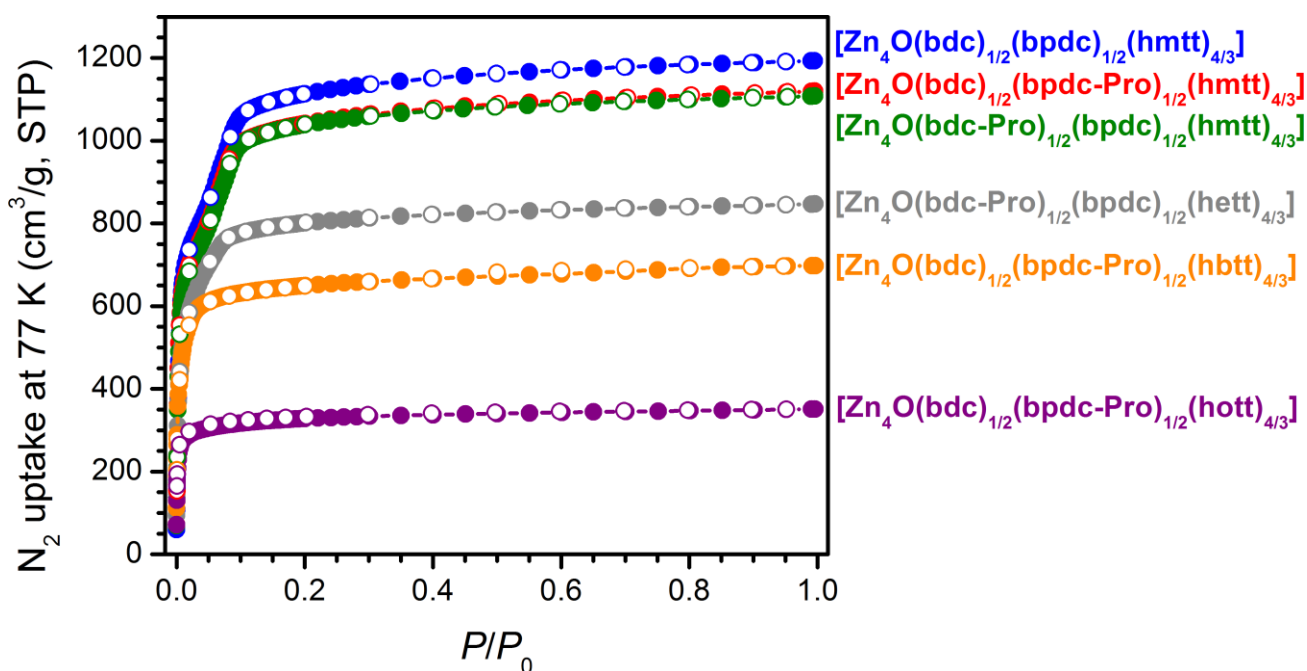


**Figure S27** Gas adsorption (filled circles) and desorption (open circles) isotherms of MOF catalysts (red, green, grey, orange and purple) compared with MUF-77, [Zn<sub>4</sub>O(bdc)<sub>1/2</sub>(bpdc)<sub>1/2</sub>(hmtt)<sub>4/3</sub>] (blue).

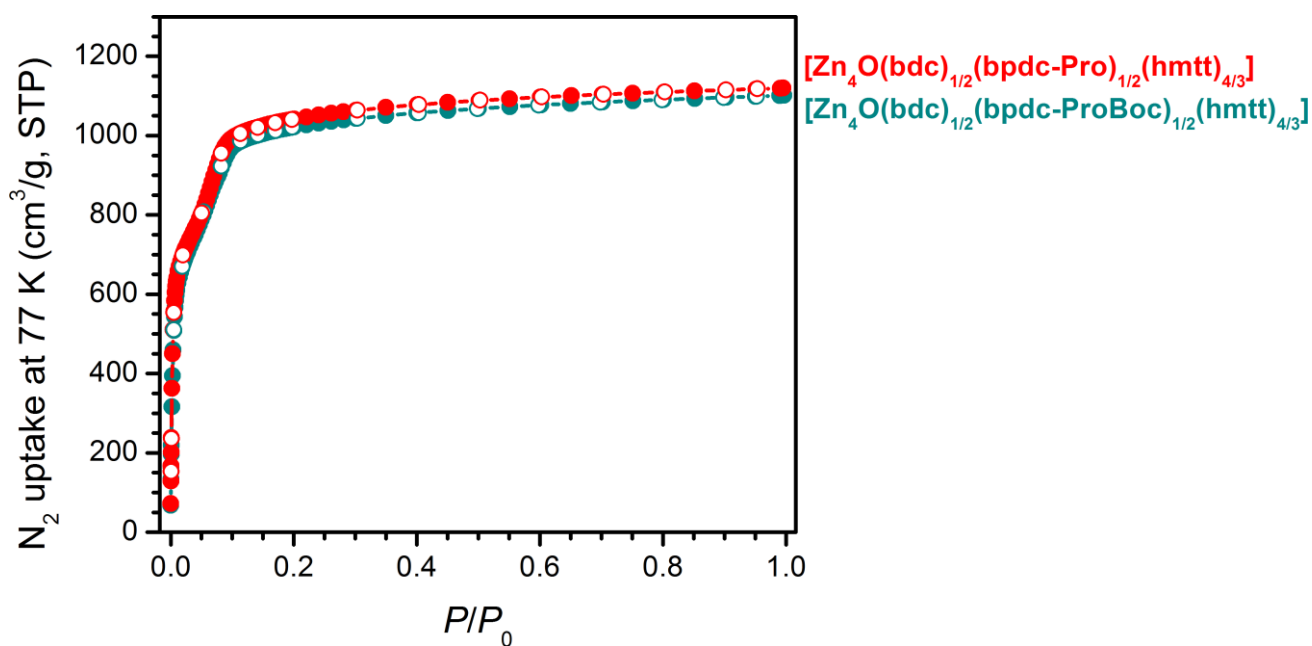


**Figure S28** Gas adsorption (filled circles) and desorption (open circles) isotherms of  $[\text{Zn}_4\text{O}(\text{bdc})_{1/2}(\text{bpdc-Pro})_{1/2}(\text{hmtt})_{4/3}]$  (red) and  $[\text{Zn}_4\text{O}(\text{bdc})_{1/2}(\text{bpdc-ProBoc})_{1/2}(\text{hmtt})_{4/3}]$  (dark cyan). As expected, the  $\text{N}_2$  uptake increases slightly after the thermolysis of Boc protecting group, consistent with retention of crystallinity and accessible pore volume.

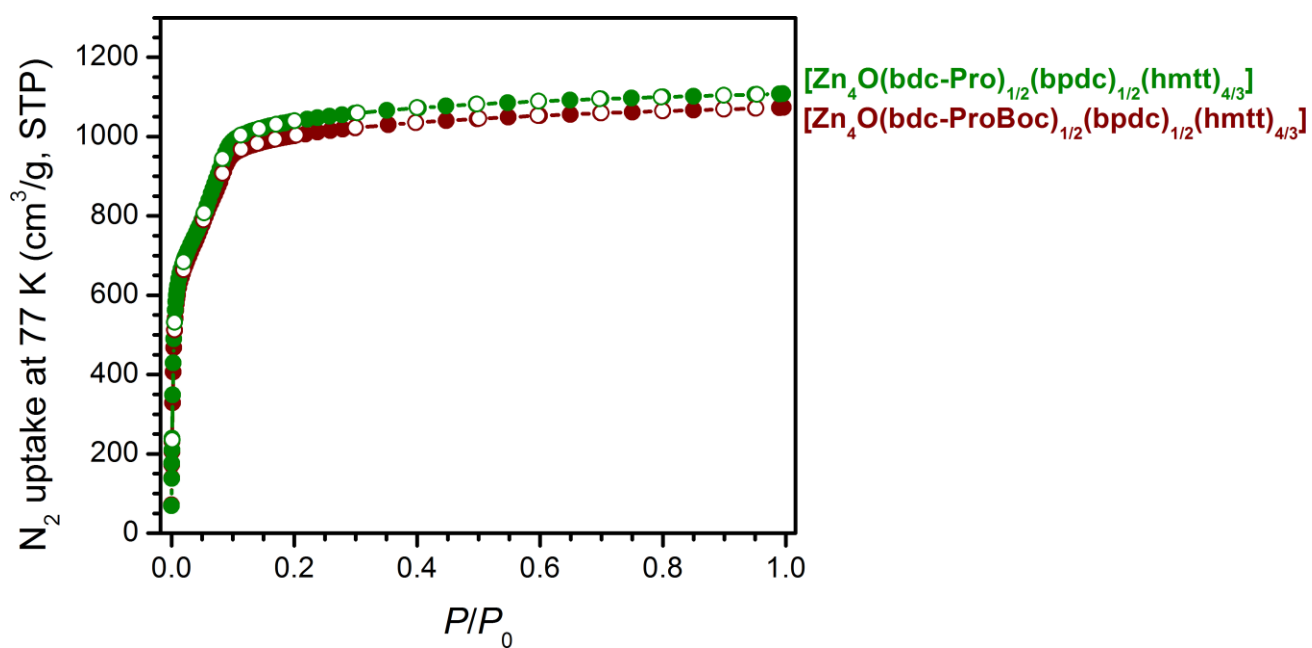


**Figure S29** Gas adsorption (filled circles) and desorption (open circles) isotherms of  $[\text{Zn}_4\text{O}(\text{bdc-Pro})_{1/2}(\text{bpdc})_{1/2}(\text{hmtt})_{4/3}]$  (green) and  $[\text{Zn}_4\text{O}(\text{bdc-ProBoc})_{1/2}(\text{bpdc})_{1/2}(\text{hmtt})_{4/3}]$  (dark red). As expected, the  $\text{N}_2$  uptake increases slightly after the thermolysis of Boc protecting group, consistent with retention of crystallinity and accessible pore volume.

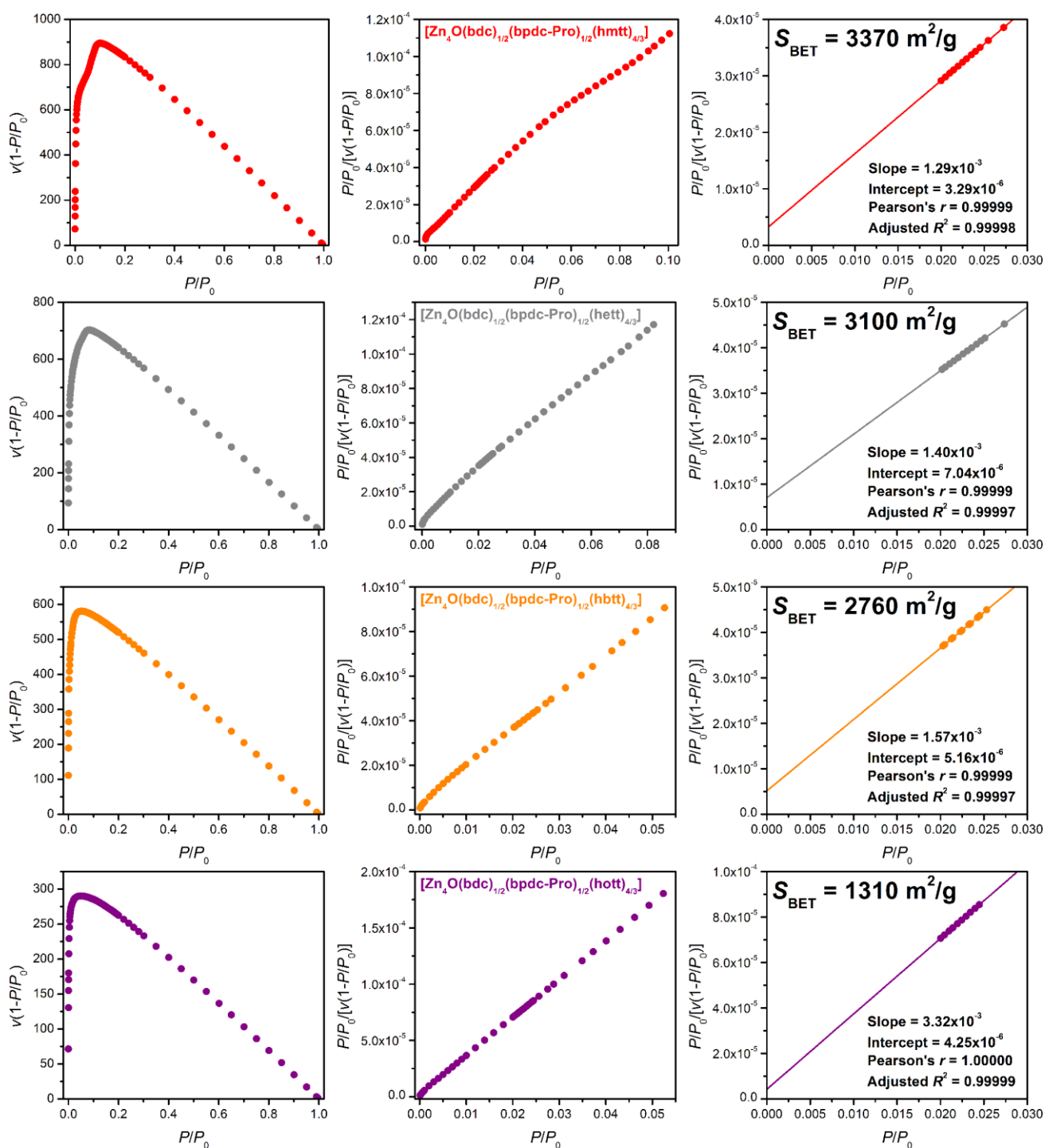


**Figure S30** BET surface area plots for  $[Zn_4O(bdc)_{1/2}(bpdc-Pro)_{1/2}(hmtt)_{4/3}]$  (red),  $[Zn_4O(bdc)_{1/2}(bpdc-Pro)_{1/2}(hett)_{4/3}]$  (grey),  $[Zn_4O(bdc)_{1/2}(bpdc-Pro)_{1/2}(hbtt)_{4/3}]$  (orange) and  $[Zn_4O(bdc)_{1/2}(bpdc-Pro)_{1/2}(hott)_{4/3}]$  (purple).

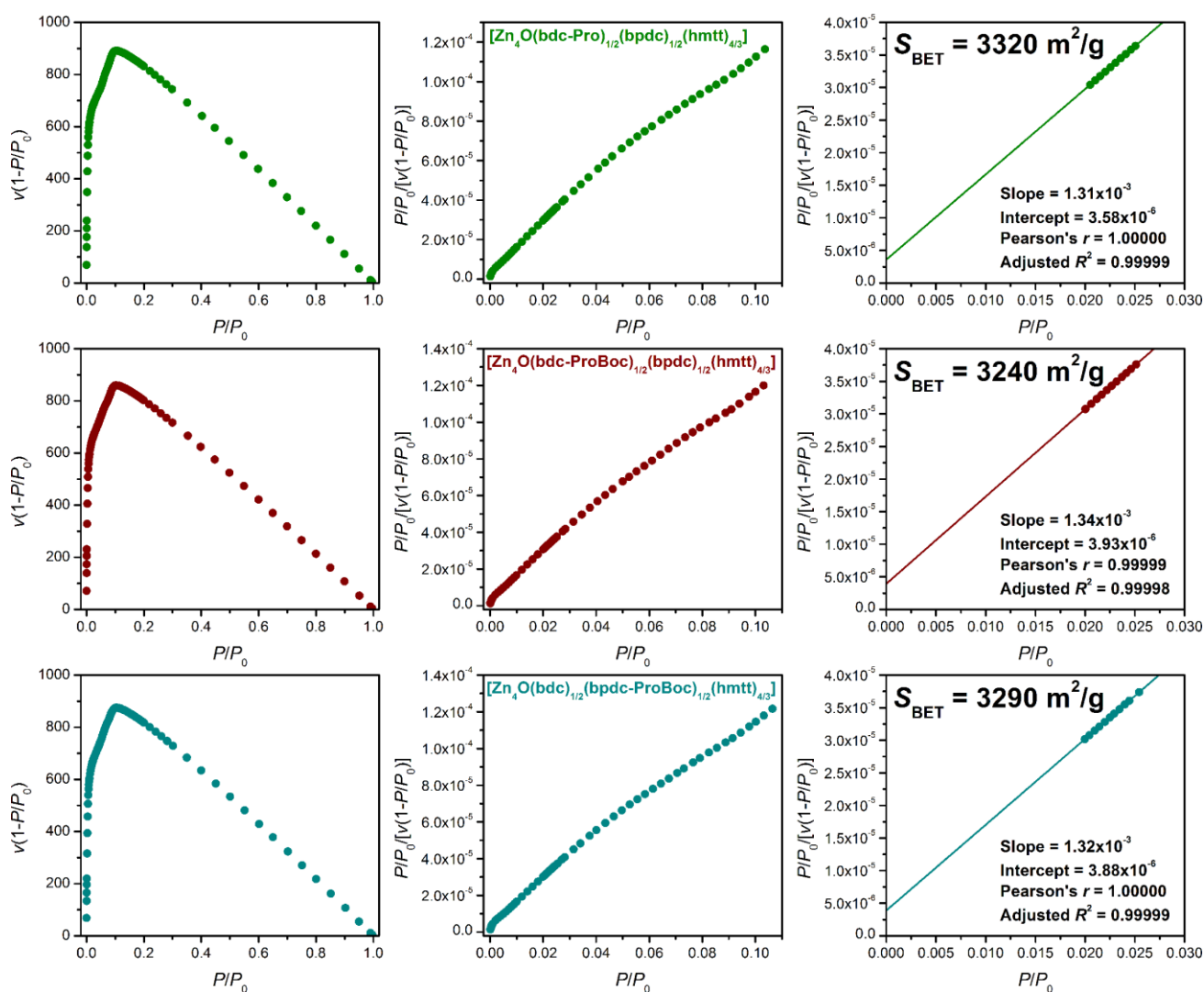


**Figure S31** BET surface area plots for  $[\text{Zn}_4\text{O}(\text{bdc-Pro})_{1/2}(\text{bpdc})_{1/2}(\text{hmtt})_{4/3}]$  (green)  $[\text{Zn}_4\text{O}(\text{bdc-ProBoc})_{1/2}(\text{bpdc})_{1/2}(\text{hmtt})_{4/3}]$  (dark red) and  $[\text{Zn}_4\text{O}(\text{bdc})_{1/2}(\text{bpdc-ProBoc})_{1/2}(\text{hmtt})_{4/3}]$  (dark cyan).

**Table S2.**  $\text{N}_2$  uptakes at saturation ( $P/P_0 = 0.995$ ), pore volumes and BET surface areas of Boc-protected MOFs and MOF catalysts as determined from  $\text{N}_2$  adsorption isotherms measured at 77K.

MOF	$\text{N}_2$ uptake at saturation ( $\text{cm}^3/\text{g}$ , STP)	Total pore volume ( $\text{cm}^3/\text{g}$ )	BET surface area ( $\text{m}^2/\text{g}$ )
$[\text{Zn}_4\text{O}(\text{bdc-ProBoc})_{1/2}(\text{bpdc})_{1/2}(\text{hmtt})_{4/3}]$	1073	1.66	3240
$[\text{Zn}_4\text{O}(\text{bdc-Pro})_{1/2}(\text{bpdc})_{1/2}(\text{hmtt})_{4/3}]$	1108	1.71	3320
$[\text{Zn}_4\text{O}(\text{bdc})_{1/2}(\text{bpdc-ProBoc})_{1/2}(\text{hmtt})_{4/3}]$	1101	1.70	3290
$[\text{Zn}_4\text{O}(\text{bdc})_{1/2}(\text{bpdc-Pro})_{1/2}(\text{hmtt})_{4/3}]$	1120	1.73	3370
$[\text{Zn}_4\text{O}(\text{bdc})_{1/2}(\text{bpdc-Pro})_{1/2}(\text{hett})_{4/3}]$	847	1.31	3100
$[\text{Zn}_4\text{O}(\text{bdc})_{1/2}(\text{bpdc-Pro})_{1/2}(\text{hbtt})_{4/3}]$	698	1.08	2760
$[\text{Zn}_4\text{O}(\text{bdc})_{1/2}(\text{bpdc-Pro})_{1/2}(\text{hott})_{4/3}]$	351	0.54	1310

### Calculated gas adsorption isotherms

Nitrogen adsorption isotherms for  $[\text{Zn}_4\text{O}(\text{bdc})_{1/2}(\text{bpdc})_{1/2}(\text{hmtt})_{4/3}]$  (MUF-77-methyl),<sup>2</sup>  $[\text{Zn}_4\text{O}(\text{bdc})_{1/2}(\text{bpdc-Pro})_{1/2}(\text{hmtt})_{4/3}]$  and  $[\text{Zn}_4\text{O}(\text{bdc-Pro})_{1/2}(\text{bpdc})_{1/2}(\text{hmtt})_{4/3}]$  were simulated using Grand Canonical Monte Carlo method with RASPA software.<sup>10</sup> Atomic coordinates were taken from the X-ray crystal structures. Disordered proline functional groups were included in just one possible orientation (where applicable).

At each pressure point the simulation involved 5000 cycles of equilibration period to ensure thermodynamic equilibrium is reached. Then another 5000 cycles of production run was performed to obtain a statistical average of  $\text{N}_2$  loading. Here, a cycle consists of  $n$  Monte Carlo steps; where  $n$  is equal to the number of nitrogen molecules (which fluctuates during a GCMC simulation). All simulations included random insertion, deletion, translation and rotation moves of  $\text{N}_2$  molecules with equal probabilities. All MOF atoms were held fixed during the simulation with their atomic coordinates taken directly from single-crystal structures. Interactions between non-bonded atoms were computed through the Lennard-Jones (LJ) potential:

$$V_{ij} = 4\varepsilon_{ij} \left[ \left( \frac{\sigma_{ij}}{r_{ij}} \right)^{12} - \left( \frac{\sigma_{ij}}{r_{ij}} \right)^6 \right]$$

where  $i$  and  $j$  are interacting atoms, and  $r_{ij}$  is the distance between atoms  $i$  and  $j$ .  $\varepsilon_{ij}$  and  $\sigma_{ij}$  are the LJ well depth and diameter, respectively. LJ parameters between atoms of different types were calculated using the Lorentz-Berthelot mixing rules (i.e., geometric average of well depths and arithmetic average of diameters). The LJ parameters for all simulations and calculations were taken from the DREIDING<sup>11</sup> force field for all framework atoms as shown in Table S3. A Lennard-Jones cut-off distance of 12.8 Å was used. The  $\text{N}_2$  molecule was modeled using the TraPPE<sup>12</sup> force field. This force field was originally fit to reproduce the vapor-liquid coexistence curve of nitrogen. In this force field the nitrogen molecule is a rigid structure where the N-N bond length is fixed at its experimental value of 1.10 Å. This model also reproduces the experimental gas-phase quadrupole moment of  $\text{N}_2$  by placing partial charges on N atoms and on a point located at the center of mass (COM) of the molecule. Partial charges of the framework atoms were calculated using the extended charge equilibration (EQeq) method.<sup>13</sup> Electric quadrupole interactions between  $\text{N}_2$  and framework atoms were also taking into consideration by calculating their Coulomb interactions. Fugacities needed to run the GCMC simulations were calculated using the Peng-Robinson equation of state.<sup>14</sup> GCMC simulations report the absolute adsorption data, which are then used to compute the excess adsorption data using the relation:

$$N_{total} = N_{excess} + \rho_{gas} \times V_p$$

where  $\rho_{gas}$  is the bulk density of the gas at simulation conditions, calculated with Peng-Robinson equation of state, and  $V_p$  is the pore volume calculated by the helium insertion method reported that mimics experiments.<sup>15</sup>

**Table S3.** LJ parameters and partial charges for framework atoms, N<sub>2</sub> and He.

Atom type	$\sigma$ (Å)	$\epsilon/k_B$ (K)	q (e)
C (MOF)	3.473	47.856	EQeq
O (MOF)	3.033	48.158	EQeq
N (MOF)	3.263	38.949	EQeq
H (MOF)	2.846	7.649	EQeq
Zn (MOF)	4.045	27.677	EQeq
N (N <sub>2</sub> )	3.31	36.0	-0.482
N_COM (N <sub>2</sub> )	0	0	0.964
He	2.64	10.9	0

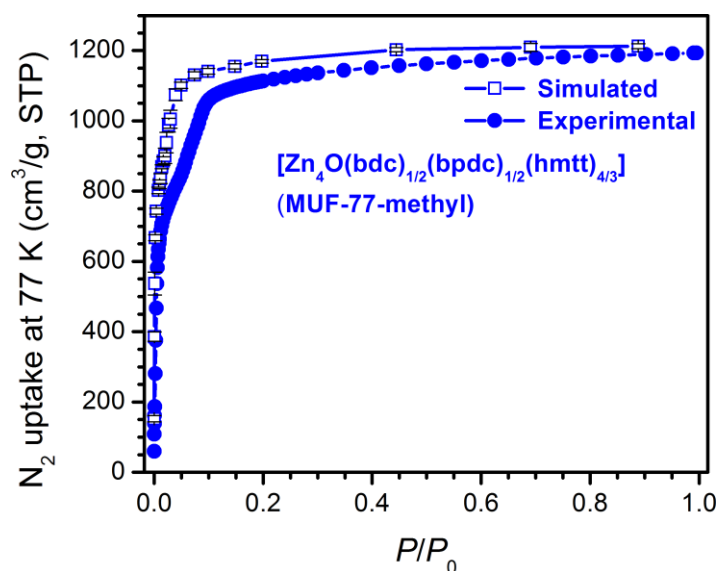


**Figure S32** Simulated (open squares) and experimentally measured<sup>2</sup> (filled circles) nitrogen adsorption isotherm for [Zn<sub>4</sub>O(bdc)<sub>1/2</sub>(bpdc)<sub>1/2</sub>(hmtt)<sub>4/3</sub>] (MUF-77) at 77 K. Standard deviations for each simulated pressure points are shown as black lines. The saturated uptake is simulated to be 1213(7) cm<sup>3</sup>/g (STP) at  $P/P_0 = 0.888$ , very close to the experimentally determined value (1194 at  $P/P_0 = 0.995$ ).

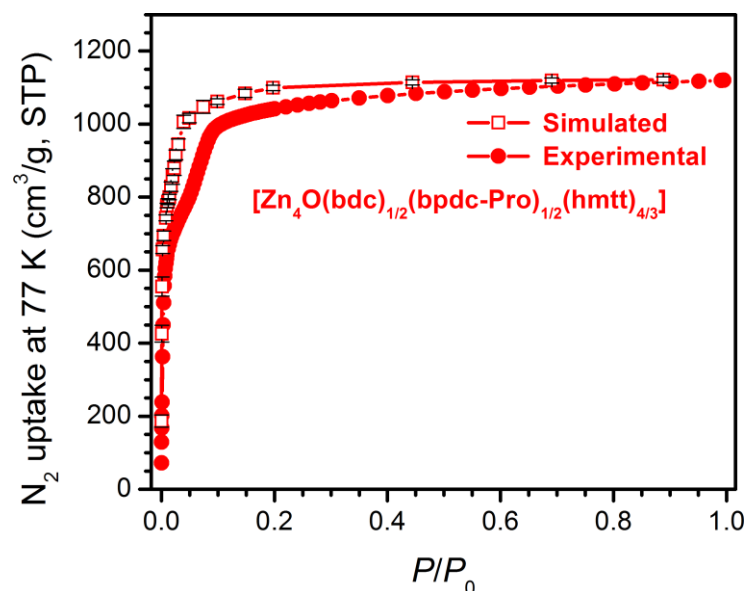


**Figure S33** Simulated (open squares) and experimentally measured (filled circles) nitrogen adsorption isotherm for  $[\text{Zn}_4\text{O}(\text{bdc})_{1/2}(\text{bpdc-Pro})_{1/2}(\text{hmtt})_{4/3}]$  at 77 K. Standard deviations for each simulated pressure points are shown as black lines. The saturated uptake is simulated to be  $1121(8) \text{ cm}^3/\text{g}$  (STP) at  $P/P_0 = 0.888$ , which is the same as the experimentally determined value ( $1120$  at  $P/P_0 = 0.995$ ).

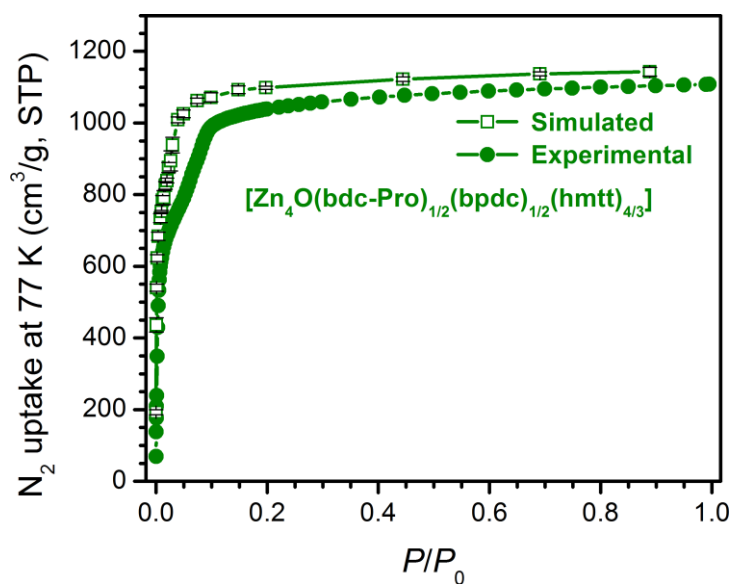


**Figure S34** Simulated (open squares) and experimentally measured (filled circles) nitrogen adsorption isotherm for  $[\text{Zn}_4\text{O}(\text{bdc-Pro})_{1/2}(\text{bpdc})_{1/2}(\text{hmtt})_{4/3}]$  at 77 K. Standard deviations for each simulated pressure points are shown as black lines. The saturated uptake is simulated to be  $1143(12) \text{ cm}^3/\text{g}$  (STP) at  $P/P_0 = 0.888$ , very close to the experimentally determined value ( $1108$  at  $P/P_0 = 0.995$ ).

## 9. Catalysis of the aldol reaction between acetone and p-nitrobenzaldehyde

**Experimental protocol.** A stock catalyst solution was prepared with 4-nitrobenzaldehyde (181 mg, 1.20 mmol), acetone (30.0 mL), water (7.50 mL), and nitrobenzene as an internal standard (121  $\mu$ L, 1.20 mmol). In a typical experiment, 1.0 mL of stock solution was added to a 1.5 mL HPLC sample vial together with a pre-weighed quantity of desolvated catalyst. The mass of catalyst was chosen so that it contained 10 mol% of prolanyl groups relative to 4-nitrobenzaldehyde. The reaction mixture was allowed to stand in the autosampler of the HPLC at 20 °C. During the reaction, 2.5  $\mu$ L of the supernatant was subjected to HPLC analysis every two hours over the initial 12 hours of the reaction and then again after 24 h. HPLC analysis was carried out under the following conditions: CHIRALPAK AS-H column; mixed solvent of hexane and isopropyl alcohol (70:30 v/v); flow rate of 0.8 ml/min. Products were detected according to their absorption of 254 nm UV light. The conversion of 4-nitrobenzaldehyde was calculated by comparing the ratio of its peak area and that of the nitrobenzene standard. The ee value of each reaction is reported based on the excess of the *R* enantiomer after a reaction time of 24 h. For accurate ee determinations the HPLC conditions were optimized to obtain baseline separations between the two enantiomers (according to the aforementioned protocol). Figure S35 shows a typical HPLC chromatogram of a reaction mixture.

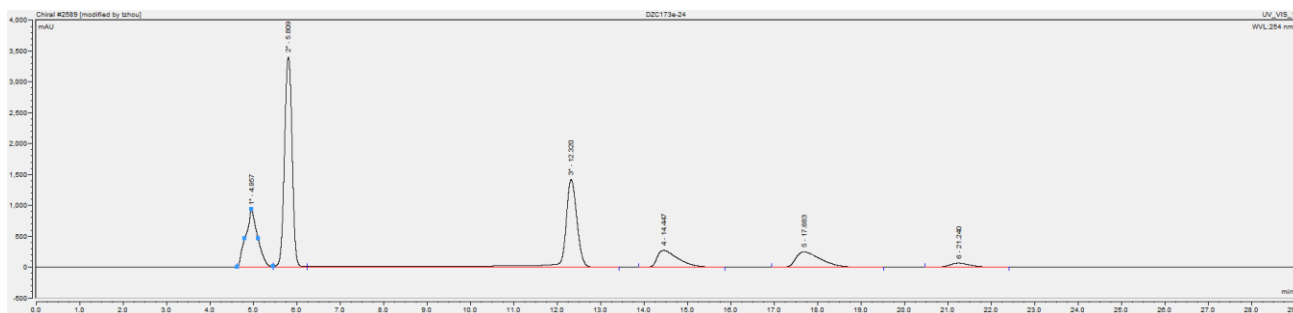


**Figure S35** A typical HPLC chromatogram (condition A, AS-H column) of the reaction mixture. Peak 1 (4.96 min): acetone; Peak 2 (5.81 min): nitrobenzene; Peak 3 (12.32 min): 4-nitrobenzaldehyde; Peak 4 (14.45 min): *R* enantiomer of aldol adduct; Peak 5 (17.68): *S* enantiomer of aldol adduct; Peak 6 (21.24): product of the elimination of H<sub>2</sub>O from the initial aldol product.

### Calculation of the observed rate constant

The rate of the aldol reaction,  $r$ , based on the consumption of 4-nitrobenzaldehyde (PNBA) can be expressed as a function of the reaction rate constant,  $k$ , and the concentration of PNBA and acetone over time,  $t$ , by assuming the reaction order of PNBA is unity:

$$r = -\frac{d[\text{PNBA}]}{dt} = k[\text{PNBA}][\text{acetone}]^a$$

Here,  $a$  is the reaction order of acetone. Since the reaction is carried out in the presence of a very large excess of acetone, the above equation can be simplified as

$$r = -\frac{d[\text{PNBA}]}{dt} = k_{obs}[\text{PNBA}]$$

where  $k_{obs}$  is the pseudo first-order observed rate constant.

Therefore

$$\ln[\text{PNBA}] = \ln[\text{PNBA}]_0 - k_{\text{obs}}t$$

Here,  $[\text{PNBA}]_0$  is the initial concentration of 4-nitrobenzaldehyde. Plotting  $\ln([\text{PNBA}]/[\text{PNBA}]_0)$  as a function of time over the initial 12 hours of the reaction yields a straight line with slope  $k_{\text{obs}}$  estimated by least squares fitting.

### Estimation of errors in $k_{\text{obs}}$ and ee

Catalysis runs using the parent catalysts,  $[\text{Zn}_4\text{O}(\text{bdc-Pro})_{1/2}(\text{bpdc})_{1/2}(\text{hmtt})_{4/3}]$  and  $[\text{Zn}_4\text{O}(\text{bdc})_{1/2}(\text{bpdc-Pro})_{1/2}(\text{hmtt})_{4/3}]$ , were repeated independently using material from either the same or different synthesis batches (Table S4, S5). The standard deviation (SD) in  $k_{\text{obs}}$  deduced from the collective data was very similar to the error estimated by the least squares fitting of the kinetic data of individual runs (which is listed in Tables S4 and S5). For all other catalysts, aldol reactions were repeated twice. SDs in  $k_{\text{obs}}$  for these catalysts were estimated as the standard error given by the least squares fitting process. While the variation in the two measured  $k_{\text{obs}}$  values is sometimes larger than the SD estimated in this way, this is justified by the data from the parent catalysts where a statistically-significant number of catalysis runs showed convergence between the standard error given for the individual runs (from least squares fitting) and the SD of the collective runs.

Standard deviations for the ee of the parent catalysts were calculated from the series of experiments on the parent catalysts (Tables S4, S5). The relative standard deviation (RSD, the ratio of the SD to the mean) is much larger for  $[\text{Zn}_4\text{O}(\text{bdc-Pro})_{1/2}(\text{bpdc})_{1/2}(\text{hmtt})_{4/3}]$  (14.0%) than for  $[\text{Zn}_4\text{O}(\text{bdc})_{1/2}(\text{bpdc-Pro})_{1/2}(\text{hmtt})_{4/3}]$  (5.9%). To extend these standard deviations to ee values observed for the remaining catalysts, we conservatively used an RSD of 14.0% for ee values between 0 and 18, and a RSD of 5.9% for ee values of 19 and above.

### Control catalysis runs

During the course of these measurements, the  $k_{\text{obs}}$  and ee of  $[\text{Zn}_4\text{O}(\text{bdc-Pro})_{1/2}(\text{bpdc})_{1/2}(\text{hmtt})_{4/3}]$  and  $[\text{Zn}_4\text{O}(\text{bdc})_{1/2}(\text{bpdc-Pro})_{1/2}(\text{hmtt})_{4/3}]$  were regularly measured for quality control purposes to ensure that they remained within one SD of the values presented in Table 1.

**Table S4** Catalysis results for  $[\text{Zn}_4\text{O}(\text{bdc-Pro})_{1/2}(\text{bpdc})_{1/2}(\text{hmtt})_{4/3}]$ .

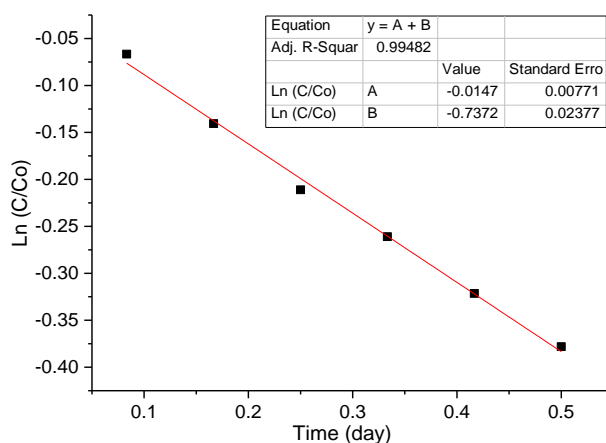
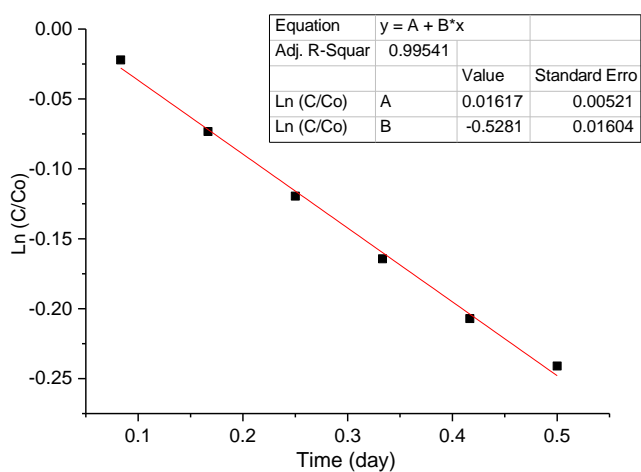
Entry	Crystal batch	ee (%)	$k_{\text{obs}}$ (L mol <sup>-1</sup> day <sup>-1</sup> )	Conversion at 24 h (%)
1	a	-3.4	0.72 ± 0.05	56.4
2	b	-4.4	0.67 ± 0.01	47.5
3	c	-4.5	0.74 ± 0.02	49.6
4	d <sup>†</sup>	-3.1	0.75 ± 0.03	53.5
5		-3.8	0.77 ± 0.04	54.4
6	e <sup>†</sup>	-4.3	0.78 ± 0.03	48.2
7		-4.6	0.74 ± 0.04	49.5
8	f <sup>†</sup>	-3.4	0.73 ± 0.03	55.0
9		-3.9	0.74 ± 0.03	54.4
<b>Average</b>		-3.93	0.74	52.06
<b>STDEV</b>		0.55	0.03	3.33
<b>Relative SD</b>		14.0%	4.1%	

<sup>†</sup> The crystals were separated into two equal amounts for two independent catalysis reactions.

**Table S5** Catalysis results for  $[\text{Zn}_4\text{O}(\text{bdc})_{1/2}(\text{bpdc-Pro})_{1/2}(\text{hmtt})_{4/3}]$ .

Entry	Crystal batch	ee (%)	$k_{\text{obs}}$ ( $\text{L mol}^{-1} \text{day}^{-1}$ )	Conversion at 24 h (%)
1	a	18.6	$0.53 \pm 0.03$	41.1
2	b	19.6	$0.53 \pm 0.02$	38.1
3	c	20.8	$0.49 \pm 0.02$	38.9
4	d <sup>†</sup>	20.3	$0.52 \pm 0.02$	44.1
5		19.2	$0.52 \pm 0.02$	42.8
6	e <sup>†</sup>	18.3	$0.47 \pm 0.01$	41.2
7		17.6	$0.55 \pm 0.01$	43.1
8	f <sup>†</sup>	22.4	$0.53 \pm 0.02$	45.8
9		23.3	$0.52 \pm 0.02$	43.2
<b>Average</b>		19.20	0.52	41.33
<b>STDEV</b>		1.13	0.03	2.21
<b>Relative SD</b>		5.9%	5.8%	

<sup>†</sup> The crystals were separated into two equal amounts for two independent catalysis reactions.

**Representative reaction kinetics plots for the parent catalysts****Figure S36** Reaction kinetics plot for the aldol reaction catalysed by  $[\text{Zn}_4\text{O}(\text{bdc-Pro})_{1/2}(\text{bpdc})_{1/2}(\text{hmtt})_{4/3}]$ .**Figure S37** Reaction kinetics plot for the aldol reaction catalysed by  $[\text{Zn}_4\text{O}(\text{bdc})_{1/2}(\text{bpdc-Pro})_{1/2}(\text{hmtt})_{4/3}]$ .

**Representative reaction kinetics plots for the other MOF catalysts**

(1)  $[\text{Zn}_4\text{O}_2(\text{bdc})_{1/2}(\text{bpdc-Pro})_1(\text{hett})_{4/3}]$

Entry	Catalyst linker set	ee (%)	$k_{\text{obs}}$ ( $\text{L mol}^{-1} \text{day}^{-1}$ )	Conversion at 24 h (%)
1	bdc/bpdc-Pro/hett	17.0	$0.33 \pm 0.02$	34.0
2		17.0	$0.30 \pm 0.01$	35.0

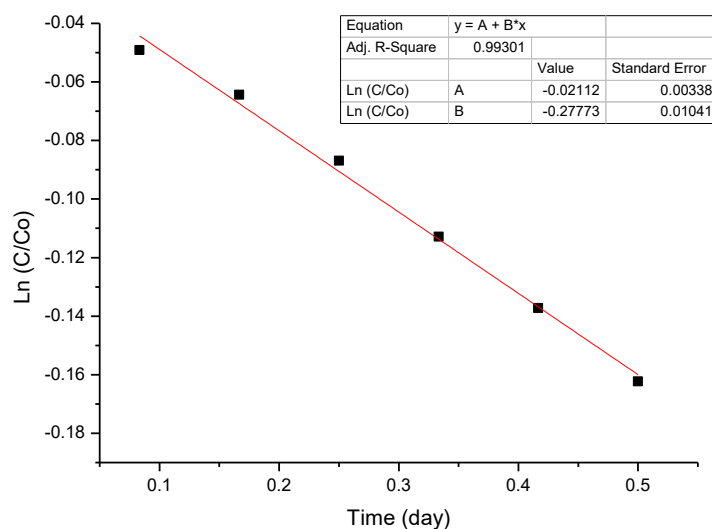


**Figure S38** Reaction kinetics plot for the aldol reaction catalysed by  $[\text{Zn}_4\text{O}(\text{bdc})_{1/2}(\text{bpdc-Pro})_{1/2}(\text{hett})_{4/3}]$ .

(2)  $[\text{Zn}_4\text{O}(\text{bdc})_{1/2}(\text{bpdc-Pro})_{1/2}(\text{hbtt})_{4/3}]$

Entry	Catalyst linker set	ee (%)	$k_{\text{obs}}$ ( $\text{L mol}^{-1} \text{day}^{-1}$ )	Conversion at 24 h (%)
1	bdc/bpdc-Pro/hbtt	16.7	$0.14 \pm 0.007$	10.4
2		18.6	$0.17 \pm 0.009$	12.6

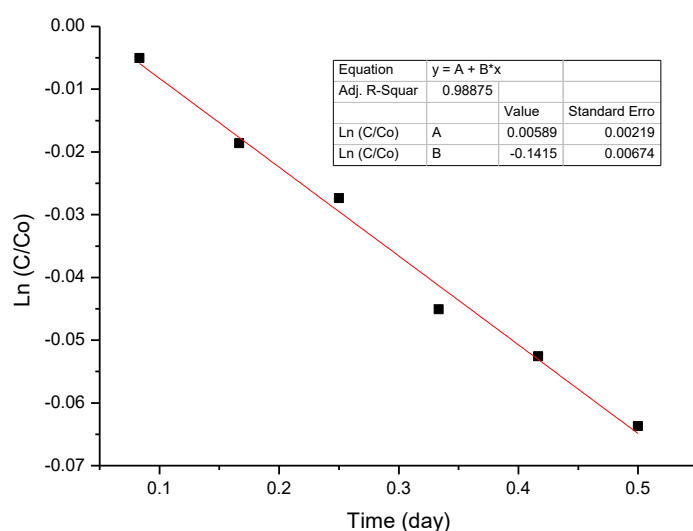


**Figure S39** Reaction kinetics plot for the aldol reaction catalysed by  $[\text{Zn}_4\text{O}(\text{bdc})_{1/2}(\text{bpdc-Pro})_{1/2}(\text{hbtt})_{4/3}]$ .

(3)  $[\text{Zn}_4\text{O}(\text{bdc})_{1/2}(\text{bpdc-Pro})_{1/2}(\text{hott})_{4/3}]$

Entry	Catalyst linker set	ee (%)	$k_{\text{obs}}$ ( $\text{L mol}^{-1} \text{day}^{-1}$ )	Conversion at 24 h (%)
1	bdc/bpdc-Pro/hott	15.9	$0.10 \pm 0.007$	9.7
2		15.4	$0.11 \pm 0.003$	10.4

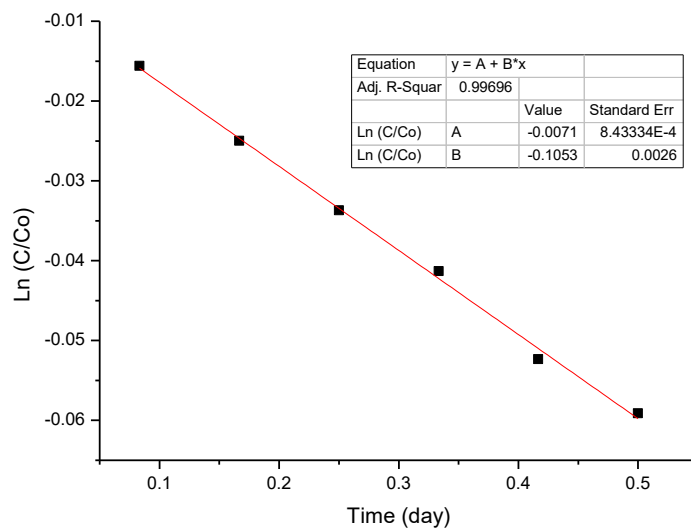


**Figure S40** Reaction kinetics plot for the aldol reaction catalysed by  $[\text{Zn}_4\text{O}(\text{bdc})_{1/2}(\text{bpdc-Pro})_{1/2}(\text{hott})_{4/3}]$ .

(4)  $[\text{Zn}_4\text{O}(\text{ndc})_{1/2}(\text{bpdc-Pro})_{1/2}(\text{hmtt})_{4/3}]$

Entry	Catalyst linker set	ee (%)	$k_{\text{obs}}$ ( $\text{L mol}^{-1} \text{day}^{-1}$ )	Conversion at 24 h (%)
1	ndc/bpdc-Pro/hmtt	24.2	$0.53 \pm 0.02$	44.4
2		24.1	$0.47 \pm 0.01$	43.2

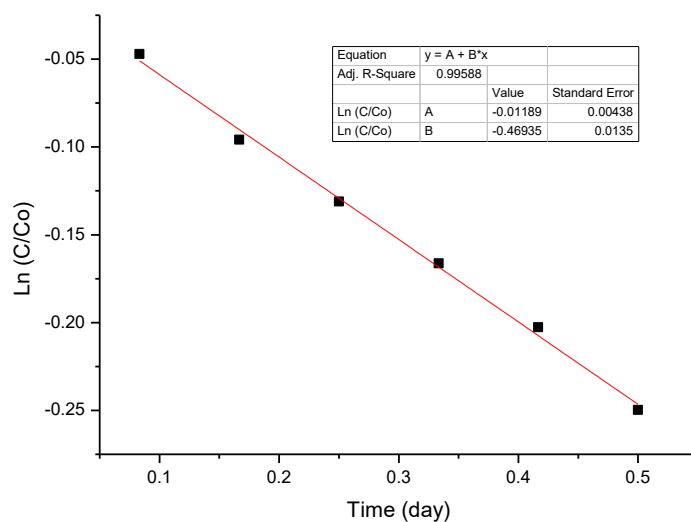


**Figure S41** Reaction kinetics plot for the aldol reaction catalysed by  $[\text{Zn}_4\text{O}(\text{ndc})_{1/2}(\text{bpdc-Pro})_{1/2}(\text{hmtt})_{4/3}]$ .

(5)  $[\text{Zn}_4\text{O}(\text{ndc})_{1/2}(\text{bpdc-Pro})_{1/2}(\text{hbtt})_{4/3}]$

Entry	Catalyst linker set	ee (%)	$k_{\text{obs}}$ ( $\text{L mol}^{-1} \text{day}^{-1}$ )	Conversion at 24 h (%)
1	ndc/bpdc-Pro/hbtt	17.8	$0.15 \pm 0.008$	16.4
2		18.3	$0.17 \pm 0.009$	15.8

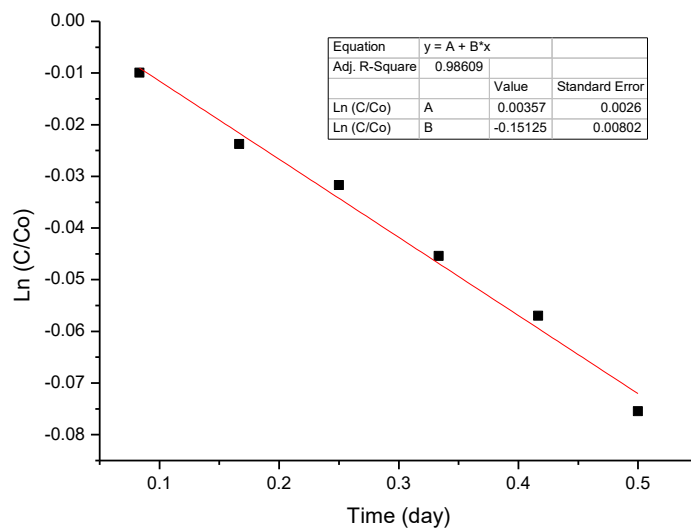


**Figure S42** Reaction kinetics plot for the aldol reaction catalysed by  $[\text{Zn}_4\text{O}(\text{ndc})_{1/2}(\text{bpdc-Pro})_{1/2}(\text{hbtt})_{4/3}]$ .

(6)  $[\text{Zn}_4\text{O}(\text{ndc})_{1/2}(\text{bpdc-Pro})_{1/2}(\text{hott})_{4/3}]$

Entry	Catalyst linker set	ee (%)	$k_{\text{obs}}$ ( $\text{L mol}^{-1} \text{day}^{-1}$ )	Conversion at 24 h (%)
1	ndc/bpdc-Pro/hott	19.0	$0.12 \pm 0.008$	13.0
2		19.2	$0.13 \pm 0.007$	14.0

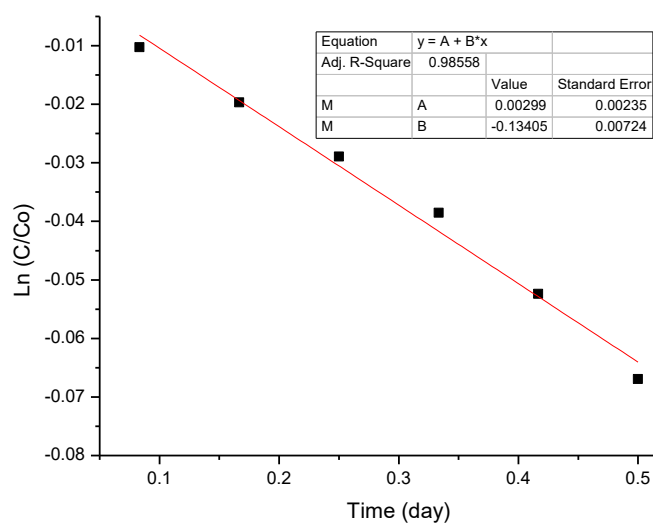


**Figure S43** Reaction kinetics plot for the aldol reaction catalysed by  $[\text{Zn}_4\text{O}(\text{ndc})_{1/2}(\text{bpdc-Pro})_{1/2}(\text{hott})_{4/3}]$ .

(7)  $[\text{Zn}_4\text{O}(\text{bdc-Pro})_{1/2}(\text{bpdc})_{1/2}(\text{hett})_{4/3}]$

Entry	Catalyst linker set	ee (%)	$k_{\text{obs}}$ ( $\text{L mol}^{-1} \text{day}^{-1}$ )	Conversion at 24 h (%)
1	bdc-Pro/bpdc/hett	-4.1	$0.68 \pm 0.04$	53.5
2		-3.7	$0.70 \pm 0.03$	55.3

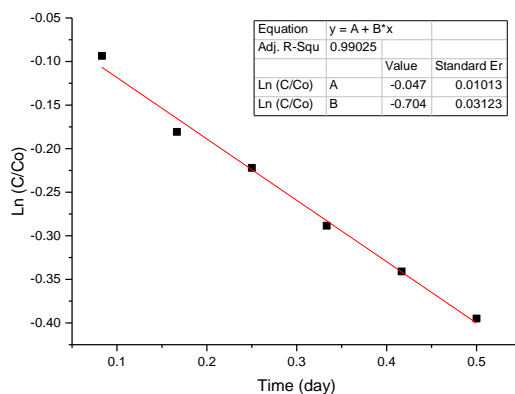


**Figure S44** Reaction kinetics plot for the aldol reaction catalysed by  $[\text{Zn}_4\text{O}(\text{bdc-Pro})_{1/2}(\text{bpdc})_{1/2}(\text{hett})_{4/3}]$ .

(8)  $[\text{Zn}_4\text{O}(\text{bdc-Pro})_{1/2}(\text{bpdc})_{1/2}(\text{hbtt})_{4/3}]$

Entry	Catalyst linker set	ee (%)	$k_{\text{obs}}$ ( $\text{L mol}^{-1} \text{day}^{-1}$ )	Conversion at 24 h (%)
1	bdc-Pro/bpdc/hbtt	4.2	$0.61 \pm 0.02$	48.1
2		4.1	$0.63 \pm 0.01$	52.7

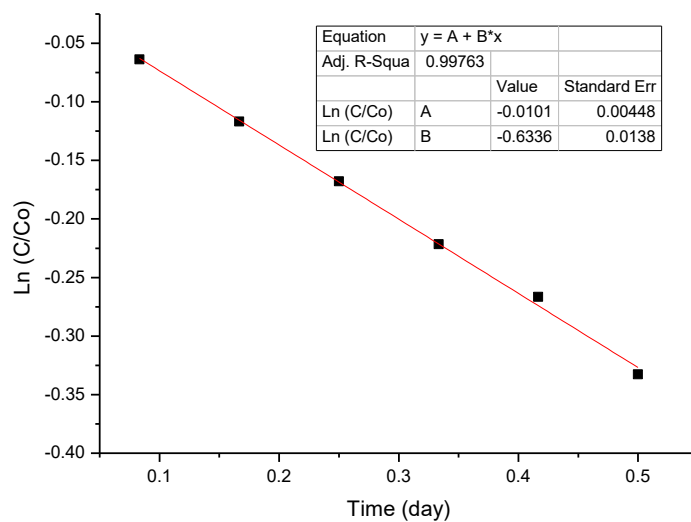


**Figure S45** Reaction kinetics plot for the aldol reaction catalysed by  $[\text{Zn}_4\text{O}(\text{bdc-Pro})_{1/2}(\text{bpdc})_{1/2}(\text{hbtt})_{4/3}]$ .

(9)  $[\text{Zn}_4\text{O}(\text{bdc-Pro})_{1/2}(\text{bpdc})_{1/2}(\text{hott})_{4/3}]$

Entry	Catalyst linker set	ee (%)	$k_{\text{obs}}$ ( $\text{L mol}^{-1} \text{day}^{-1}$ )	Conversion at 24 h (%)
1	bdc-Pro/bpdc/hott	+1.6	$0.44 \pm 0.02$	40.5
2		+1.9	$0.40 \pm 0.02$	38.8

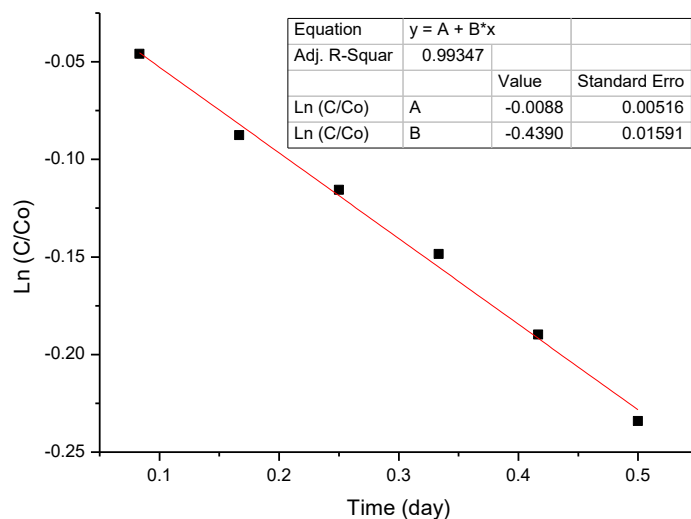


**Figure S46** Reaction kinetics plot for the aldol reaction catalysed by  $[\text{Zn}_4\text{O}(\text{bdc-Pro})_{1/2}(\text{bpdc})_{1/2}(\text{hott})_{4/3}]$ .

(10)  $[\text{Zn}_4\text{O}(\text{bdc-Pro})_{1/2}(\text{dppdc})_{1/2}(\text{hmtt})_{4/3}]$

Entry	Catalyst linker set	ee (%)	$k_{\text{obs}}$ ( $\text{L mol}^{-1} \text{day}^{-1}$ )	Conversion at 24 h (%)
1	bdc-Pro/dppdc/hmtt	-26.1	$0.28 \pm 0.01$	21.3
2	bdc-Pro/dppdc/hmtt	-27.0	$0.25 \pm 0.01$	21.9

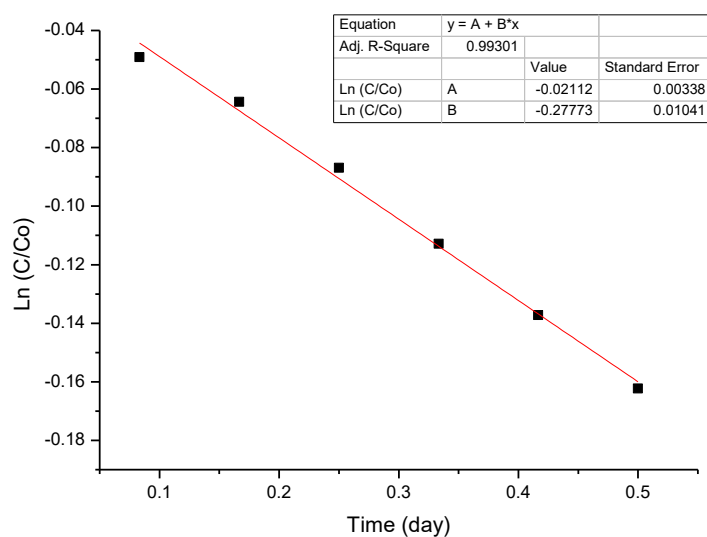


**Figure S47** Reaction kinetics plot for the aldol reaction catalysed by  $[\text{Zn}_4\text{O}(\text{bdc-Pro})_{1/2}(\text{dppdc})_{1/2}(\text{hmtt})_{4/3}]$ .

(11)  $[\text{Zn}_4\text{O}(\text{bdc-Pro})_{1/2}(\text{pcdc})_{1/2}(\text{hmtt})_{4/3}]$

Entry	Catalyst linker set	ee (%)	$k_{\text{obs}}$ ( $\text{L mol}^{-1} \text{day}^{-1}$ )	Conversion at 24 h (%)
1	bdc-Pro/pcdc/hmtt	-9.5	$0.046 \pm 0.002$	6.1
2	bdc-Pro/pcdc/hmtt	-11.0	$0.058 \pm 0.003$	5.7

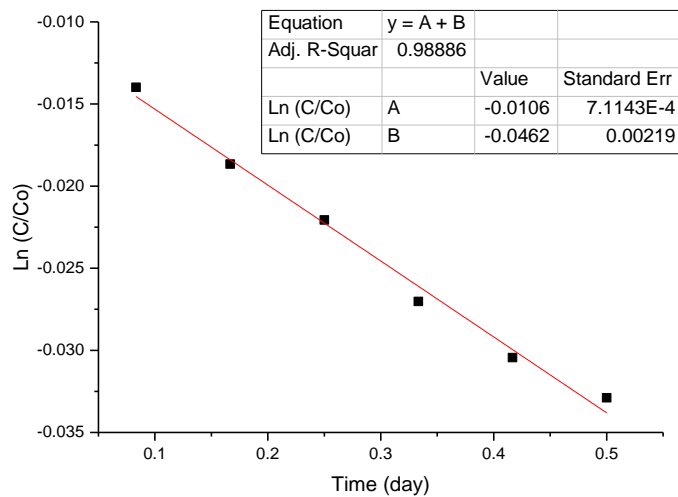


**Figure S48** Reaction kinetics plot for the aldol reaction catalysed by  $[\text{Zn}_4\text{O}(\text{bdc-Pro})_{1/2}(\text{pcdc})_{1/2}(\text{hmtt})_{4/3}]$ .

(12) Homogeneous catalysis by Me<sub>2</sub>bdc-Pro

Entry	Catalyst	ee (%)	k <sub>obs</sub> (L mol <sup>-1</sup> day <sup>-1</sup> )	Conversion at 24 h (%)
1	Me <sub>2</sub> bdc-Pro	8.9	3.98	98.3
2		8.4	3.90	98.1

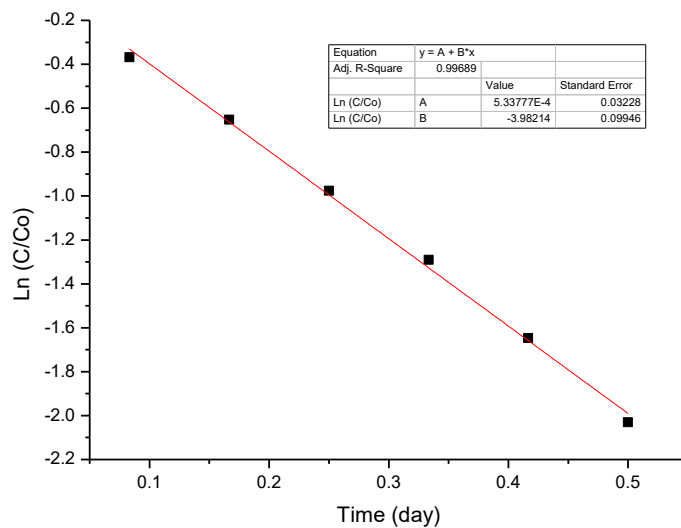


Figure S49 Reaction kinetics plot for the aldol reaction catalysed by Me<sub>2</sub>bdc-Pro.

(13) Homogeneous catalysis by Me<sub>2</sub>bpdc-Pro

Entry	Catalyst	ee (%)	k <sub>obs</sub> (L mol <sup>-1</sup> day <sup>-1</sup> )	Conversion at 24 h (%)
1	Me <sub>2</sub> bpdc-Pro	30.6	0.49	37.4
2		30.0	0.49	39.5

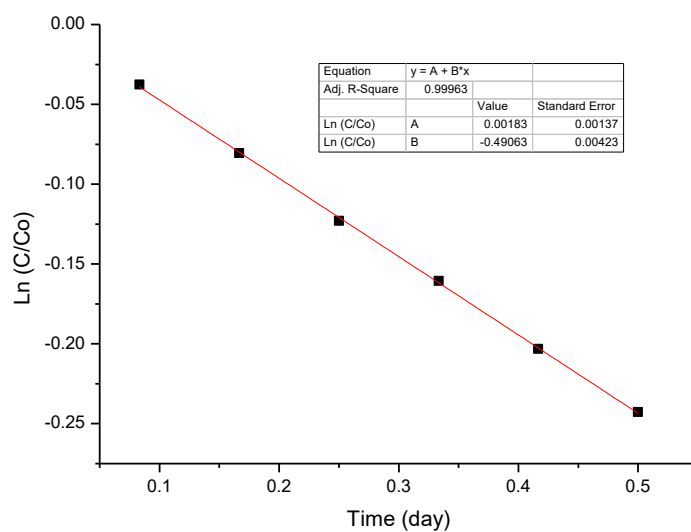
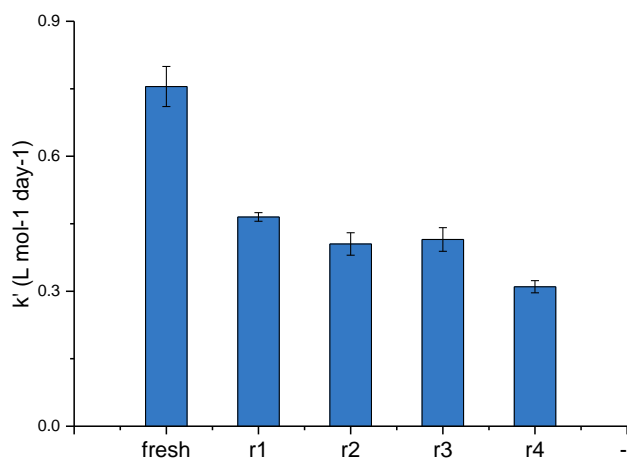


Figure S50 Reaction kinetics plot for the aldol reaction catalysed by Me<sub>2</sub>bpdc-Pro.

### Recycling experiments

For recycling experiments, 1.0 mL of stock solution was added in to the vial preloaded with desolvated catalyst. After each cycle, the catalyst was washed with acetone at least three times and then immersed in minimum amount of acetone before adding the stock solution for the next cycle. As expected, due to the increase total volume of acetone after the first cycle, the concentration of 4-nitrobenzaldehyde decreases slightly and causes a slight drop in  $k_{\text{obs}}$  between the first and second catalytic cycles. Each rate constant value is the average of results from two independent, side-by-side experiments.



**Figure S51** A plot showing  $k_{\text{obs}}$  measured over five successive runs using the same sample of  $[\text{Zn}_4\text{O}(\text{bdc-Pro})_{1/2}(\text{bpdc})_{1/2}(\text{hmtt})_{4/3}]$  demonstrating the recyclability of this catalyst.

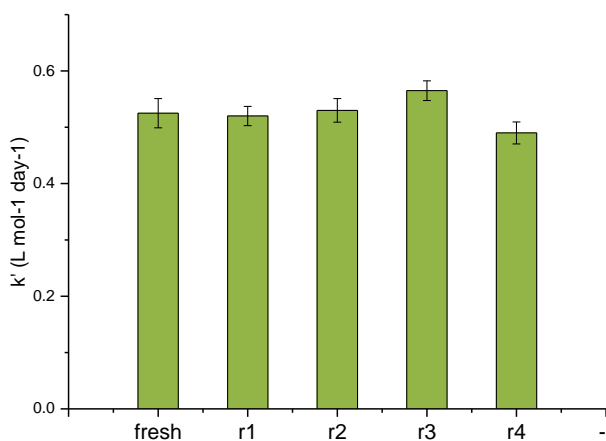


**Figure S52** A plot showing  $k_{\text{obs}}$  measured over five successive runs using the same sample of  $[\text{Zn}_4\text{O}(\text{bdc})_{1/2}(\text{bpdc-Pro})_{1/2}(\text{hmtt})_{4/3}]$  demonstrating the recyclability of this catalyst.

**Monitoring the catalysis until the completion of the reaction**

To confirm the aldol reaction with acetone is first order reaction in PNBA, the reaction catalyzed by  $[Zn_4O(bdc-Pro)_{1/2}(bpdc)_{1/2}(hmtt)_{4/3}]$  was monitored by HPLC over a period of 42 h, at which point the conversion had exceeded 95%. The kinetic plot, shown below, maintains linearity until the PNBA is fully consumed.

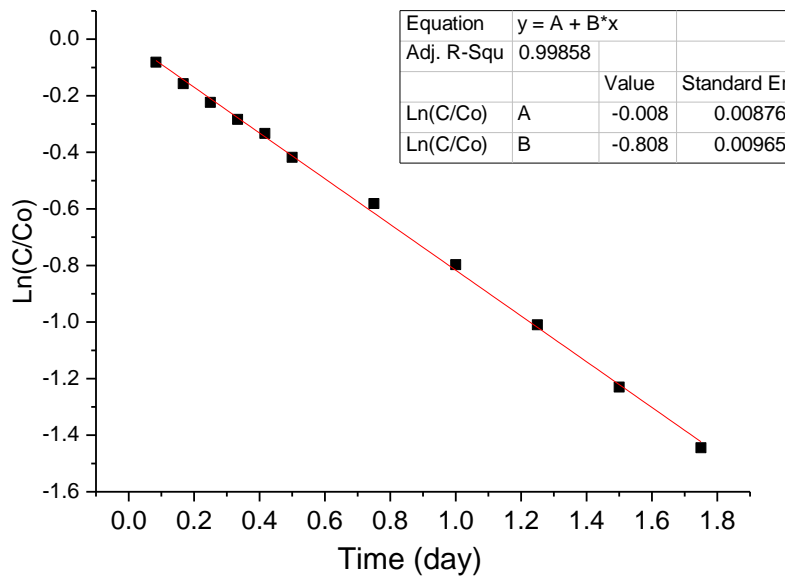


**Figure S53** Reaction kinetic plot for the aldol reaction catalysed by  $[Zn_4O(bdc-Pro)_{1/2}(bpdc)_{1/2}(hmtt)_{4/3}]$  over an extended time period.

**Characterization of the MOF after catalysis**

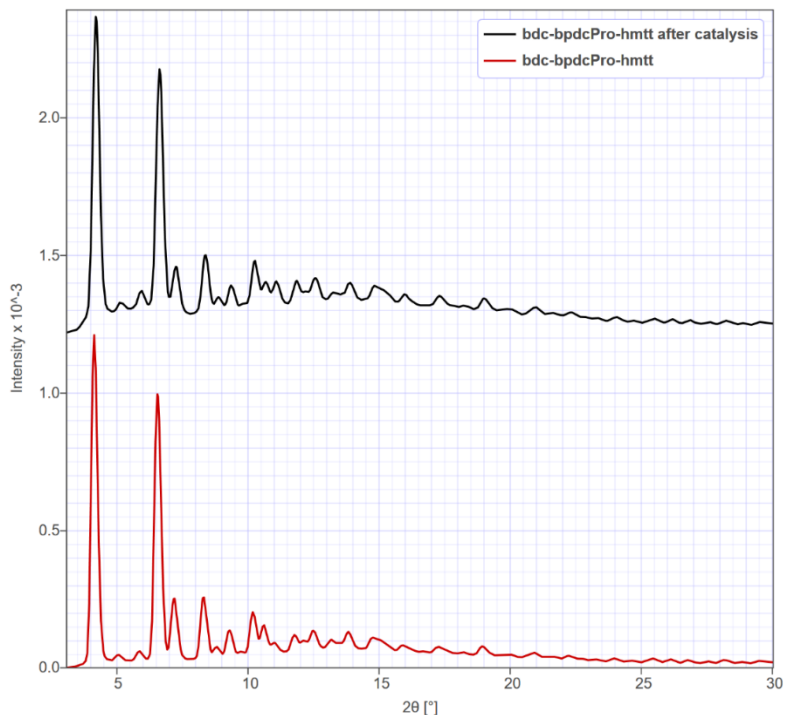


**Figure S54** PXRD patterns of  $[Zn_4O(bdc)_{1/2}(bpdc-Pro)_{1/2}(hmtt)_{4/3}]$  before (red) and after (black) catalysis.

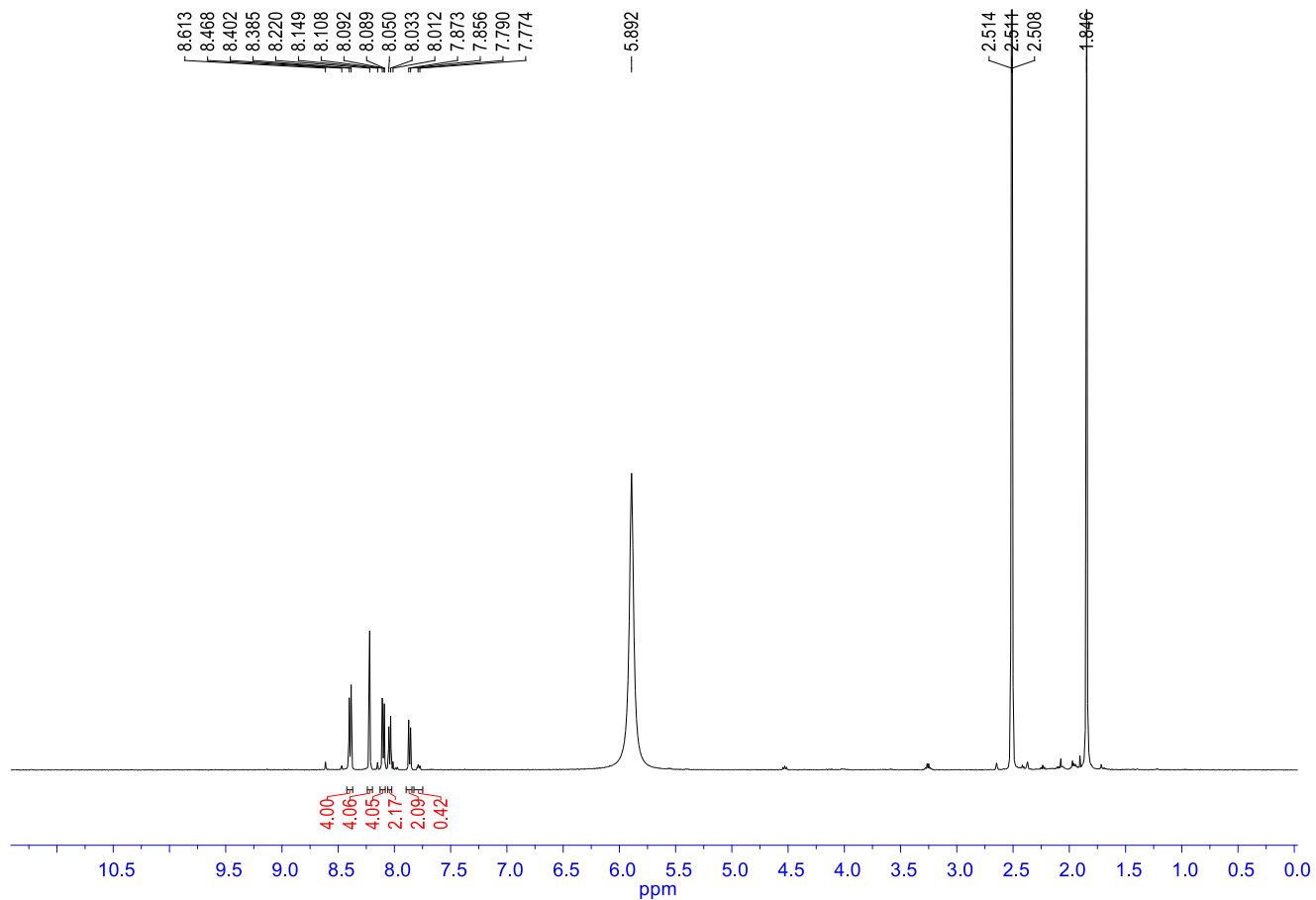


**Figure S55**  $^1H$  NMR spectrum of  $[Zn_4O(bdc-Pro)_{1/2}(bpdc)_{1/2}(hmtt)_{4/3}]$  digested following catalysis.

## 10. Catalysis of the aldol reaction between cyclopentanone and p-nitrobenzaldehyde

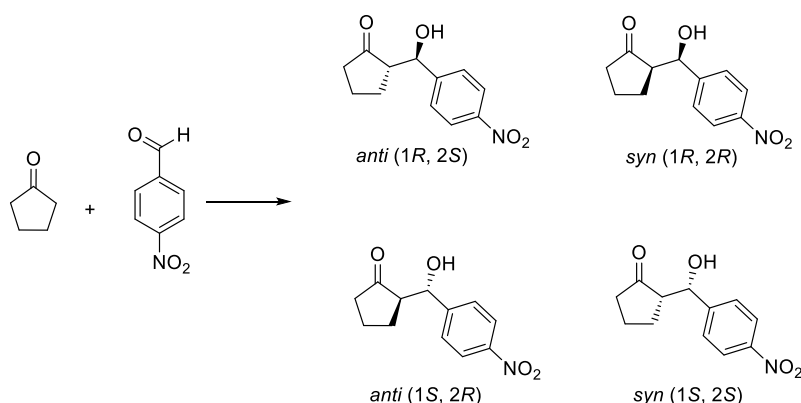


**Figure S56** The aldol reaction between cyclopentanone and p-nitrobenzaldehyde.

### Experimental protocol

A stock catalyst solution was prepared with 4-nitrobenzaldehyde (PNBA, 54.4 mg, 0.36 mmol) and water-saturated cyclopentanone (10 mL). In a typical experiment, 1.0 mL of stock solution was added to a 1.5 mL HPLC sample vial together with a pre-weighed quantity of desolvated catalyst. The mass of catalyst was chosen so that it contained 10 mol% of prolinyl groups relative to 4-nitrobenzaldehyde. The reaction mixture was allowed to stand in the autosampler of the HPLC at 20 °C. Over the course reaction, 2.5  $\mu$ L of the supernatant was subjected to HPLC analysis every 24 hours. HPLC analysis was carried out under the following conditions: CHIRALPAK AS-H column; mixed solvent of hexane and isopropyl alcohol (80/20 v/v); flow rate of 1.0 ml/min. The remaining PNBA and the products were detected according their absorption of 254 nm UV light. The assignments of the product isomers were made on the basis of related literature.<sup>1,16</sup> The ee values for each diastereomer was calculated according to the formula  $ee = \frac{(\text{peak area of slow-eluting enantiomer}) - (\text{peak area of fast-eluting enantiomer})}{\text{total peak area}} \times 100$  (Figure S57). The MOF catalysts were tested in parallel. The isomer distributions of the individual runs agreed closely, and average values are given in Table S6.

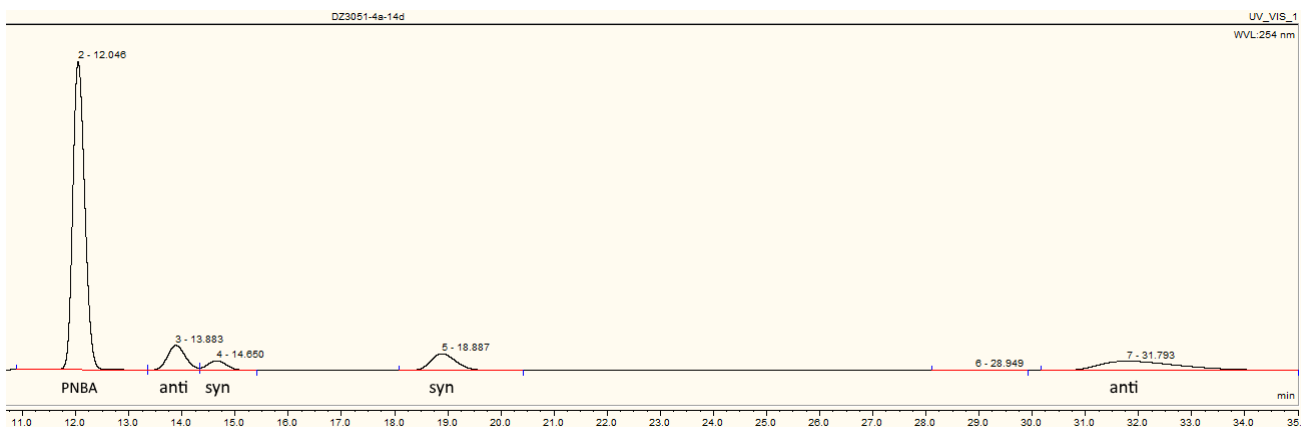


**Figure S57** HPLC chromatogram of the aldol reaction between cyclopentanone and p-nitrobenzaldehyde.

**Table S6** Summary of the reaction between cyclopentanone and p-nitrobenzaldehyde catalyzed by MUF-77 analogs and comparison with related homogenous catalysts.

Entry	Catalyst	Conversion after 10 days	dr <sup>a</sup> <i>syn:anti</i>	<i>syn ee (%)</i> <sup>a</sup>	<i>anti ee (%)</i> <sup>a</sup>
1	[Zn <sub>4</sub> O(bdc-Pro) <sub>1/2</sub> (bpdc) <sub>1/2</sub> (hmtt) <sub>4/3</sub> ]	68.9	1.74:1	-2.8	-35.8
2	[Zn <sub>4</sub> O(bdc) <sub>1/2</sub> (bpdc-Pro) <sub>1/2</sub> (hmtt) <sub>4/3</sub> ]	32.6	0.55:1	37.2	16.8
3	[Zn <sub>4</sub> O(bdc-Pro) <sub>1/2</sub> (dppdc) <sub>1/2</sub> (hmtt) <sub>4/3</sub> ]	41.3	2.14:1	3.4	-10.2
4	[Zn <sub>4</sub> O(ndc) <sub>1/2</sub> (bpdc-Pro) <sub>1/2</sub> (hmtt) <sub>4/3</sub> ]	16.7	0.64:1	40.3	24.3
5	Me <sub>2</sub> bdc-Pro	63.6	0.33:1	44.9	-18.6
6	Me <sub>2</sub> bpdc-Pro	61.6	0.41:1	68.4	19.8

<sup>a</sup> Determined by HPLC.

## 11. Photographs and microscopy images

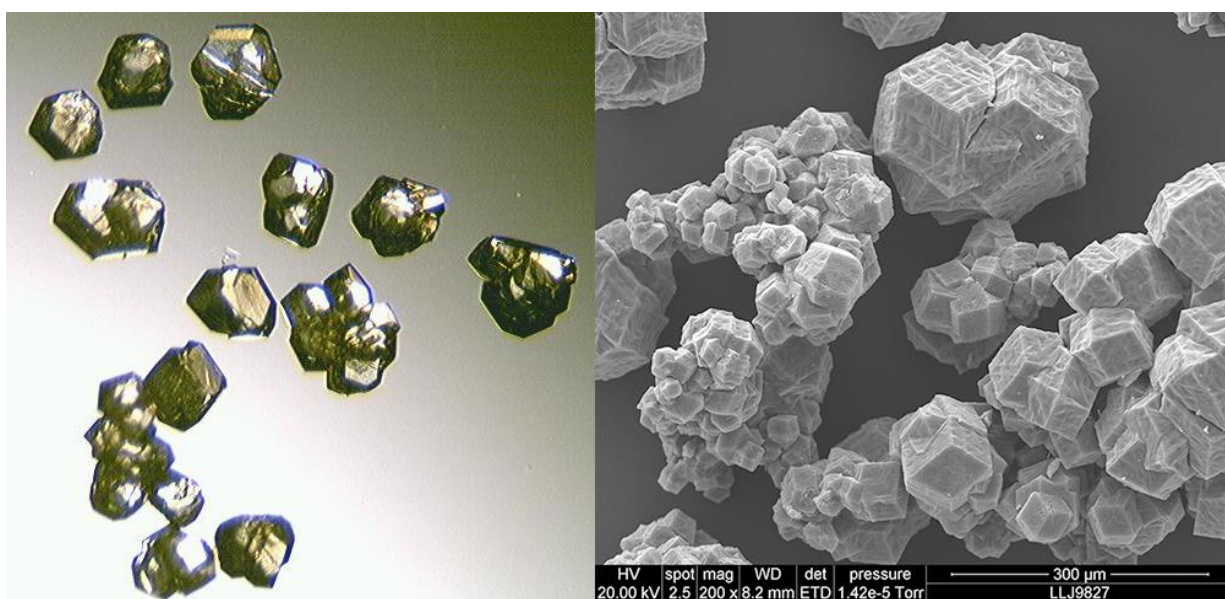


**Figure S58** Optical (left) and SEM (right) microscopy images of [Zn<sub>4</sub>O(bpdc-Pro)<sub>1/2</sub>(bdc)<sub>1/2</sub>(hmtt)<sub>4/3</sub>] crystals produced by thermolysis of [Zn<sub>4</sub>O(bpdc-ProBoc)<sub>1/2</sub>(bdc)<sub>1/2</sub>(hmtt)<sub>4/3</sub>]. The transparency and integrity of the crystals are very well maintained after thermolysis.

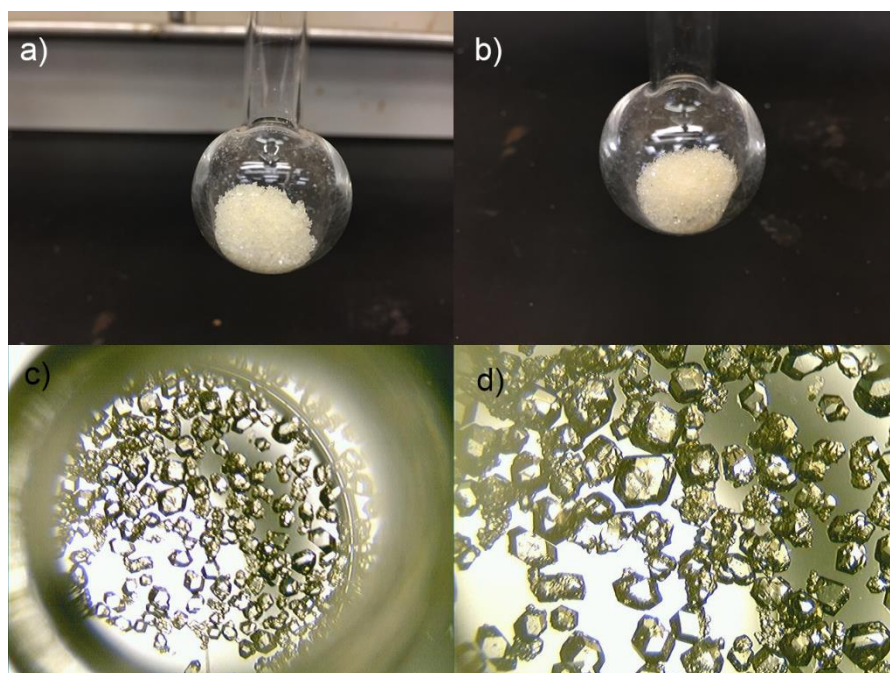


**Figure S59** a) Desolvated  $[\text{Zn}_4\text{O}(\text{bdc-ProBoc})_{1/2}(\text{bpdc})_{1/2}(\text{hmtt})_{4/3}]$  crystals in a sample tube; b)  $[\text{Zn}_4\text{O}(\text{bdc-Pro})_{1/2}(\text{bpdc})_{1/2}(\text{hmtt})_{4/3}]$  produced by thermolysis of the crystals shown in (a) by heating under vacuum; c) A small quantity of  $[\text{Zn}_4\text{O}(\text{bdc-Pro})_{1/2}(\text{bpdc})_{1/2}(\text{hmtt})_{4/3}]$  crystals was transferred to a glass vial with an inner diameter of 6 mm showing the size of these crystals with respect to the vial; d) A zoomed area of image (c).

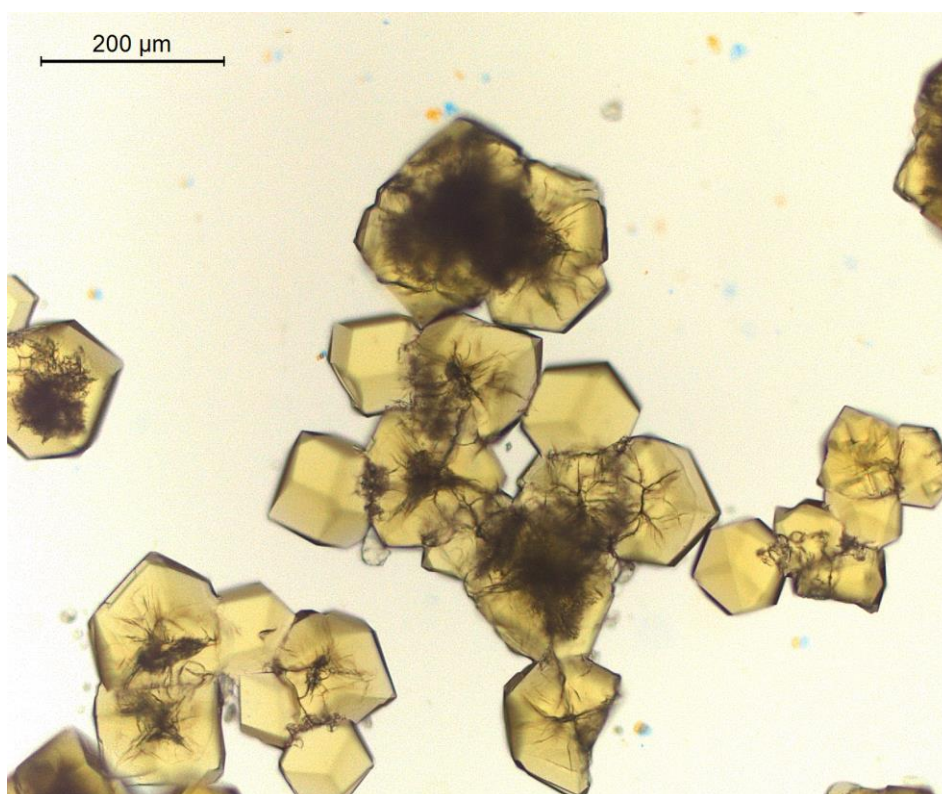


**Figure S60** Desolvated  $[\text{Zn}_4\text{O}(\text{bdc-Pro})_{1/2}(\text{bpdc})_{1/2}(\text{hmtt})_{4/3}]$  crystals following catalysis showing that the transparency and morphology of the crystals are retained.

## 12. References

1. Lun, D. J.; Waterhouse, G. I. N.; Telfer, S. G. *J. Am. Chem. Soc.* **2011**, *133*, 5806-5809.
2. Liu, L.; Telfer, S. G. *J. Am. Chem. Soc.* **2015**, *137*, 3901-3909.
3. Das, S.; Kim, H.; Kim, K. *J. Am. Chem. Soc.* **2009**, *131*, 3814-3815.
4. Ol'khovik, V. K.; Vasilevskii, V. A.; Galinovskii, N. A. *Russ. J. Org. Chem.* **2010**, *46*, 1167-1172.
5. Rigaku; Rigaku Corporation: Tokyo, Japan, 1996.
6. Sheldrick, G. M. *Acta Cryst.* **2008**, *A64*, 112-122.
7. Dolomanov, O. V.; Bourhis, L. J.; Gildea, R. J.; Howard, J. A. K.; Puschmann, H. *J. Appl. Crystallogr.* **2009**, *42*, 339-341.
8. Rigaku; 1.0.3.4 ed.; Rigaku Corporation: 2011.
9. Walton, K. S.; Snurr, R. Q. *J. Am. Chem. Soc.* **2007**, *129*, 8552-8556.
10. Dubbeldam, D.; Calero, S.; Ellis, D. E.; Snurr, R. Q. *Mol. Simul.* **2015**, 1-21.
11. Mayo, S. L.; Olafson, B. D.; Goddard, W. A. *J. Phys. Chem.* **1990**, *94*, 8897-8909.
12. Potoff, J. J.; Siepmann, J. I. *AIChE J.* **2001**, *47*, 1676-1682.
13. Wilmer, C. E.; Kim, K. C.; Snurr, R. Q. *J. Phys. Chem. Lett.* **2012**, *3*, 2506-2511.
14. Peng, D.-Y.; Robinson, D. B. *Ind. Eng. Chem. Fundam.* **1976**, *15*, 59-64.
15. Frost, H.; Düren, T.; Snurr, R. Q. *J. Phys. Chem. B* **2006**, *110*, 9565-9570.
16. Cobb, A. J. A.; Shaw, D. M.; Longbottom, D. A.; Gold, J. B.; Ley, S. V. *Org. Biol. Chem.* **2005**, *3*, 84-96.